DISCOVERY AND CHARACTERIZATION OF SKELETAL MUSCLE-DERIVED MYOKINES

by
Hannah C. Little

A dissertation submitted to Johns Hopkins University in conformity with the requirements for the degree of Doctor of Philosophy

Baltimore, MD
May 2019

© 2019 Hannah C. Little
All Rights Reserved

ABSTRACT

Obesity, diabetes, and associated co-morbidities are part of a major health epidemic in the United States, and they are becoming more rampant globally as well. Much still remains to be understood regarding the intricate mechanisms controlling whole-body energy balance and how dysregulation leads to disease. Regular exercise benefits systemic health, and it is hypothesized that myokines secreted from contracting skeletal muscle can mediate these effects. To identify novel exercise-regulated myokines, we measured the levels of 66 cytokines in serum and in glycolytic and oxidative muscles from wildtype mice subjected to either a sprint, endurance run, or one week of voluntary wheel running. Overall, many significant changes were observed in both serum and muscle in response to exercise, and our study identified 22 novel exercise-regulated myokines. Additionally, this is the first report comparing the cytokine profiles between muscle fiber types in response to different exercise regimes, and we demonstrated that there were more differences than commonalities between oxidative and glycolytic muscle. Lastly, a subset of the cytokine changes observed in circulation did not reflect changes in the skeletal muscle but rather correlated with gene expression changes in adipose tissue or liver. In another study, we focused on elucidating the role of a specific myokine, myonectin, in regulating systemic energy metabolism using a genetic knockout mouse model. Loss of myonectin had minimal or negligible effects on glucose metabolism, lipid metabolism, and exercise capacity in male and female mice fed a control, low-fat diet. However, when challenged with a high-fat diet to induce obesity, myonectin deficiency altered lipid handling and storage in males. Specifically, knockout mice exhibited a striking impairment in clearing serum lipids following a meal or oral lipid gavage compared to their wildtype littermates. Additionally, myonectin deficiency resulted in a dramatic reduction of high-fat diet-induced hepatic steatosis and, in parallel, a significant increase in adipose tissue mass

with concomitant adipocyte hypertrophy. The increased adiposity in knockout mice was promoted, in part, through increased adipose tissue lipoprotein lipase activity. In sum, our studies highlight novel and important functions of myokines in exercise and lipid metabolism, linking skeletal muscle to systemic energy homeostasis.

Thesis advisor: Guang William Wong, Ph.D.

Thesis reader: Paul A. Watkins, M.D., Ph.D.

ACKNOWLEDGEMENTS

I would like to start by acknowledging those who supported my research beginnings – Dr. Zhibin Guan and Dr. Hanxiang Zeng. I am extremely thankful to Dr. Guan for the opportunity to conduct research as an undergraduate in his lab at UC Irvine. Hanxiang, a PhD student at the time, was patient, kind, and an incredible mentor. My experience in this lab instilled in me a love for conducting basic research.

I am extremely grateful for the mentorship of my current PI, Dr. Will Wong, and the opportunity to conduct my PhD research in his lab. His enthusiasm for science is unrivaled, making his lab an enjoyable and exciting place to work. I especially appreciate his balance in mentoring style; he was always available and happy to provide guidance, but he also allowed me the freedom to explore, which expedited my growth as a scientist. I also value his level of trust in me as a scientist and in my data, and his principle to follow the data and not get distracted based on what we *a priori* expected the results to say. Overall, Will's guidance was instrumental in my scientific development.

I could not have asked for better labmates to have worked with over the years, including Marcus, Stefanie, Pia, Risa, Susie, Shelley, Ashley, Dylan, Gel, and Francesca. I really enjoy how collaborative our lab is and that my peers were always willing to help me with a mouse experiment or brainstorm with me about complicated data. Not only do I appreciate their scientific help and insight, but they are an incredibly friendly and fun group of people that I enjoyed spending many hours with.

I am still amazed at how quickly my BCMB classmates and I bonded and became very close friends. Their friendship has been incredibly important to me. Not only did we provide a framework of support for one another, but we had an amazingly fun time during grad school. They

will undoubtedly be friends for life. The same is true for other friends I met during graduate school, including those in CBI whom I met through Rick, climbing friends, and yoga friends. I am also thankful for the support and encouragement of my friends from High School and Undergrad, some of whom made the long trip to Baltimore to visit me during my years here.

Of course, I owe much of my success and my happiness in life to the love and support of my family. I cannot express in words my gratitude for everything they have done and continue to do for me. Thank you, Mama, Papa, Kim, Meghan, and Brittany! And thank you to my future in-laws for supporting me as if I'm already part of the family!

Lastly, thank you to my fiancé, Rick Hooy. You encourage me to pursue my dreams, you help me celebrate the successes, and you support me during hardship. I could not have done this without you.

TABLE OF CONTENTS

CHAPTER 1:

Introduction

Obesity, diabetes, and associated co-morbidities

The recent dramatic increase in the prevalence of obesity is alarming, with recent estimates categorizing nearly 40% of adults and more than 18% of children in the United States as clinically obese (1). Approximately 13% of the world's population is obese, a figure which has nearly tripled in the last four decades (2). It is widely accepted that obesity is causally related to the development of comorbidities such as type 2 diabetes and cardiovascular disease, both of which are among the leading causes of death in the United States (3–6). Not only do these metabolic health issues have a negative impact on the well-being of affected individuals, but also they pose an enormous economic burden on society (5–7). There is a dire need to understand the basic biology underlying metabolic dysregulation associated with excess caloric intake and a sedentary lifestyle, novel findings of which may lead to innovative treatments or preventative measures.

Systemic control of energy homeostasis

Controlling energy homeostasis is a complex, systems-level task for an organism. Fundamentally, this requires balancing food intake and energy expenditure to promote survival in times of fluctuating energy supply and demand. To do so, the body has to adapt its metabolism to its current metabolic state. For example, feeding stimulates anabolic processes to promote nutrient storage whereas fasting is dominated by catabolic processes to break down stored nutrients for energy utilization (8, 9). Exercise presents a unique metabolic challenge to an animal whereby high energy substrates are directed to the working skeletal muscle for ATP production, and fuel selection is dependent on exercise intensity (8). Proper control of nutrient intake, storage, and utilization specific to the metabolic state is dependent on the ability of different organs and organ systems to communicate their status and needs to other parts of the body. This inter-organ crosstalk

is mediated by nutrient flow, neuronal signals, and the endocrine system. Integration of these signals results in activation or suppression of specific metabolic pathways in a tissue-specific manner to maintain whole-body metabolic homeostasis. (8, 9). Secreted proteins represent a major part of the endocrine system, and greater than 10 percent of all protein-coding genes in the human genome are predicted to be secreted proteins based on the presence of a signal peptide (10). Most major metabolic organs are capable of both receiving endocrine signals as well as producing secreted proteins for inter-organ communication, including the gut, liver, adipose, and skeletal muscle (9). When energy balance is perturbed by overconsumption of calories and a sedentary lifestyle, the resulting disruption of signaling pathways regulated by these circulating hormones not only exacerbates the metabolic phenotype but also can lead to the development of comorbidities (11). Thus, studying the function of secreted proteins in normal physiology and metabolic disease may facilitate the discovery of novel therapeutic targets or strategies.

Myokines

Proteins secreted from the skeletal muscle are called myokines, and they can act in an autocrine, paracrine, and/or endocrine manner (12). Myostatin was the first characterized myokine, and it was discovered in the process of identifying new transforming growth factor beta (TGF-β) superfamily members. It is most well-known for its autocrine and paracrine roles as a negative regulator of muscle growth (13). Since then, numerous other myokines have been identified and characterized, spanning diverse roles in physiology. These include interleukin (IL)-7, IL-8, leukemia inhibitory factor (LIF), IL-15, brain-derived neurotrophic factor (BDNF), irisin, fibroblast growth factor 21 (FGF21), decorin, and secreted protein acidic and rich in cysteine (SPARC), among others (14, 15). Many proteomic studies have been carried out to characterize

the entire skeletal muscle secretome. Depending on the experimental design and method used, most of these studies have estimated that there are hundreds of myokines actively produced and secreted by skeletal muscle (16–20); hence, many remain to be characterized.

Myokines and exercise

Well before the discovery of myostatin, the existence of myokines was postulated, specifically in the context of exercise; it was hypothesized that exercising skeletal muscle must secrete some "exercise factor" into circulation in order to explain the observations that exercise is sufficient to reduce blood glucose by promoting glucose uptake and utilization in both exercising and non-exercising skeletal muscle, and that these effects are independent of the nervous system (21). Regular exercise is protective against many diseases, including cardio-metabolic disorders, whereas physical inactivity is a major risk factor for disease and premature mortality (15). However, the underlying mechanisms linking the inverse relationship between exercise and disease are not fully understood. Thus, there have been major efforts to identify "exercise factors" or "exerkines" which may mediate the beneficial health effects of exercise. Interleukin-6 (IL-6), the most extensively studied myokine, was the first protein shown to be secreted from contracting skeletal muscle. In the context of exercise, it functions in an endocrine manner to mobilize energy substrates and then in an autocrine fashion to promote substrate uptake and utilization in the skeletal muscle (15). However, in the context of injury or infection, IL-6 functions as a pro-inflammatory molecule and plays a role in activating the adaptive immune response (22). In addition to acute inflammation, elevated baseline IL-6 levels are partly responsible for chronic low-grade inflammation that is characteristic of obesity and type 2 diabetes (23). With regular exercise, resting levels of IL-6 are actually decreased while expression of the receptor IL-6Ra is

upregulated, thereby increasing IL-6 sensitivity and preventing IL-6-mediated chronic inflammation (15). Thus, IL-6 is a prime example of a myokine with acute functions in exercise that mechanistically links chronic exercise with improved health.

Finding novel exercise-induced myokines

Various approaches have been taken to identify novel exercise-induced myokines that could mediate the beneficial effects of exercise, similarly to IL-6. One method is *in vitro* studies using differentiated myotubes in culture that are stimulated to contract with electrical pulses. The conditioned media is then examined with proteomics methods to identify secreted proteins (24). The major advantage to this approach is the ability to detect *bona-fide* myokines; whatever was detected in the media came *directly* from the muscle cells. However, cell culture is an imperfect mimic of skeletal muscle *in vivo*: the organ is comprised of other cell types in addition to myotubes, electrical pulse stimulation does not fully reproduce the physiological changes exhibited in contracting skeletal muscle, and not all local and systemic factors that interact with the muscle are represented *in vitro* (24, 25). There have also been many human studies. Most often, blood and muscle biopsies are taken before and after exercise and subjected to transcriptomics or proteomics to identify changes induced by exercise (24). One drawback to human studies is that muscle biopsies are most often taken from a large leg muscle like the vastus lateralis, which contains a mix of muscle fiber types, so it is not feasible to determine the contribution of individual muscle fiber types (24). Additionally, it is not practical in humans to take tissue samples from other metabolic organs to assess if changes seen in the serum are due to protein expression and secretion in non-muscle tissues as a secondary response to myokine signaling from the exercising skeletal muscle. In general, a major limitation to the traditional proteomics approach using mass

spectrometry is that it is not sensitive enough to detect factors that are at very low abundance (25). Many circulating factors in the serum are known to be in the ng/mL or even pg/mL range and thus would not even be detected by these methods even though small changes in concentration of some circulating proteins are known to exert significant biological effects (25). Lastly, many *in vitro* and *in vivo* studies rely on mRNA expression data only and infer that those changes reflect protein levels, which may produce misleading conclusions (25). Chapter 2 describes a study that overcomes many of these limitations and provides novel insights regarding exercise-regulated changes in secreted proteins.

Adiponectin and C1q/TNF Related Proteins (CTRPs)

While the focus of the study detailed in Chapter 2 is on finding novel myokines, Chapter 3 describes a study characterizing the physiological role of a particular myokine called complement component 1q (C1q)/tumor necrosis factor (TNF)-related protein 15 (CTRP15). CTRP15 is part of the CTRP family of secreted proteins. CTRPs were first discovered in 2004 from a database of expressed sequence tags based on homology to adiponectin (26). Adiponectin is an extensively studied adipokine (hormone secreted from the adipose tissue) having pleiotropic roles in metabolism. The hormone sensitizes the body to insulin by stimulating AMP-activated protein kinase (AMPK) signaling in liver and skeletal muscle to enhance fat oxidation and glucose uptake and reduce hepatic gluconeogenesis (27). Despite being almost exclusively expressed in and secreted from adipose tissue, circulating adiponectin levels are paradoxically reduced in obese humans and mice (28, 29). The same holds true for diabetic patients (30). In fact, studies suggest that adiponectin can be a causative link between obesity and metabolic co-morbidities: a combination of genetic factors (e.g. single-nucleotide polymorphisms (SNPs) in the adiponectin

gene) and environmental factors that lead to obesity (e.g. high-fat diet) result in lower adiponectin levels, and adiponectin action is further decreased due to lower expression of its receptors in the obese state. This reduction in adiponectin action has been causatively linked to the development of insulin resistance, type 2 diabetes, metabolic syndrome, and atherosclerosis (27). Given the significant role adiponectin plays in metabolism and the etiology of metabolic diseases, the impetus to study the novel family of adiponectin paralogs in the context of metabolism was obvious.

CTRP structure

CTRPs share the same domain structure as adiponectin: an N-terminal signal peptide to promote secretion, a short variable domain with one or more conserved cysteine residues, a collagen-like domain, and a C-terminal globular c1q domain (**Fig. 1**) (11). The c1q domain is homologous to the complement protein of the same name and is structurally similar to TNFα, inspiring the name of the protein family (C1q/TNF related protein) (26). All CTRPs form trimers and many form higher order oligomeric structures, the formation of which is mediated by disulfide bond formation between conserved cysteine residues in the variable N-terminal domain (11). Different oligomeric forms of adiponectin have been shown to have different functions *in vivo* (31). Whether the same holds true for CTRPs remains largely unexplored. The exception is CTRP12 in which different isoforms form different oligomeric complexes and preferentially activate different signaling pathways: the full-length isoform forms trimers and larger complexes and activates protein kinase B (AKT) signaling whereas the cleaved, globular isoform forms dimers and activates mitogen-activated protein kinase (MAPK) signaling (32). Interestingly, many CTRPs have been shown to form hetero-oligomeric complexes with other CTRPs or with

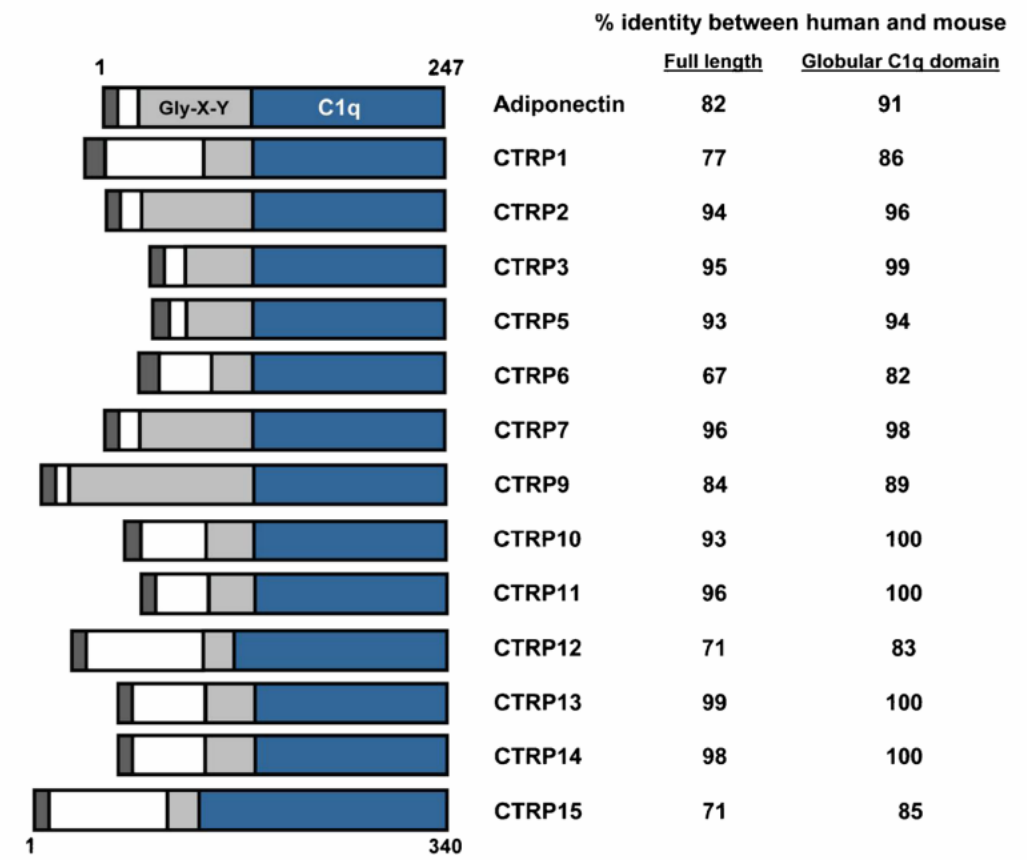

Figure 1. Schematic of CTRPs. With the exception of CTRP4, every CTRP consists of four domains: a signal peptide for secretion (*dark grey*), an N-terminal domain with one or more conserved Cys residues (*white*), a collagen domain with varying numbers of Gly-X-Y repeats (*light gray*), and a C-terminal globular domain homologous to the immune complement C1q (*blue*). The numbers on the right refer to the percent amino acid identity between human and mouse orthologs when comparing the full-length protein (first column) or the C-terminal globular domain (second column). CTRP4 and CTRP8 are omitted – the former consists of only two tandem C1q domains, while the latter is absent in the mouse genome. **(figure and figure legend copied with permission from reference 11)**

adiponectin (33–38); the physiological significance is currently unknown but it is possible that hetero-oligomers function in a manner different from the homo-oligomers, which would functionally increase the CTRP gene-to-ligand ratio (33). Many CTRPs are also glycosylated, which is likely to be important for protein folding in the endoplasmic reticulum, stability, and secretion (39). However, the functional significance of post-translational modifications of CTRPs has not been explored, with the exception of CTRP12. Cleavage of CTRP12 to generate the

globular isoform is regulated, in part, by N-linked glycosylation on a conserved asparagine residue in close proximity to the cleavage site (40).

CTRP function

All CTRPs are highly conserved throughout vertebrate evolution, implicating that each has a significant role in biology (11). Like adiponectin, many CTRPs are expressed in and secreted from white adipose tissue, but in general their tissue expression profiles in mice and humans are broader than that of adiponectin (11). For most CTRPs, expression and/or circulating levels are altered by acute or chronic metabolic state in mice ([reviewed in 11], 41–45). The functional roles of CTRPs have begun to be elucidated using overexpression and knockout mouse models. As expected based on homology to adiponectin, many of these mouse models have significant metabolic phenotypes, including differences in body weight (42, 46, 47), glucose homeostasis (44, 45), lipid homeostasis, or both glucose and lipid metabolism (41, 43, 46–48) (metabolic phenotypes also reviewed in 11). The relevance to human physiology has been confirmed with studies that have correlated serum or tissue CTRP levels with metabolic state or metabolic pathology including obesity, type 2 diabetes, and/or non-alcoholic fatty liver disease ([reviewed in 11], 43–45, 49–58). With an increasing focus on investigating CTRP function using rodent models, many CTRPs have been found to have physiological roles outside of nutrient metabolism, including inflammation (44, 45, 59), cardiac function (60–64), blood pressure (65), kidney function (data in press), bone function (66), atherogenesis (67–69), tissue fibrosis (45, 62), vascular remodeling (70), neuroinflammation/brain function (71), autophagy (72), and iron metabolism (73–75) (non-metabolic phenotypes also reviewed in 11). In humans, tissue or serum levels of CTRPs have been associated (positively or negatively) with the following disease states

in addition to nutrient metabolism: congestive heart failure (76), coronary artery disease (67, 77), late onset retinal degeneration, pulmonary arterial hypertension (78), polycystic ovarian syndrome (79), and anemia (80–82) (non-metabolic disease states correlated with CTRPs also reviewed in 11). One major limitation to the study of CTRP function is that there is limited research regarding their receptors. CTRP8 was shown to bind to and activate the G-protein-coupled receptor (GPCR) relaxin receptor 1 (RXFP1) in human glioblastoma cells, inducing cell migration and production of cathepsin B, a lysosomal protease correlated with tumor invasion (83). This interaction outside of the context of glioblastoma has not been investigated. CTRP9 can activate adiponectin receptor 1 (AdipoR1) to promote vasorelaxation in mouse aorta, which may have implications in endothelial dysfunction in cardiovascular disease (84). Lastly, CTRPs 10, 11, 13, and 14 were shown to bind to brain-specific angiogenesis inhibitor 3 (BAI3), a cell-adhesion GPCR, and the c1q globular domains were sufficient to decrease the excitatory synapse density in cultured neurons (85). However, the *in vivo* physiological relevance has not yet been determined. Given the diverse roles of the CTRP family of proteins and their relevance to so many disease states, further study of CTRP function and elucidation of relevant receptors will not only provide insight into normal physiology but also may provide a basis for therapeutic strategies aimed at developing receptor agonists or antagonists.

CTRP15/myonectin/erythroferrone

CTRP15 is unique among the CTRP family in that it is almost exclusively expressed in skeletal muscle in both humans and mice in normal conditions (38) whereas other members display a broader expression profile (11). For this reason, CTRP15 is also referred to as “myonectin.” Interestingly, the expression of most known myokines is not restricted to the skeletal muscle but

rather they are more widely expressed, so it seems myonectin is unique among myokines in its very limited expression profile under basal conditions (38). Myonectin expression in the skeletal muscle is upregulated after exercise (38, 64), and mouse studies have linked this exercise-induced increase in myonectin with improved outcomes after myocardial ischemia-reperfusion injury (64). However, during stress erythropoiesis in mice stimulated by blood loss or erythropoietin (EPO) administration, myonectin is highly induced in erythroblasts in the bone marrow and spleen (75). Under these circumstances, myonectin signals to the liver to suppress hepcidin expression, a negative regulator of iron mobilization, thereby increasing iron availability for new red blood cells (75). Based on this discovery, myonectin is also referred to as "erythroferrone" (75). The relevance to iron metabolism in humans has also been demonstrated. In patients with anemia due to chronic kidney disease, serum levels of myonectin rise in response to EPO or erythropoiesis-stimulating agents (86, 87). Similarly, blood loss or EPO administration to healthy individuals is sufficient to increase circulating levels of myonectin (81). Basal levels of myonectin are higher in patients with iron deficiency anemia (80) and beta thalassemia (81), and lower in patients with anemia of inflammation (82), implying myonectin's involvement in pathogenesis or response to anemia diseases.

The first piece of evidence for myonectin's role in nutrient metabolism is its unique expression pattern in mice based on metabolic state: mRNA and circulating levels are at low, basal levels during fasting but are dramatically upregulated upon re-feeding following an overnight fast (38). Interestingly, it seems that any nutrient flux through the muscle is sufficient to stimulate the expression and release of myonectin – both lipid and glucose administration are independently sufficient to show the same effect both *in vivo* and in cultured myotubes (38). In line with its postprandial expression pattern, myonectin stimulates nutrient uptake into peripheral tissues:

injection of recombinant myonectin into wildtype mice is sufficient to lower serum free fatty acid levels, and myonectin acts directly on adipocytes and hepatocytes in culture to stimulate fatty acid uptake from the media (38). Additionally, myonectin serves as a postprandial cue to stimulate the mammalian target of rapamycin (mTOR) pathway in the liver to inhibit autophagy, an intracellular recycling process that is activated during fasting (72). In humans, serum levels of myonectin have been correlated with metabolic pathologies: myonectin is higher in patients with metabolic syndrome than controls (57), and people with newly diagnosed type 2 diabetes have more myonectin than those with impaired glucose tolerance who, in turn, have higher myonectin than control patients (58). So far, these myonectin studies with respect to metabolism have been limited to recombinant protein infusion into mice, *in vitro* experiments using immortalized cell lines, and human correlational studies. Chapter 3 describes a study that investigates the *in vivo* physiological function of myonectin in regulating metabolic homeostasis in normal physiological conditions or in the context of metabolic disease using a genetic loss-of-function mouse model.

REFERENCES

1. Hales CM, Carroll MD, Fryar CD, Ogden CL. Prevalence of obesity among adults and youth: United States, 2015–2016. NCHS data brief, no 288. Hyattsville, MD: National Center for Health Statistics. 2017.

2. Obesity and overweight. The world health organization. 16 Feb. 2018: https://www.who.int/news-room/fact-sheets/detail/obesity-and-overweight

3. Kahn, S. E., Hull, R. L., and Utzschneider, K. M. (2006) Mechanisms linking obesity to insulin resistance and type 2 diabetes. *Nature* **444**, 840–846

4. Ortega, F. B., Lavie, C. J., and Blair, S. N. (2016) Obesity and Cardiovascular Disease. *Circulation Research* **118**, 1752–1770

5. Benjamin, E. J., Muntner, P., Alonso, A., Bittencourt, M. S., Callaway, C. W., Carson, A. P., Chamberlain, A. M., Chang, A. R., Cheng, S., Das, S. R., Delling, F. N., Djousse, L., Elkind, M., Ferguson, J. F., Fornage, M., Jordan, L., Khan, S. S., Kissela, B. M., Knutson, K. L., Kwan, T. W., Lackland, D. T., Lewis, T. T., Lichtman, J. H., Longenecker, C. T., Loop, M., Lutsey, P. L., Martin, S. S., Matsushita, K., Moran, A. E., Mussolino, M. E., O'Flaherty, M., Pandey, A., Perak, A. M., Rosamond, W. D., Roth, G. A., Sampson, U., tou, G., Schroeder, E. B., Shah, S. H., Spartano, N. L., Stokes, A., Tirschwell, D. L., Tsao, C. W., Turakhia, M. P., VanWagner, L. B., Wilkins, J. T., Wong, S. S., and Virani, S. S. (2019) Heart Disease and Stroke Statistics—2019 Update: A Report From the American Heart Association. *Circulation* **139**, e56

6. Centers for Disease Control and Prevention. National Diabetes Statistics Report, 2017. Atlanta, GA: Centers for Disease Control and Prevention, U.S. Dept of Health and Human Services; 2017.

7. Tremmel, M., Gerdtham, U.-G., Nilsson, P., and Saha, S. (2017) Economic Burden of Obesity: A Systematic Literature Review. *Int J Environ Res Pu* **14**, 435

8. Smith, R. L., Soeters, M. R., Wüst, R. C., and Houtkooper, R. H. (2018) Metabolic flexibility as an adaptation to energy resources and requirements in health and disease. *Endocrine reviews* **39**, 489-517

9. Lempradl, A., Pospisilik, A. J., and Penninger, J. M. (2015) Exploring the emerging complexity in transcriptional regulation of energy homeostasis. *Nature Reviews Genetics* **16**, 665–681

10. Uhlén, M., Fagerberg, L., Hallström, B. M., Lindskog, C., Oksvold, P., Mardinoglu, A., Sivertsson, Å., Kampf, C., Sjöstedt, E., Asplund, A., Olsson, I., Edlund, K., Lundberg, E., Navani, S., Szigyarto, C., Odeberg, J., Djureinovic, D., Takanen, J., Hober, S., Alm, T., Edqvist, P.-H., Berling, H., Tegel, H., Mulder, J., Rockberg, J., Nilsson, P., hwenk, J., Hamsten, M., von Feilitzen, K., Forsberg, M., Persson, L., Johansson, F., Zwahlen, M., von Heijne, G., Nielsen, J., and Pontén, F. (2015) Tissue-based map of the human proteome. *Science* **347**, 1260419

11. Seldin, M., Tan, S. Y., and Wong, W. G. (2014) Metabolic function of the CTRP family of hormones. *Reviews in Endocrine and Metabolic Disorders* **15**, 111–123

12. Pedersen, B., Steensberg, A., Fischer, C., Keller, C., Keller, P., Plomgaard, P., Febbraio, M., and Saltin, B. (2003) Searching for the exercise factor: is IL-6 a candidate? *Journal of muscle research and cell motility* **24**, 113–119

13. McPherron, A., Lawler, A., and Lee, S.-J. (1997) Regulation of skeletal muscle mass in mice by a new TGF-beta superfamily member. *Nature* **387**, 83–90

14. Lee, J. and Jun, H.-S. (2019) Role of Myokines in Regulating Skeletal Muscle Mass and Function. *Frontiers in Physiology* **10**, 42

15. Pedersen, B. K. and Febbraio, M. A. (2012) Muscles, exercise and obesity: skeletal muscle as a secretory organ. *Nature Reviews Endocrinology* **8**, 457

16. Hartwig, S., Raschke, S., Knebel, B., Scheler, M., Irmler, M., Passlack, W., Muller, S., Hanisch, F.-G., Franz, T., Li, X., Dicken, H.-D., Eckardt, K., Beckers, J., de Angelis, M., Weigert, C., Häring, H.-U., Al-Hasani, H., Ouwens, M. D., Eckel, J., Kotzka, J., and Lehr, S. (2014) Secretome profiling of primary human skeletal muscle cells. *Biochimica et Biophysica Acta (BBA) - Proteins and Proteomics* **1844**, 1011–1017

17. Catoire, M., Mensink, M., Kalkhoven, E., Schrauwen, P., and Kersten, S. (2014) Identification of human exercise-induced myokines using secretome analysis. *Physiological Genomics* **46**, 256–267

18. Henningsen, J., Rigbolt, K. T., Blagoev, B., Pedersen, B., and Kratchmarova, I. (2010) Dynamics of the Skeletal Muscle Secretome during Myoblast Differentiation. *Molecular & Cellular Proteomics* **9**, 2482–2496

19. Norheim, F., Raastad, T., Thiede, B., Rustan, A. C., Drevon, C. A., and Haugen, F. (2011) Proteomic identification of secreted proteins from human skeletal muscle cells and expression in response to strength training. *American Journal of Physiology-Endocrinology and Metabolism* **301**, E1013–E1021

20. Yoon, J., Yea, K., Kim, J., Choi, Y., Park, S., Lee, H., Lee, C., Suh, P., and Ryu, S. (2009) Comparative proteomic analysis of the insulin-induced L6 myotube secretome. *PROTEOMICS* **9**, 51–60

21. Goldstein. (1961) Humoral Nature of the Hypoglycemic Factor of Muscular Work. *Diabetes* **10**, 232–234

22. Scheller, J., Chalaris, A., Schmidt-Arras, D., and Rose-John, S. (2011) The pro- and anti-inflammatory properties of the cytokine interleukin-6. *Biochimica Et Biophysica Acta Bba - Mol Cell Res* **1813**, 878–888

23. Pedersen, B. K. (2009) Edward F. Adolph Distinguished Lecture: Muscle as an endocrine organ: IL-6 and other myokines. *Journal of Applied Physiology* **107**, 1006–1014

24. Peake, J., Gatta, P., Suzuki, K., and Nieman, D. (2015) Cytokine expression and secretion by skeletal muscle cells: regulatory mechanisms and exercise effects.*Exerc Immunol Rev* **21**, 8–25

25. Whitham, M. and Febbraio, M. A. (2016) The ever-expanding myokinome: discovery challenges and therapeutic implications. *Nature Reviews Drug Discovery* **15**, 719–729

26. Wong, G. W., Wang, J., Hug, C., Tsao, T.-S., and Lodish, H. F. (2004) A family of Acrp30/adiponectin structural and functional paralogs. *Proceedings of the National Academy of Sciences of the United States of America* **101**, 10302–10307

27. Kadowaki, T. and Yamauchi, T. (2005) Adiponectin and Adiponectin Receptors. *Endocrine Reviews* **26**, 439–451

28. Arita, Y., Kihara, S., Ouchi, N., Takahashi, M., Maeda, K., Miyagawa, J., Hotta, K., Shimomura, I., Nakamura, T., Miyaoka, K., Kuriyama, H., Nishida, M., Yamashita, S., Okubo, K., Matsubara, K., Muraguchi, M., Ohmoto, Y., Funahashi, T., and Matsuzawa, Y. (2012) Paradoxical decrease of an adipose-specific protein, adiponectin, in obesity. 1999. *Biochemical and biophysical research communications* **425**, 560–564

29. Hu, E., Liang, P., and iegelman, B. (1996) AdipoQ Is a Novel Adipose-specific Gene Dysregulated in Obesity. *Journal of Biological Chemistry* **271**, 10697–10703

30. Hotta, K., Funahashi, T., Arita, Y., Takahashi, M., Matsuda, M., Okamoto, Y., Iwahashi, H., Kuriyama, H., Ouchi, N., Maeda, K., Nishida, M., Kihara, S., Sakai, N., Nakajima, T., Hasegawa, K., Muraguchi, M., Ohmoto, Y., Nakamura, T., Yamashita, S., Hanafusa, T., and Matsuzawa, Y. (2000) Plasma Concentrations of a Novel, Adipose-Specific Protein, Adiponectin, in Type 2 Diabetic Patients. *Arteriosclerosis, Thrombosis, and Vascular Biology* **20**, 1595–1599

31. Wang, Y., Lam, K. S., Yau, M. H., and Xu, A. (2008) Post-translational modifications of adiponectin: mechanisms and functional implications. *The Biochemical journal* **409**, 623–633

32. Wei, Z., Lei, X., Seldin, M., and Wong, W. G. (2012) Endopeptidase Cleavage Generates a Functionally Distinct Isoform of C1q/Tumor Necrosis Factor-related Protein-12 (CTRP12) with an Altered Oligomeric State and Signaling Specificity. *Journal of Biological Chemistry* **287**, 35804–35814

33. Wong, W., Krawczyk, S., Kitidis-Mitrokostas, C., Revett, T., Gimeno, R., and Lodish, H. (2008) Molecular, biochemical and functional characterizations of C1q/TNF family members: adipose-tissue-selective expression patterns, regulation by PPAR-γ agonist, cysteine-mediated oligomerizations, combinatorial associations and metabolic functions. *Biochem J* **416**, 161–177

34. Wong, G., Krawczyk, S. A., Kitidis-Mitrokostas, C., Ge, G., Spooner, E., Hug, C., Gimeno, R., and Lodish, H. F. (2009) Identification and characterization of CTRP9, a novel secreted glycoprotein, from adipose tissue that reduces serum glucose in mice and forms heterotrimers with adiponectin. *FASEB journal : official publication of the Federation of American Societies for Experimental Biology* **23**, 241–258

35. Peterson, J. M., Wei, Z., and Wong, W. G. (2009) CTRP8 and CTRP9B are novel proteins that hetero-oligomerize with C1q/TNF family members. *Biochemical and biophysical research communications* **388**, 360–365

36. Wei, Z., Seldin, M., Natarajan, N., Djemal, D. C., Peterson, J. M., and Wong, W. G. (2013) C1q/Tumor Necrosis Factor-related Protein 11 (CTRP11), a Novel Adipose Stroma-derived Regulator of Adipogenesis. *Journal of Biological Chemistry* **288**, 10214–10229

37. Wei, Z., Peterson, J. M., and Wong, W. G. (2011) Metabolic Regulation by C1q/TNF-related Protein-13 (CTRP13) ACTIVATION OF AMP-ACTIVATED PROTEIN KINASE AND SUPPRESSION OF FATTY ACID-INDUCED JNK SIGNALING. *Journal of Biological Chemistry* **286**, 15652–15665

38. Seldin, M., Peterson, J. M., Byerly, M. S., Wei, Z., and Wong, W. G. (2012) Myonectin (CTRP15), a Novel Myokine That Links Skeletal Muscle to Systemic Lipid Homeostasis. *Journal of Biological Chemistry* **287**, 11968–11980

39. Jayaprakash, N. and Surolia, A. (2017) Role of glycosylation in nucleating protein folding and

stability. *Biochemical Journal* **474**, 2333–2347

40. Stewart, A. N., Tan, S. Y., Clark, D. J., Zhang, H., and Wong, W. G. (2018) N-linked glycosylation dependent and independent mechanisms regulating CTRP12 cleavage, secretion, and stability. *Biochemistry* **58**, 727-741

41. Peterson, J., Seldin, M., Tan, S., and Wong, W. (2014) CTRP2 Overexpression Improves Insulin and Lipid Tolerance in Diet-Induced Obese Mice. *Plos One* **9**, e88535

42. Byerly, M. S., Petersen, P. S., Ramamurthy, S., Seldin, M., Lei, X., Provost, E., Wei, Z., Ronnett, G. V., and Wong, G. (2014) C1q/TNF-related protein 4 (CTRP4) is a unique secreted protein with two tandem C1q domains that functions in the hypothalamus to modulate food intake and body weight. *The Journal of biological chemistry* **289**, 4055–4069

43. Lei, X., Rodriguez, S., Petersen, P. S., Seldin, M., Bowman, C. E., Wolfgang, M. J., and Wong, G. (2016) Loss of CTRP5 improves insulin action and hepatic steatosis. *American journal of physiology. Endocrinology and metabolism* **310**, E1036-52

44. Lei, X., Seldin, M., Little, H. C., Choy, N., Klonisch, T., and Wong, G. (2017) C1q/TNF-related protein 6 (CTRP6) links obesity to adipose tissue inflammation and insulin resistance. *The Journal of biological chemistry* **292**, 14836–14850

45. Petersen, P. S., Lei, X., Wolf, R. M., Rodriguez, S., Tan, S. Y., Little, H. C., Schweitzer, M. A., Magnuson, T. H., Steele, K. E., and Wong, G. (2017) CTRP7 deletion attenuates obesity-linked glucose intolerance, adipose tissue inflammation, and hepatic stress. *American journal of physiology. Endocrinology and metabolism* **312**, E309–E325

46. Rodriguez, S., Lei, X., Petersen, P., Tan, S., Little, H., and Wong, W. (2016) Loss of CTRP1 disrupts glucose and lipid homeostasis. *Am J Physiology Endocrinol Metabolism* **311**, E678–E697

47. Wei, Z., Lei, X., Petersen, P. S., Aja, S., and Wong, G. (2014) Targeted deletion of C1q/TNF-related protein 9 increases food intake, decreases insulin sensitivity, and promotes hepatic steatosis in mice. *American journal of physiology. Endocrinology and metabolism* **306**, E779-90

48. Tan, S. Y., Little, H. C., Lei, X., Li, S., Rodriguez, S., and Wong, G. (2016) Partial deficiency of CTRP12 alters hepatic lipid metabolism. *Physiological genomics* **48**, 936–949

49. Shabani, P., Khaledi, N. H., Beigy, M., Emamgholipour, S., Parvaz, E., Poustchi, H., and Doosti, M. (2015) Circulating level of CTRP1 in patients with nonalcoholic fatty liver disease (NAFLD): is it through insulin resistance? *PloS one* **10**, e0118650

50. Wolf, R. M., Steele, K. E., Peterson, L. A., Magnuson, T. H., Schweitzer, M. A., and Wong, G. (2015) Lower Circulating C1q/TNF-Related Protein-3 (CTRP3) Levels Are Associated with Obesity: A Cross-Sectional Study. *PloS one* **10**, e0133955

51. Emamgholipour, S., Moradi, N., Beigy, M., Shabani, P., Fadaei, R., Poustchi, H., and Doosti, M. (2015) The association of circulating levels of complement-C1q TNF-related protein 5 (CTRP5) with nonalcoholic fatty liver disease and type 2 diabetes: a case-control study. *Diabetology & metabolic syndrome* **7**, 108

52. Wang, M., Tang, X., Li, L., Liu, D., Liu, H., Zheng, H., Deng, W., Zhao, X., and Yang, G. (2018)

C1q/TNF-related protein-6 is associated with insulin resistance and the development of diabetes in Chinese population. *Acta diabetologica* **55**, 1221–1229

53. Jia, Y., Luo, X., Ji, Y., Xie, J., Jiang, H., Fu, M., and Li, X. (2017) Circulating CTRP9 levels are increased in patients with newly diagnosed type 2 diabetes and correlated with insulin resistance. *Diabetes research and clinical practice* **131**, 116–123

54. Wolf, R. M., Steele, K. E., Peterson, L. A., Zeng, X., Jaffe, A. E., Schweitzer, M. A., Magnuson, T. H., and Wong, G. (2016) C1q/TNF-Related Protein-9 (CTRP9) Levels Are Associated With Obesity and Decrease Following Weight Loss Surgery. *The Journal of clinical endocrinology and metabolism* **101**, 2211–2217

55. Bai, B., Ban, B., Liu, Z., Zhang, M. M., Tan, B. K., and Chen, J. (2017) Circulating C1q complement/TNF-related protein (CTRP) 1, CTRP9, CTRP12 and CTRP13 concentrations in Type 2 diabetes mellitus: In vivo regulation by glucose. *PloS one* **12**, e0172271

56. Shanaki, M., Fadaei, R., Moradi, N., Emamgholipour, S., and Poustchi, H. (2016) The Circulating CTRP13 in Type 2 Diabetes and Non-Alcoholic Fatty Liver Patients. *PloS one* **11**, e0168082

57. Mi, Q., Li, Y., Wang, M., Yang, G., Zhao, X., Liu, H., Zheng, H., and Li, L. (2019) Circulating C1q/TNF-related protein isoform 15 is a marker for the presence of metabolic syndrome. *Diabetes/metabolism research and reviews* **35**, e3085

58. Li, K., Liao, X., Wang, K., Mi, Q., Zhang, T., Jia, Y., Xu, X., Luo, X., Zhang, C., Liu, H., Zhen, H., Li, L., and Yang, G. (2018) Myonectin Predicts the Development of Type 2 Diabetes. *The Journal of clinical endocrinology and metabolism* **103**, 139–147

59. Petersen, P. S., Wolf, R. M., Lei, X., Peterson, J. M., and Wong, G. (2016) Immunomodulatory roles of CTRP3 in endotoxemia and metabolic stress. *Physiological reports* **4**, e12735

60. Ma, Z.-G., Yuan, Y.-P., Zhang, X., Xu, S.-C., Kong, C.-Y., Song, P., Li, N., and Tang, Q.-Z. (2018) C1q-tumor necrosis factor-related protein-3 exacerbates cardiac hypertrophy in mice. *Cardiovascular research* **115**, 1067-1077

61. Zheng, W.-F., Zhang, S.-Y., Ma, H.-F., Chang, X.-W., and Wang, H. (2019) C1qTNF-related protein-6 protects against doxorubicin-induced cardiac injury. *Journal of cellular biochemistry* **120**, 10748–10755

62. Lei, H., Wu, D., Wang, J.-Y., Li, L., Zhang, C.-L., Feng, H., Fu, F.-Y., and Wu, L.-L. (2015) C1q/tumor necrosis factor-related protein-6 attenuates post-infarct cardiac fibrosis by targeting RhoA/MRTF-A pathway and inhibiting myofibroblast differentiation. *Basic research in cardiology* **110**, 35

63. Yuasa, D., Ohashi, K., Shibata, R., Mizutani, N., Kataoka, Y., Kambara, T., Uemura, Y., Matsuo, K., Kanemura, N., Hayakawa, S., Hiramatsu-Ito, M., Ito, M., Ogawa, H., Murate, T., Murohara, T., and Ouchi, N. (2016) C1q/TNF-related protein-1 functions to protect against acute ischemic injury in the heart. *FASEB journal : official publication of the Federation of American Societies for Experimental Biology* **30**, 1065–1075

64. Otaka, N., Shibata, R., Ohashi, K., Uemura, Y., Kambara, T., Enomoto, T., Ogawa, H., Ito, M., Kawanishi, H., Maruyama, S., Joki, Y., Fujikawa, Y., Narita, S., Unno, K., Kawamoto, Y., Murate, T., Murohara, T., and Ouchi, N. (2018) Myonectin Is an Exercise-Induced Myokine That Protects the Heart

From Ischemia-Reperfusion Injury. *Circulation research* **123**, 1326–1338

65. Han, S., Jeong, A. L., Lee, S., Park, J. S., Buyanravjikh, S., Kang, W., Choi, S., Park, C., Han, J., Son, W.-C., Yoo, K. H., Cheong, J. H., Oh, G. T., Lee, W.-Y., Kim, J., Suh, S. H., Lee, S.-H., Lim, J.-S., Lee, M.-S., and Yang, Y. (2018) C1q/TNF-α-Related Protein 1 (CTRP1) Maintains Blood Pressure Under Dehydration Conditions. *Circulation research* **123**, e5–e19

66. Li, Q., Wu, J., Xi, W., Chen, X., Wang, W., Zhang, T., Yang, A., and Wang, T. (2019) Ctrp4, a new adipokine, promotes the differentiation of osteoblasts. *Biochemical and biophysical research communications* **512**, 224-229

67. Li, C., Chen, J. W., Liu, Z. H., Shen, Y., Ding, F. H., Gu, G., Liu, J., Qiu, J. P., Gao, J., Zhang, R. Y., Shen, W. F., Wang, X. Q., and Lu, L. (2018) CTRP5 promotes transcytosis and oxidative modification of low-density lipoprotein and the development of atherosclerosis. *Atherosclerosis* **278**, 197–209

68. Huang, C., Zhang, P., Li, T., Li, J., Liu, T., Zuo, A., Chen, J., and Guo, Y. (2019) Overexpression of CTRP9 attenuates the development of atherosclerosis in apolipoprotein E-deficient mice. *Molecular and cellular biochemistry* **455**, 99–108

69. Wang, C., Xu, W., Liang, M., Huang, D., and Huang, K. (2019) CTRP13 inhibits atherosclerosis via autophagy-lysosome-dependent degradation of CD36. *FASEB journal : official publication of the Federation of American Societies for Experimental Biology* **33**, 2290–2300

70. Ogawa, H., Ohashi, K., Ito, M., Shibata, R., Kanemura, N., Yuasa, D., Kambara, T., Matsuo, K., Hayakawa, S., Hiramatsu-Ito, M., Otaka, N., Kawanishi, H., Yamaguchi, S., Enomoto, T., Abe, T., Kaneko, M., Takefuji, M., Murohara, T., and Ouchi, N. (2019) Adipolin/CTRP12 protects against pathological vascular remodeling through suppression of smooth muscle cell growth and macrophage inflammatory response. *Cardiovascular research* [Epub ahead of print]

71. Zhao, L., Chen, S., Sherchan, P., Ding, Y., Zhao, W., Guo, Z., Yu, J., Tang, J., and Zhang, J. H. (2018) Recombinant CTRP9 administration attenuates neuroinflammation via activating adiponectin receptor 1 after intracerebral hemorrhage in mice. *Journal of neuroinflammation* **15**, 215

72. Seldin, M., Lei, X., Tan, S., Stanson, K., Wei, Z., and Wong, W. (2013) Skeletal Muscle-derived Myonectin Activates the Mammalian Target of Rapamycin (mTOR) Pathway to Suppress Autophagy in Liver. *J Biol Chem* **288**, 36073–36082

73. Kautz, L., Jung, G., Du, X., Gabayan, V., Chapman, J., Nasoff, M., Nemeth, E., and Ganz, T. (2015) Erythroferrone contributes to hepcidin suppression and iron overload in a mouse model of β-thalassemia. *Blood* **126**, 2031–2037

74. Kautz, L., Jung, G., Nemeth, E., and Ganz, T. (2014) Erythroferrone contributes to recovery from anemia of inflammation. *Blood* **124**, 2569–2574

75. Kautz, L., Jung, G., Valore, E. V., Rivella, S., Nemeth, E., and Ganz, T. (2014) Identification of erythroferrone as an erythroid regulator of iron metabolism. *Nature genetics* **46**, 678–684

76. Yang, Y., Liu, S., Zhang, R.-Y., Luo, H., Chen, L., He, W.-F., Lei, R., Liu, M.-R., Hu, H.-X., and Chen, M. (2017) Association Between C1q/TNF-Related Protein-1 Levels in Human Plasma and Epicardial Adipose Tissues and Congestive Heart Failure. *Cellular physiology and biochemistry : international journal of experimental cellular physiology, biochemistry, and pharmacology* **42**, 2130–

2143

77. Fadaei, R., Moradi, N., Kazemi, T., Chamani, E., Azdaki, N., Moezibady, S. A., Shahmohamadnejad, S., and Fallah, S. (2019) Decreased serum levels of CTRP12/adipolin in patients with coronary artery disease in relation to inflammatory cytokines and insulin resistance. *Cytokine* **113**, 326–331

78. Li, Y., Geng, X., Wang, H., Cheng, G., and Xu, S. (2016) CTRP9 Ameliorates Pulmonary Arterial Hypertension Through Attenuating Inflammation and Improving Endothelial Cell Survival and Function. *Journal of cardiovascular pharmacology* **67**, 394–401

79. Shanaki, M., Moradi, N., Fadaei, R., Zandieh, Z., Shabani, P., and Vatannejad, A. (2018) Lower circulating levels of CTRP12 and CTRP13 in polycystic ovarian syndrome: Irrespective of obesity. *PloS one* **13**, e0208059

80. El Gendy, F. M., El-Hawy, M. A., Shehata, A. M., and Osheba, H. E. (2018) Erythroferrone and iron status parameters levels in pediatric patients with iron deficiency anemia. *European journal of haematology* **100**, 356–360

81. Ganz, T., Jung, G., Naeim, A., Ginzburg, Y., Pakbaz, Z., Walter, P. B., Kautz, L., and Nemeth, E. (2017) Immunoassay for human serum erythroferrone. *Blood* **130**, 1243–1246

82. Boshuizen, M., Binnekade, J. M., Nota, B., van de Groep, K., Cremer, O. L., Tuinman, P. R., Horn, J., Schultz, M. J., van Bruggen, R., and Juffermans, N. P. (2018) Iron metabolism in critically ill patients developing anemia of inflammation: a case control study. *Annals of intensive care* **8**, 56

83. Glogowska, A., Kunanuvat, U., Stetefeld, J., Patel, T. R., Thanasupawat, T., Krcek, J., Weber, E., Wong, W. G., Bigio, M. R., Hoang-Vu, C., Hombach-Klonisch, S., and Klonisch, T. (2013) C1q-tumour necrosis factor-related protein 8 (CTRP8) is a novel interaction partner of relaxin receptor RXFP1 in human brain cancer cells. *The Journal of Pathology* **231**, 466–479

84. Zheng, Q., Yuan, Y., Yi, W., Lau, W., Wang, Y., Wang, X., Sun, Y., Lopez, B. L., Christopher, T. A., Peterson, J. M., Wong, W. G., Yu, S., Yi, D., and Ma, X.-L. (2011) C1q/TNF-Related Proteins, A Family of Novel Adipokines, Induce Vascular Relaxation Through the Adiponectin Receptor-1/AMPK/eNOS/Nitric Oxide Signaling Pathway. *Arteriosclerosis, Thrombosis, and Vascular Biology* **31**, 2616–2623

85. Bolliger, M. F., Martinelli, D. C., and Südhof, T. C. (2011) The cell-adhesion G protein-coupled receptor BAI3 is a high-affinity receptor for C1q-like proteins. *Proceedings of the National Academy of Sciences* **108**, 2534–2539

86. Honda, H., Kobayashi, Y., Onuma, S., Shibagaki, K., Yuza, T., Hirao, K., Yamamoto, T., Tomosugi, N., and Shibata, T. (2016) Associations among Erythroferrone and Biomarkers of Erythropoiesis and Iron Metabolism, and Treatment with Long-Term Erythropoiesis-Stimulating Agents in Patients on Hemodialysis. *PloS one* **11**, e0151601

87. Hanudel, M. R., Rappaport, M., Chua, K., Gabayan, V., Qiao, B., Jung, G., Salusky, I. B., Ganz, T., and Nemeth, E. (2018) Levels of the erythropoietin-responsive hormone erythroferrone in mice and humans with chronic kidney disease. *Haematologica* **103**, e141–e142

CHAPTER 2:

Multiplex quantification identifies novel exercise-regulated myokines/cytokines in plasma and in glycolytic and oxidative skeletal muscle*

*Text and figures in this chapter were published in *Molecular and Cellular Proteomics* in 2018:

Little, H. C., Tan, S. Y., Cali, F., Rodriguez, S., Lei, X., Wolfe, A., Hug, C., and Wong, G. W. (2018) Multiplex Quantification Identifies Novel Exercise-regulated Myokines/Cytokines in Plasma and in Glycolytic and Oxidative Skeletal Muscle. *Mol Cell Proteomics* **17**, 1546–1563

ABSTRACT

Exercise is known to confer major health benefits, but the underlying mechanisms are not well understood. The systemic effects of exercise on multi-organ systems are thought to be partly due to myokines/cytokines secreted by skeletal muscle. The extent to which exercise alters cytokine expression and secretion in different muscle fiber types has not been systematically examined. Here, we assessed changes in 66 mouse cytokines in serum, and in glycolytic (plantaris) and oxidative (soleus) muscles, in response to sprint, endurance, or chronic wheel running. Both acute and short-term exercise significantly altered a large fraction of cytokines in both serum and muscle, twenty-two of which are considered novel exercise-regulated myokines. Most of the secreted cytokine receptors profiled were also altered by physical activity, suggesting an exercise-regulated mechanism that modulates the generation of soluble receptors found in circulation. A greater overlap in cytokine profile was seen between endurance and chronic wheel running. Between fiber types, both acute and chronic exercise induced significantly more cytokine changes in oxidative compared to glycolytic muscle. Further, changes in a subset of circulating cytokines were not matched by their changes in muscle, but instead reflected altered expression in liver and adipose tissues. Lastly, exercise-induced changes in cytokine mRNA and protein were only minimally correlated in soleus and plantaris. In sum, our results indicate that exercise regulates a large number of cytokines whose pleiotropic actions may be linked to positive health outcomes. These data provide a framework to further understand potential crosstalk between skeletal muscle and other organ compartments.

INTRODUCTION

Physical inactivity is a major risk factor contributing to cardio-metabolic disorders in modern society (1, 2). Conversely, regular exercise confers systemic health benefits (3-6). The underlying mechanisms responsible for the positive physiological effects of exercise, however, are not well understood (7, 8). The systemic effects of exercise on multi-organ systems has long thought to be, at least in part, due to myokines and cytokines secreted by skeletal muscle in response to exercise (9-11). These exercise-induced myokines are believed to mediate crosstalk between skeletal muscle and other organ compartments. Depending on the method used and biological contexts, proteomics-based analyses of the muscle "secretome" have identified hundreds of proteins secreted by muscle cells (12-19). The functions for most of these muscle-derived secretory proteins are poorly defined, and it is unclear whether their expression and secretion are regulated by muscle contraction *in vivo*. Importantly, biologically potent molecules, such as cytokines, that normally exist at low levels (typically in the ng/mL and pg/mL range) are generally not detected by current proteomics methods.

The cytokine interleukin (IL)-6 is one of the first myokines shown to be actively secreted by contracting skeletal muscle in human (20, 21). Since its discovery, other cytokines such as IL-7 (22), IL-15 (23), leukemia inhibitory factor (LIF) (24), and vascular endothelial growth factor (VEGF) (25) have also been shown to be functionally relevant exercise-induced myokines, either acting in an autocrine/paracrine manner within muscle, or acting via an endocrine fashion to affect biological processes in non-muscle tissues. Recent *in vitro* studies using electrical pulse stimulation of primary human myotubes and antibody-based detection approaches also identified significant numbers of contraction-induced myokines/cytokines (26, 27). While these *in vitro* studies allow the unequivocal identification of *bona fide* muscle cell-derived myokines, limitations

to these cell models have also been noted. Although differentiated primary myotubes in culture serve as a reasonable proxy for mature muscle cells, they do not capture the three-dimensional muscle fibers in the context of other potentially important accessory cell types (e.g., vascular endothelial cells, satellite cells, immune cells, and sympathetic nerve cells), nor do the cultured myotubes fully resemble the metabolically distinct glycolytic and oxidative fiber types. Further, electrical pulse stimulation of myotubes does not fully recapitulate both the stimulatory and inhibitory pathways induced by exercising skeletal muscle (28). As such, *in vivo* studies in humans or animal models will complement and extend the *in vitro* studies, enabling a more complete understanding of skeletal muscle's response to exercise.

Cytokines, chemokines, and secreted cytokine receptors constitute a large family of secretory proteins with pleiotropic immune and non-immune functions (29-33). As such, changes in local and systemic levels of these molecules in response to exercise could potentially account, at least in part, for the positive effects of physical activities. The present study aimed to address three related questions. First, while a handful of cytokines has thus far been shown to be secreted by exercising muscle *in vivo*, the extent to which different types of physical activity (sprint, endurance, voluntary wheel running) regulates cytokine expression and secretion in glycolytic versus oxidative muscle fibers has not been systematically examined. Most human exercise studies examined transcriptional and protein changes in vastus lateralis, a quadriceps muscle with mixed fiber types. The metabolism of *in vitro* differentiated primary human myotubes also tended to be glycolytic rather than oxidative. Thus, the use of mouse exercise models allows us to address questions that are difficult to study in humans and primary cell culture system. Secondly, it is generally assumed that changes in serum cytokine in response to exercise are directly related to changes in their expression and secretion in skeletal muscle. It remains unknown to what extent

the changes in plasma cytokine levels are due to secondary adaptive changes in their expression and secretion in non-muscle tissues in response to exercise. This could potentially occur if the primary exercise-induced cytokines in turn stimulate the expression and secretion of secondary cytokines in other non-muscle tissues. Thirdly, several transcriptomics studies have been carried out to look at changes in human muscle gene expression in response to exercise (34-37). Whether changes in mRNA level translate into changes in protein level in human skeletal muscle are often not examined, in large part limited by the availability of protein-specific antibodies and the cost of validating a large number of candidate proteins.

With the use of the conventional ELISA method, it is not feasible to simultaneously measure the levels of large numbers of cytokines in a mouse due to limited blood volume that could be sampled. Technological advancement in recent years has made it feasible now to simultaneously quantify a large number of cytokines in serum and tissues using only small volume of blood or quantity of tissue. Using a bead-based multiplex profiling method, we seek to measure cytokine levels in mice in response to an acute sprint or endurance run, or a short-term access to a running wheel for one week (representing chronic exercise). Here, we examined a total of 66 known cytokines (including secreted cytokine receptors and acute phase proteins) that represent a well-studied set of molecules with diverse functions and activities. These cytokines act on diverse cell types to modulate a variety of biological processes that include inflammation, chemotaxis, apoptosis, metabolism, angiogenesis, and cell proliferation (38). Given the pleiotropic systemic effects of exercise, we hypothesized that acute and chronic exercise would dynamically alter cytokine levels in circulation and in different muscle fiber types (e.g., oxidative and glycolytic). Indeed, our results show that exercise modulates the expression of a large number of cytokines in different muscle fiber types depending on the type of physical activity (sprint, endurance, or

chronic wheel running). Many of these cytokines are considered novel exercise-regulated myokines. Concordance between mRNA and protein level was observed for only a small subset of cytokines. Further, we showed that a subset of circulating cytokines is likely induced and secreted in non-muscle tissues in response to exercise, highlighting the primary skeletal muscle response to exercise and the secondary adaptive response in non-muscle tissues.

EXPERIMENTAL PROCEDURES

Animals

Eight-week-old C57BL/6J male mice were purchased from The Jackson Labs. All mice were housed in polycarbonate cages under a 12:12-h light-dark photocycle (6 AM – 6 PM) and had access to food and water *ad libitum* throughout the study period. Mice were allowed to acclimate for one week before experimentation. All animal experiments were approved by the Animal Care and Use Committee of The Johns Hopkins University School of Medicine.

Mice were randomly divided into 4 groups of 10 mice for the following control or exercise paradigms: sedentary, sprint exercise, endurance exercise, and voluntary exercise. At 9 weeks of age, blood was collected from the tail vein for pre-exercise measurements from all mice, including the sedentary group. While serum samples from the sedentary group were not used for analysis, blood was still collected from this group to normalize treatment and handling among all groups. Samples were collected at the same time of day for all mice (10:30 AM). Serum was separated using Microvette® CB 300 LH (The SARSTEDT Group, Numbrecht, Germany), and separated serum was stored at -80°C until analysis.

For sprint and endurance exercise conditions, mice were acclimatized to the treadmill (Exer 3/6 treadmill; Columbus Instruments) for 3 days before the exercise test as follows: day 1: mice

were placed on the stationary treadmill for 10 min (with the shock grid on); day 2: mice were run on the treadmill at a speed of 5 m/min for 10 min at a 10° incline; day 3: mice were run on the treadmill at 10 m/min for 10 min at a 10° incline. A shock grid at the back of the treadmill encouraged mice to continue running by administering a mild shock each time they stepped off the belt. The acute exercise tests were performed on the fourth day when the mice were 10 weeks of age.

Sprint exercise: Baseline blood glucose and lactate levels were measured with glucose and lactate meters (Nova Biomedical) from a drop of blood obtained through the tail vein. Mice were run on the treadmill set to a fixed incline of 15° until exhaustion using the following speed protocol: 5 m/min for 1 min, 10 m/min for 2 min, then 2 min intervals of the following speeds (m/min): 10, 14, 18, 22, 26, 28, 30, 32, 34, 36, 38, 40. Mice were run in multiple groups beginning at 9:30 AM. A mouse was considered exhausted when it remained on the shock grid for 5 continuous seconds and, after being blown by one puff of air at 5 sec, still didn't move back to treadmill within 2 sec of the air puff. Immediately after finishing the run, blood glucose and lactate levels were measured (**Table 1**). Within 5 min of finishing the run, mice were anesthetized with isoflurane, euthanized with cervical dislocation, and the following tissues were collected: blood from the retro-orbital sinus via heparin-coated capillary tubes (Fisher 22-362-566), soleus, plantaris, and gastrocnemius muscles, visceral (epididymal) and subcutaneous (inguinal) white adipose tissue, and liver. Separated serum and tissues were flash frozen in liquid nitrogen, and all samples were stored at -80°C until analysis.

Endurance exercise: Baseline blood glucose and lactate levels were measured and then mice were run on the treadmill at a fixed incline of 10° until exhaustion using the following speed protocol: 10 m/min for 30 min, then an increase of 2 m/min every 15 min thereafter. Mice were

run in multiple groups beginning at 9:30 AM. Mice were considered exhausted using the same criteria as detailed above. After measuring post-run glucose and lactate values (**Table 1**), mice were euthanized within 5 min of finishing the run and tissues were collected in the same manner as described above.

	Body weight (g)	Pre-exercise Glucose (mg/dL)	Pre-exercise Lactate (mM)	Total run Time (min)	Total run distance (m)	Post-exercise Glucose (mg/dL)	Post-exercise Lactate (mM)
Sprint	25.7 ± 0.6	186 ± 6	2.0 ± 0.3	11 ± 1	156 ± 20	199 ± 9	11.0 ± 0.6
Endurance run	26.6 ± 0.6	176 ± 5	3.0 ± 0.4	72 ± 5	912 ± 85	210 ± 6	5.5 ± 0.3
Voluntary wheel running	25.7 ± 0.5	183 ± 5	--				
Sedentary	25.3 ± 0.4	193 ± 6	2.3 ± 0.2				

Table 1. Body weight, total run time and distance, and pre- and post-exercise blood glucose and lactate levels. All values shown as average ± S.E. N=10 mice per group.

Voluntary exercise: At 10 weeks of age, mice were separated into individual cages and a running wheel (Columbus Instrument) was placed in each cage such that mice had free access to it. This represents a form of chronic exercise. After one week, mice were sacrificed and tissues were collected as described above. Running wheels were left in the cages until the time of sacrifice (10:30 AM).

Sedentary control: At 10 weeks of age, mice that were normally housed in the cage (with no running wheel) were sacrificed and tissues were collected as described above. Mice were sacrificed at 10:00 AM.

Throughout the study, all mice were treated in the exact same manner, with the exception of the exercise itself, to facilitate accurate analysis by minimizing any potential confounding factors.

Muscle lysate preparation

One plantaris and one soleus muscle from each mouse was used. Muscles were lysed in 500 μL PBS supplemented with protease inhibitor cocktail (Sigma). First, muscles were homogenized with a 1 mL glass dounce homogenizer (Wheaton), using the loose pestle followed by the tight pestle. Subsequently, the suspension was subjected to sonication to complete the tissue lysis (Branson Sonifier 150; 5-10 s at the lowest setting). Homogenates were centrifuged at 12,000 x *g* for 20 min at 4°C and the supernatant was transferred to a new tube. Total protein content in the supernatant was quantified with a Bradford protein assay (Sigma), and the cleared lysate was stored at -80°C until analysis.

Multiplex assays for measuring cytokine protein level

Multiplex assays for 66 mouse cytokines (covering the majority of the well-studied cytokines) were performed using a Luminex bead-based multiplex system according to manufacturer's protocol (EMD Millipore, Billerica, MA). This method is sensitive and reproducible (39, 40) and has been validated in multiple studies (27, 41). The following 4 assay kits (covering 66 analytes according to their dynamic range) from Millipore were used to measure the concentrations of cytokines in mouse serum, soleus homogenate, and plantaris homogenate: MCYTOMAG-70K, MECY2MAG-73K, MSCRMAG-42K, and MTH17MAG-47K. IFN-γ protein levels in soleus and plantaris were measured with the kit MCYTOMAG-70K. However, IFN-γ levels in serum were measured using a more sensitive assay kit MECY2MAG-73K. Many cytokine receptors are known to be proteolytic cleaved and the soluble ligand-binding ectodomain circulates in plasma (42). Thus, secreted sCD30, sIL-1RI, sIL-1RII, sIL-2Ra, sIL-4R, sIL-6R, sTNFRI, sTNFRII, sVEGFR1, sVEGFR2, sVEGFR3, sgp130, and sRAGE were also measured as

part of the 66 cytokines profiled. The experiments were set up according to the manufacturer's protocol and the assays were performed as we have previously described (43). In brief, standards were provided for each mouse cytokine, from which standard curves were generated. Serum was diluted according to the manufacturer's protocol and cleared muscle lysates were assayed undiluted. For soleus lysates, an average of 18.05 ± 6.79 pg protein was added per well, and for plantaris lysates, an average of 38.84 ± 10.43 pg protein was added per well. All samples (n=10 mice per group) and standards were analyzed using a Luminex 200 instrument (Luminex, Austin, TX) and XPonent 3.1 Software (Millipore, Billerica, MA). Concentrations were determined for each of the 66 mouse cytokines relative to an appropriate 6-point regression standard curve in which the mean fluorescence for each cytokine standard was transformed into known concentrations (pg/mL or ng/mL). For muscle lysates, cytokine concentrations were normalized to total protein before further analysis. The multiplex assays were carried out on three separate occasions, each time with different samples: 1) pre- and post- exercise serum from sprint and endurance mice, 2) pre- and post- exercise serum from voluntary running mice, and 3) all muscle lysates from all 4 exercise regimes. All samples that were used for direct comparison or normalization were run on the same plate.

QuantiGene Plex assay (QGP) for measuring cytokine mRNA level

QuantiGene Plex assays enable simultaneous quantification of up to 80 genes of interest in a single well of a 96-well plate. This method is hybridization-based and incorporates branched DNA (bDNA) technology (44, 45). Because it relies on signal amplification rather than target amplification for direct measurement of RNA transcripts, no RNA isolation and reverse transcription is needed. QuantiGene assay has comparable or better linear range and relative

accuracy when compared to standard real-time PCR method (46). All Gene-specific QuantiGene probes were validated and provided by Thermo Fisher Scientific. Soleus and plantaris muscle fibers harvested from mice were weighed, and placed on dry ice until ready to process. 5-15 mg of tissue was used in sample preparation. Tissues were lysed in 300 µL of homogenizing solution (QGP Assay Kit, Thermo Fisher Scientific, Waltham, MA) per 10 mg tissue, using an MP24 fastprep (MP Biomedicals, Santa Ana, CA) with MP lysing matrix A tubes (Cat #6910-100, MP Biomedicals). Tissue homogenates were heated at 65°C for 1 h, with vortexing every 10 min. Heated samples were centrifuged at room temperature for 15 min at 16,000 x *g* to sediment the matrix, and the supernatant was transferred to clean microcentrifuge tubes. The supernatant was clarified by repeating the above centrifugation step, and the resultant supernatant transferred to another clean microcentrifuge tube. Supernatants were added directly to the QGP hybridization plate following the addition of master mix prepared according to manufacturer's instructions. The hybridization plate was incubated overnight at 57°C with shaking at 600 rpm. The next day, the plate was processed according to manufacturer's instructions, and read on a Luminex 200 instrument (Luminex, Austin, TX). Data was analyzed and fold change calculated according to manufacturer's instructions, using *Hprt* and *Actb* as reference genes. Statistical analyses were performed using a one-way ANOVA with Dunnett's post-test with the sedentary group as the control.

Quantitative real-time PCR analysis

Total RNA was isolated from liver, visceral (epididymal) and subcutaneous (inguinal) white adipose tissues using Trizol® (Life Technologies). Random primers and GoScript reverse transcriptase (Promega) were used to generate cDNA. Quantitative real-time PCR analyses were

performed on CFX Connect Real-Time system (Bio-Rad) using iTaq Universal SYBR Green Supermix (Bio-Rad). The data were normalized to 36B4 (also known as acidic ribosomal phosphoprotein P0 (RPLP0)) to generate a ΔCt value, and then a ΔΔCt was obtained by normalizing the data to the mean ΔCt of the control group (47). 36B4 gene was selected for normalization because it had the least variation across tissue samples. All primers used for real-time PCR analyses are listed in **Table 2**.

Gene	Forward primer	Reverse primer
CXCL1 (KC)	CTGGGATTCACCTCAAGAACATC	CAGGGTCAAGGCAAGCCTC
EPO	ACTCTCCTTGCTACTGATTCCT	ATCGTGACATTTTCTGCCTCC
IL-20	TCTTGCCTTTGGACTGTTCTCC	GTTTGCAGTAATCACACAGCTTC
IL-17a	TTTAACTCCCTTGGCGCAAAA	CTTTCCCTCCGCATTGACAC
IL-17f	TGCTACTGTTGATGTTGGGAC	AATGCCCTGGTTTTGGTTGAA
sgp130 (IL-6ST)	CCGTGTGGTTACATCTACCCT	CGTGGTTCTGTTGATGACAGTG
IL-16	AAGAGCCGGAAATCCACGAAA	GTCTCAAAAGGGTCAGGGTACT
CCL17 (TARC)	GACGACAGAAGGGTACGGC	GCATCTGAAGTGACCTCATGGTA
IFN-γ	ATGAACGCTACACACTGCATC	CCATCCTTTTGCCAGTTCCTC
CX3CL1 (Fractalkine)	ACGAAATGCGAAATCATGTGC	CTGTGTCGTCTCCAGGACAA
TIMP-1	GCAACTCGGACCTGGTCATAA	CGGCCCGTGATGAGAAACT
IL-4R	TCTGCATCCCGTTGTTTTGC	GCACCTGTGCATCCTGAATG
TNF-RII	ACACCCTACAAACCGGAACC	AGCCTTCCTGTCATAGTATTCCT
CXCL10 (IP10)	CCAAGTGCTGCCGTCATTTTC	GGCTCGCAGGGATGATTTCAA
TNF-RI	CCGGGAGAAGAGGGATAGCTT	TCGGACAGTCACTCACCAAGT
G-CSF	ATGGCTCAACTTTCTGCCCAG	CTGACAGTGACCAGGGGAAC
CCL12 (MCP-5)	ATTTCCACACTTCTATGCCTCCT	ATCCAGTATGGTCCTGAAGATCA
CCL20 (MIP-3a)	GCCTCTCGTACATACAGACGC	CCAGTTCTGCTTTGGATCAGC
36B4	AGATTCGGGATATGCTGTTGGC	TCGGGTCCTAGACCAGTGTTC

Table 2. Quantitative real-time PCR primers used in the study

Confirmatory experiment with a second cohort of mice

A second independent cohort of endurance and sedentary mice was used to confirm some of the findings obtained from the multiplex assays. As before, 8 week-old C57BL/6J mice were

purchased from Jackson Labs for the experiments with N=10 per group. However, data for the endurance group reflects N=6 because 2 mice refused to run despite being adequately acclimated to the treadmill and 2 mice were running when the treadmill experienced technical issues so had to be taken out of the study. The experiments were conducted exactly as described previously with the exception of timing of the pre-exercise blood draws. Given that a large volume of serum was needed to satisfy the volume requirements for multiple ELISAs, blood was drawn on two separate occasions before the exercise experiment: once 3 weeks before the endurance run and once 2 weeks before the run. Serum from both blood draws was combined before it was assayed. Mice were allowed to recover for two full weeks after the last pre-exercise blood draw as opposed to the one week of recovery with the first cohort. Thus, the mice in this second cohort were approximately 2 weeks older and a few grams heavier than their counterparts in the first cohort on the day of the experiment. Otherwise, all data including time to exhaustion, blood glucose, and blood lactate levels matched very well between the two cohorts. Soleus and plantaris lysates were prepared as described except both muscles were used and the volume of buffer was reduced to 350 μL. These changes were implemented to increase the signal in the ELISAs.

The following cytokines were measured via ELISA in the pre- and post- exercise serum from the endurance group and soleus and plantaris lysates from all endurance and sedentary mice: MCP-5, KC, MIP-2, MIP-3, IFNγ, and sTNFRI. ELISAs for all targets were purchased from R&D Systems with the exception of sTNFRI, which was purchased from Thermo Scientific. Assays were carried out according to the manufacturer's protocol. Muscle lysates were assayed undiluted, and cytokine concentrations in these samples were first normalized to total protein before further analysis.

Data analysis

For a given analyte, not all samples were successfully detected in the multiplex analysis. Data for a given analyte was analyzed when analyte levels were detected in at least 3 out of the 10 samples. To enable paired t-test analysis (where $N \geq 3$), serum analyte levels must be detected in both pre- and post-exercise samples from the same mouse. It should be noted that the vast majority (~90%) of statistically significant data were obtained from sample size N=9-10. For statistical analysis, a paired t-test was used to analyze pre-exercise versus post-exercise serum data. The nonparametric Wilcoxon matched pairs test was used to analyze data in which the differences (post minus pre) were not Gaussian. Lysate data were analyzed by 1-way-ANOVA. The means from each exercise condition were compared to that from the sedentary condition using Dunnett's post-test. $P < 0.05$ was considered significant. All data is reported as mean ± SEM. Data was analyzed using Graph Pad Prism 7 software. For each data set, false discovery rate analysis was also performed with GraphPad Prism 7 using the recommended two-stage step-up method of Benjamini, Krieger and Yekutieli. The false discovery rate (Q) was set to 5%.

RESULTS

Using multiplex technology to measure cytokine levels

Three exercise paradigms—sprint, endurance exercise, and voluntary wheel running—representing an acute and chronic forms of physical activity, were used in the present study to assess changes in circulating serum cytokines, as well as their protein levels in glycolytic (plantaris) and oxidative (soleus) muscles. A bead-based multiplex profiling method was used to quantify 66 cytokines in both serum and muscle lysates. We could reliably detect and measure up to 52 cytokines from among the 66 cytokines profiled (**Tables 3 and 4**). This is not surprising

Table 3

Serum cytokine

Analyte	Sprint		Endurance		1-week wheel running	
	Pre-exercise (pg/mL)	Post-exercise (pg/mL)	Pre-exercise (pg/mL)	Post-exercise (pg/mL)	Pre-exercise (pg/mL)	Post-exercise (pg/mL)
G-CSF	290 ± 26	341 ± 73	343 ± 69	250 ± 33	3244 ± 457	**787 ± 149** ***
Eotaxin-1/CCL11	1265 ± 171	1526 ± 233	1417 ± 261	1654 ± 216	1344 ± 378	1475 ± 342
GM-CSF	77 ± 32	52 ± 10	--	30 ± 9	48 ± 11	69 ± 30
IFN-β1	--	--	--	--	--	--
IFN-γ	491 ± 50	**337 ± 49** **	472 ± 37	**285 ± 36** ***	367 ± 54	**113 ± 10** **
IL-1α	111 ± 15	125 ± 12	125 ± 25	122 ± 22	148 ± 27	247 ± 84
IL-1β	37 ± 15	20 ± 7	21 ± 5	37 ± 14	--	23 ± 6
IL-2	--	--	--	--	8 ± 1	6 ± 3
IL-3	--	--	--	--	--	--
IL-4	--	--	--	--	--	--
IL-5	13 ± 2	9 ± 1		15 ± 3	11 ± 1	11 ± 2
IL-6	15 ± 4	30 ± 11	11 ± 2	9 ± 0	56 ± 10	**15 ± 3** *
IL-7	13 ± 2				5 ± 1	6 ± 1
IL-9	377 ± 131	443 ± 308	669 ± 549	501 ± 155	229 ± 45	272 ± 40
IL-10	13 ± 3	10 ± 2	--	--	4 ± 1	9 ± 4
IL-11	304 ± 49	274 ± 21	416 ± 40	476 ± 115	--	--
IL-12 (p40)	15 ± 3	17 ± 2	10 ± 1	14 ± 3	15 ± 5	15 ± 4
IL-12 (p70)		20 ± 5		26 ± 9	12 ± 5	17 ± 6
IL-13	36 ± 4	42 ± 1	32 ± 0	40 ± 4	11 ± 2	10 ± 2
IL-15	33 ± 17	42 ± 17	64 ± 51	78 ± 26	63 ± 27	100 ± 36
IL-16	3525 ± 311	**2590 ± 431** *	4062 ± 338	**2321 ± 186** ***	4761 ± 747	**1509 ± 147** **
IL-17A	--	--	--	--	--	--
IL-17A/F	1922 ± 77	**1567 ± 73** *	1919 ± 126	1828 ± 295	286 ± 39	203 ± 15
IL-17F	--	--	--		10 ± 5	14 ± 8
IL-20	1431 ± 187	**2183 ± 343** *	1568 ± 220	2427 ± 446	434 ± 91	359 ± 76
IL-21	--	--	--	--	--	--
IL-22	7 ± 3	53 ± 49	9 ± 2	10 ± 2	15 ± 5	9 ± 2
IL-23	388 ± 66	884 ± 212	410 ± 53	762 ± 106	735 ± 91	352 ± 61
IL-27	1212 ± 186	1311 ± 137	920 ± 120	1110 ± 72	1307 ± 307	1201 ± 102
IL-28B	--	17104 ± 9808	--	--	--	119 ± 22
IL-33	--	2062 ± 2016	--	98 ± 31	--	--
IP-10/CXCL10	159 ± 9	154 ± 19	172 ± 13	**109 ± 19** *	246 ± 19	229 ± 7
KC/CXCL1	125 ± 25	**309 ± 78** *	143 ± 27	**284 ± 30** **	619 ± 110	**392 ± 52** *
LIF	--	--	--	--	--	--
LIX/CXCL5	5100 ± 1955	4250 ± 1027	3935 ± 1499	4771 ± 1302	717 ± 224	2998 ± 1013
MCP-1/CCL2	102 ± 25	102 ± 13	61 ± 8	77 ± 7	27 ± 6	49 ± 9
M-CSF	21 ± 7	35 ± 10		23 ± 9	14 ± 3	14 ± 4
MIG/CXCL9	171 ± 13	208 ± 17	188 ± 22	172 ± 17	136 ± 14	151 ± 20
MIP-1α/CCL3	74 ± 11	90 ± 7	68 ± 5	85 ± 16	40 ± 11	51 ± 14
MIP-1β/CCL4	41 ± 6	38 ± 4	35 ± 0	36 ± 13	46 ± 5	37 ± 4
MIP-2/CXCL2	199 ± 32	215 ± 21	124 ± 13	**169 ± 15** *	206 ± 56	270 ± 28
RANTES/CCL5	24 ± 4	26 ± 3	17 ± 2	19 ± 2	16 ± 2	16 ± 3

Table 3 - continued

Serum cytokine

Analyte	Sprint		Endurance		1-week wheel running	
	Pre-exercise (pg/mL)	Post-exercise (pg/mL)	Pre-exercise (pg/mL)	Post-exercise (pg/mL)	Pre-exercise (pg/mL)	Post-exercise (pg/mL)
TNF-α	9 ± 0	11 ± 2	9 ± 1	14 ± 3	15 ± 4	15 ± 4
VEGF	--	--	--	--	--	--
Exodus-2/CCL21	10433 ± 392	10817 ± 635	11022 ± 379	11095 ± 433	20853 ± 1796	20777 ± 1125
Fractalkine/CX3CL1	2431 ± 92	2607 ± 116	2427 ± 57	**2770 ± 119** *	609 ± 47	730 ± 47
MDC/CCL22	394 ± 46	492 ± 53	496 ± 48	455 ± 40	161 ± 34	136 ± 20
MCP-5/CCL12	416 ± 36	392 ± 33	368 ± 37	**293 ± 31** *	252 ± 36	**160 ± 23** **
MIP-3α/CCL20	269 ± 11	237 ± 9	272 ± 11	**215 ± 10** *	102 ± 6	**74 ± 4** **
MIP-3β/CCL19	687 ± 52	676 ± 71	745 ± 70	776 ± 122	143 ± 29	77 ± 12
TARC/CCL17	327 ± 13	**227 ± 12** ***	359 ± 61	**176 ± 9** **	73 ± 10	56 ± 6
TIMP-1	4641 ± 198	4515 ± 678	4842 ± 222	**2905 ± 52** ***	5184 ± 372	**3313 ± 179** ***
sCD30	--	--	--	--	--	67 ± 0
sgp130	658 ± 69	**430 ± 53** *	527 ± 32	459 ± 43	616 ± 56	649 ± 54
sIL-1RI	1760 ± 298	1679 ± 198	2189 ± 263	1705 ± 210	2914 ± 362	1966 ± 378
sIL-1RII	6343 ± 149	6348 ± 117	6445 ± 153	6685 ± 134	11780 ± 446	11412 ± 281
sIL-2Ra	366 ± 25	376 ± 20	367 ± 14	392 ± 32	467 ± 21	448 ± 26
sIL-4R	2434 ± 477	1851 ± 257	2481 ± 311	**1601 ± 153** **	2859 ± 204	2302 ± 163
sIL-6R	11627 ± 508	10710 ± 437	11691 ± 226	11713 ± 487	19337 ± 639	17804 ± 754
sRAGE	252 ± 63	332 ± 140	347 ± 154	--	--	--
sTNFRI	2786 ± 205	2823 ± 196	3032 ± 252	**2101 ± 139** ***	8200 ± 597	**6461 ± 372** *
sTNFRII	5833 ± 559	5028 ± 292	5851 ± 663	**5156 ± 589** **	9591 ± 572	**7926 ± 288** *
sVEGFR1	997 ± 349	618 ± 100	507 ± 70	507 ± 74	368 ± 79	707 ± 240
sVEGFR2	33031 ± 1833	28423 ± 2901	29170 ± 1504	36032 ± 1903	--	--
sVEGFR3	26831 ± 1438	28009 ± 711	29247 ± 448	29785 ± 888	61281 ± 2402	62438 ± 2043
EPO	1257 ± 98	**1393 ± 82** *	1030 ± 85	1143 ± 73	123 ± 10	100 ± 16
# of cytokine detected	48		45		49	
# of cytokine changed	8		13		10	
% of cytokine changed	17%		29%		20%	

Table 3. Summary of cytokine protein levels in serum in response to sprint, endurance run, or voluntary wheel running for 1 week. All values shown as average ± S.E. Those cytokines that are below the detection limit of the assay are indicated by "--". N=10 mice per group. *p< 0.05; **p<0.01; ***p<0.001.

Table 4

Analyte	Soleus (protein) Sprint/ Sedentary (Fold change)	Soleus (protein) Endurance/ Sedentary (Fold change)	Soleus (protein) Voluntary wheel running/ Sedentary (Fold change)	Plantaris (protein) Sprint/ Sedentary (Fold change)	Plantaris (protein) Endurance/ Sedentary (Fold change)	Plantaris (protein) Voluntary wheel running/ Sedentary (Fold change)
G-CSF	--	--	--	--	--	--
Eotaxin-1/CCL11	1.09 ± 0.08	0.82 ± 0.03	*** **0.57 ± 0.01**	1.10 ± 0.07	0.96 ± 0.10	** **0.64 ± 0.05**
GM-CSF	1.57 ± 0.34	1.35 ± 0.21	--	0.36 ± 0.08	0.43 ± 0.13	0.17 ± 0.03
IFN-β1	--	--	--	--	--	--
IFN-γ	* **1.47 ± 0.12**	* **1.55 ± 0.22**	*** **0.10 ± 0.01**	0.67 ± 0.10	0.97 ± 0.21	** **0.15 ± 0.02**
IL-1α	* **1.23 ± 0.10**	*** **1.40 ± 0.08**	*** **0.20 ± 0.01**	0.83 ± 0.07	1.05 ± 0.18	** **0.31 ± 0.02**
IL-1β	* **1.57 ± 0.17**	*** **1.86 ± 0.18**	1.13 ± 0.03	1.17 ± 0.08	* **1.36 ± 0.10**	0.78 ± 0.05
IL-2	1.21 ± 0.08	* **1.28 ± 0.09**	*** **0.18 ± 0.01**	0.80 ± 0.08	1.02 ± 0.17	** **0.32 ± 0.02**
IL-3	--	--	--	--	--	--
IL-4	1.07 ± 0.13	0.81 ± 0.13	--	0.76 ± 0.09	0.97 ± 0.18	** **0.32 ± 0.02**
IL-5	2.16 ± 0.46	1.14 ± 0.20	0.36 ± 0.06	0.63 ± 0.21	0.49 ± 0.18	0.20 ± 0.10
IL-6	* **1.29 ± 0.10**	** **1.42 ± 0.12**	*** **0.17 ± 0.01**	0.81 ± 0.08	1.06 ± 0.18	*** **0.22 ± 0.01**
IL-7	--	--	--	0.74 ± 0.15	1.48 ± 0.54	--
IL-9	1.13 ± 0.06	*** **1.35 ± 0.07**	*** **0.22 ± 0.02**	0.86 ± 0.08	1.08 ± 0.14	*** **0.19 ± 0.02**
IL-10	* **2.22 ± 0.51**	1.33 ± 0.17	1.08 ± 0.26	0.79 ± 0.14	0.94 ± 0.20	1.24 ± 0.16
IL-11	--	--	--	--	--	--
IL-12 (p40)	** **1.73 ± 0.18**	*** **2.10 ± 0.15**	*** **0.16 ± 0.01**	0.75 ± 0.13	0.86 ± 0.13	*** **0.10 ± 0.01**
IL-12 (p70)	--	--	--	--	--	--
IL-13	--	--	--	0.48 ± 0.11	0.75 ± 0.19	0.21 ± 0.03
IL-15	1.65 ± 0.22	** **2.06 ± 0.21**	* **0.14 ± 0.02**	* **0.56 ± 0.10**	0.76 ± 0.11	*** **0.05 ± 0.01**
IL-16	0.89 ± 0.08	0.71 ± 0.03	*** **1.88 ± 0.18**	1.14 ± 0.08	0.98 ± 0.09	0.90 ± 0.11
IL-17A	--	--	--	0.63 ± 0.10	0.90 ± 0.18	--
IL-17A/F	--	--	--	--	--	--
IL-17F	--	--	--	--	--	--
IL-20	1.23 ± 0.08	1.56 ± 0.13	* **1.70 ± 0.19**	0.71 ± 0.13	1.62 ± 0.54	0.97 ± 0.23
IL-21	--	--	--	--	--	--
IL-22	* **1.51 ± 0.18**	1.35 ± 0.17	** **0.28 ± 0.01**	0.83 ± 0.11	0.71 ± 0.11	*** **0.23 ± 0.01**
IL-23	1.28 ± 0.13	1.22 ± 0.26	--	0.47 ± 0.06	0.53 ± 0.08	--
IL-27	--	--	--	0.77 ± 0.08	0.91 ± 0.17	--
IL-28B	--	--	--	0.65 ± 0.07	0.71 ± 0.11	--
IL-33	1.04 ± 0.11	* **0.61 ± 0.07**	* **0.64 ± 0.06**	1.27 ± 0.17	0.86 ± 0.12	0.62 ± 0.07
IP-10/CXCL10	* **1.58 ± 0.14**	* **1.61 ± 0.19**	1.01 ± 0.13	0.81 ± 0.05	0.96 ± 0.10	*** **0.25 ± 0.05**
KC/CXCL1	1.52 ± 0.11	** **1.72 ± 0.26**	* **0.45 ± 0.02**	0.61 ± 0.0769	1.01 ± 0.17	*** **0.12 ± 0.01**
LIF	--	--	--	--	--	--
LIX/CXCL5	--	--	--	0.49 ± 0.09	0.85 ± 0.21	--
MCP-1/CCL2	1.22 ± 0.16	1.46 ± 0.31	0.96 ± 0.18	1.21 ± 0.19	1.15 ± 0.14	0.91 ± 0.20
M-CSF	1.68 ± 0.32	0.90 ± 0.21	0.34 ± 0.03	0.75 ± 0.07	0.89 ± 0.16	*** **0.24 ± 0.01**
MIG/CXCL9	1.51 ± 0.09	1.56 ± 0.21	1.35 ± 0.27	1.06 ± 0.06	1.01 ± 0.08	*** **0.39 ± 0.07**
MIP-1α/CCL3	1.45 ± 0.16	1.54 ± 0.14	1.18 ± 0.06	1.22 ± 0.09	*** **1.51 ± 0.10**	** **0.60 ± 0.07**
MIP-1β/CCL4	--	--	--	--	--	--
MIP-2/CXCL2	1.58 ± 0.29	*** **2.89 ± 0.39**	1.30 ± 0.18	0.45 ± 0.12	0.82 ± 0.26	0.18 ± 0.05
RANTES/CCL5	* **1.46 ± 0.15**	* **1.49 ± 0.18**	*** **0.21 ± 0.01**	0.76 ± 0.10	0.73 ± 0.13	*** **0.19 ± 0.02**

Table 4 - continued

Analyte	Soleus (protein) Sprint/ Sedentary (Fold change)	Soleus (protein) Endurance/ Sedentary (Fold change)	Soleus (protein) Voluntary wheel running/ Sedentary (Fold change)	Plantaris (protein) Sprint/ Sedentary (Fold change)	Plantaris (protein) Endurance/ Sedentary (Fold change)	Plantaris (protein) Voluntary wheel running/ Sedentary (Fold change)
TNF-α	--	--	--	--	--	--
VEGF	** **0.64 ± 0.09**	*** **0.63 ± 0.05**	*** **0.38 ± 0.03**	*** **0.62 ± 0.05**	** **0.70 ± 0.05**	* **0.76 ± 0.07**
Exodus-2/CCL21	0.70 ± 0.12	* **0.54 ± 0.11**	0.69 ± 0.06	1.08 ± 0.07	0.80 ± 0.05	* **0.66 ± 0.11**
Fractalkine/CX3CL1	--	--	** **0.62 ± 0.05**	--	1.09 ± 0.34	--
MDC/CCL22	1.12 ± 0.10	1.16 ± 0.10	0.80 ± 0.06	0.87 ± 0.07	1.04 ± 0.17	0.63 ± 0.11
MCP-5/CCL12	0.61 ± 0.08	* **0.42 ± 0.06**	* **1.51 ± 0.18**	0.73 ± 0.08	0.73 ± 0.15	0.92 ± 0.24
MIP-3α/CCL20	1.11 ± 0.06	* **1.20 ± 0.05**	*** **0.33 ± 0.01**	0.84 ± 0.06	0.90 ± 0.14	*** **0.29 ± 0.03**
MIP-3β/CCL19	1.20 ± 0.16	1.00 ± 0.11	** **1.65 ± 0.14**	0.96 ± 0.09	1.15 ± 0.08	0.86 ± 0.11
TARC/CCL17	--	--	--	--	--	--
TIMP-1	0.76 ± 0.09	0.55 ± 0.06	*** **4.16 ± 0.67**	0.87 ± 0.11	0.78 ± 0.13	* **3.01 ± 1.01**
sCD30	0.95 ± 0.05	0.82 ± 0.07		0.77 ± 0.03	0.88 ± 0.13	0.83 ± 0.26
sgp130	1.09 ± 0.11	1.34 ± 0.11	* **0.60 ± 0.09**	1.39 ± 0.11	1.64 ± 0.25	2.02 ± 1.12
sIL-1RI	1.10 ± 0.09	1.14 ± 0.04	*** **0.57 ± 0.03**	0.86 ± 0.06	1.03 ± 0.07	** **0.66 ± 0.06**
sIL-1RII	1.04 ± 0.10	0.78 ± 0.05	0.78 ± 0.06	* **1.65 ± 0.33**	1.19 ± 0.08	0.82 ± 0.11
sIL-2Ra	--	--	--	--	--	--
sIL-4R	--	--	--	--	--	--
sIL-6R	1.08 ± 0.17	0.80 ± 0.10	0.94 ± 0.07	** **2.10 ± 0.41**	1.48 ± 0.14	0.69 ± 0.07
sRAGE	1.19 ± 0.10	1.28 ± 0.14	*** **0.17 ± 0.01**	0.73 ± 0.06	0.82 ± 0.13	*** **0.16 ± 0.06**
sTNFRI	0.87 ± 0.06	** **0.73 ± 0.06**	0.82 ± 0.05	1.10 ± 0.07	1.07 ± 0.05	0.82 ± 0.14
sTNFRII	0.89 ± 0.06	0.70 ± 0.05	*** **1.66 ± 0.13**	1.11 ± 0.07	1.08 ± 0.06	1.05 ± 0.14
sVEGFR1	1.05 ± 0.06	* **0.79 ± 0.03**	*** **0.64 ± 0.03**	1.23 ± 0.12	1.32 ± 0.09	0.71 ± 0.07
sVEGFR2	* **0.84 ± 0.04**	*** **0.61 ± 0.03**	* **0.83 ± 0.04**	0.91 ± 0.05	0.79 ± 0.06	0.88 ± 0.10
sVEGFR3	0.89 ± 0.11	0.90 ± 0.07	0.88 ± 0.04	1.52 ± 0.10	1.49 ± 0.15	1.46 ± 0.37
EPO	1.24 ± 0.10	* **1.40 ± 0.09**	--	0.63 ± 0.08	0.90 ± 0.17	--
# of cytokines detected	45	45	42	51	52	44
# of cytokines changed	11	21	26	4	3	22
% of cytokines changed	24%	47%	62%	8%	6%	50%

Table 4. Summary of cytokine protein levels in soleus and plantaris muscles in response to sprint, endurance run, or voluntary wheel running for 1 week. All values are normalized to the control sedentary group and shown as fold change ± S.E. Those cytokines that are below the detection limit of the assay are indicated by "--". N=10 mice per group. *p< 0.05; **p<0.01; ***p<0.001.

given that some cytokines are expressed at very low levels and are only upregulated in the context of immune activation in response to infection. Remarkably, a large fraction of the cytokines

detected were significantly altered by acute and chronic exercise (**Tables 3 and 4**). When adjusted for false discovery, most of the significant changes still remain (**Tables 5-7**). Using a second independent cohort of mice subjected to an endurance run, we confirmed the validity of the multiplex assay using the standard, conventional ELISA method. Of the six chosen targets analysed, three (MCP-5/CCL12, KC/CXCL1, and MIP-2/CXCL2) were significantly different between pre- and post-exercise serum, and the direction of change matched that of the multiplex data (**Fig. 1**). Similarly, three targets were significantly different between sedentary and exercised soleus, and the direction of change matched that of the multiplex data (MCP-5/CCL12, IFN-γ, and sTNFRI). In agreement with the multiplex data, none of the targets (except sTNFRI) were significantly different between sedentary and exercised plantaris as measured by ELISA (**Fig. 1**).

Changes in serum cytokine levels in response to different exercise regimes

In serum, we observed significant changes in eight (17%), thirteen (29%), and ten (20%) circulating cytokines in response to a single bout of sprint, endurance run, and 1-week voluntary wheel running, respectively (**Table 3**). A much greater overlap was seen between a single bout of endurance run and voluntary wheel running (**Fig. 2**). With the exception of CXCL1, the direction of change in serum levels was consistent among all the overlapping cytokines in three of the exercise paradigms. While there was overlap, a single bout of sprint and endurance run also altered different sets of cytokines (**Fig. 2**). Of the serum cytokines altered by acute or chronic exercise, 4 were upregulated and 14 were downregulated.

Table 5

Serum cytokine

Analyte	Sprint		Endurance		1-week wheel running	
	Un-adjusted p-value	Adjusted p-value (FDR)	Un-adjusted p-value	Adjusted p-value (FDR)	Un-adjusted p-value	Adjusted p-value (FDR)
G-CSF	0.5550	0.9079	0.2812	0.4488	**0.0007** ***	**0.0162** *
Eotaxin-1/CCL11	0.6523	0.9197	0.5283	0.7269	0.8043	0.9290
GM-CSF					0.9609	0.9428
IFN-β1						
IFN-γ	**0.0022** **	0.0543	**0.0002** ***	**0.0027****	**0.0039** **	**0.0360** *
IL-1α	0.5432	0.9079	0.9188	0.8866	0.3478	0.5951
IL-1β	0.7188	0.9387	0.8125	0.8531		
IL-2					0.7500	0.9116
IL-3						
IL-4						
IL-5	0.5000	0.9079			0.6250	0.7944
IL-6					**0.0312** *	0.1602
IL-7						
IL-9	0.8750	0.9387	0.8125	0.8531	0.4154	0.6618
IL-10					0.5000	0.7202
IL-11	0.6136	0.9154	0.9531	0.8866		
IL-12 (p40)	0.6307	0.9154	0.2296	0.3983	0.8750	0.9401
IL-12 (p70)					0.3750	0.6188
IL-13	0.5000	0.9079			0.8707	0.9401
IL-15	0.8750	0.9387	0.6250	0.7793	0.9999	0.9428
IL-16	**0.016** *	0.2632	**0.0001** ***	**0.0020** **	**0.0020** **	**0.0308** *
IL-17A						
IL-17A/F	**0.0293** *	0.2755	0.2031	0.3859	0.0550	0.1966
IL-17F					0.5000	0.7202
IL-20	**0.0478** *	0.2949	0.0604	0.1663	0.2329	0.4483
IL-21						
IL-22	0.8750	0.9387	0.9999	0.8866	0.1471	0.3524
IL-23	0.2500	0.7711	0.0625	0.1663	0.0625	0.1966
IL-27	0.5703	0.9079	0.1875	0.3859	0.9999	0.9428
IL-28B						
IL-33						
IP-10/CXCL10	0.8331	0.9387	**0.0469** *	0.1439	0.4331	0.6670
KC/CXCL1	**0.0281** *	0.2755	**0.0016** **	**0.0128** *	**0.0371** *	0.1714
LIF						
LIX/CXCL5	0.9102	0.9557	0.6684	0.8068	0.0568	0.1966
MCP-1/CCL2	0.8438	0.9387	0.1875	0.3859	0.1400	0.3524
M-CSF	0.3750	0.8813			0.9870	0.9428
MIG/CXCL9	0.1866	0.7084	0.3499	0.5171	0.6316	0.7944
MIP-1α/CCL3	0.3350	0.8701	0.2513	0.4178		
MIP-1β/CCL4	0.3750	0.8813	0.9999	0.8866	0.2158	0.4483
MIP-2/CXCL2	0.6134	0.9154	**0.0463** *	0.1439	0.9999	0.9428

Table 5 - continued

Serum cytokine

Analyte	Sprint		Endurance		1-week wheel running	
	Un-adjusted p-value	Adjusted p-value (FDR)	Un-adjusted p-value	Adjusted p-value (FDR)	Un-adjusted p-value	Adjusted p-value (FDR)
RANTES/CCL5	0.6875	0.9387	0.6875	0.8068	0.8566	0.9401
TNF-α	0.5000	0.9079	0.7500	0.8522		
VEGF						
Exodus-2/CCL21	0.5497	0.9079	0.8754	0.8866	0.9731	0.9428
Fractalkine/CX3CL1	0.1825	0.7084	**0.0192 ***	0.0766	0.0681	0.1966
MDC/CCL22	0.1100	0.4935	0.3008	0.4616	0.7695	0.9116
MCP-5/CCL12	0.4405	0.9079	**0.0391 ***	0.1418	**0.0098 ****	0.0755
MIP-3α/CCL20	0.0924	0.4935	**0.0109 ***	**0.0483 ***	**0.0032 ****	**0.0360 ***
MIP-3β/CCL19	0.8609	0.9387	0.7689	0.8522	0.0625	0.1966
TARC/CCL17	**0.0001 *****	**0.0049 ****	**0.0039 ****	**0.0222 ***	0.2324	0.4483
TIMP-1	0.4922	0.9079	**0.0001 *****	**0.0020 ****	**0.0005 *****	**0.0162 ***
sCD30						
sgp130	**0.0426 ***	0.2949	0.2009	0.3859	0.6362	0.7944
sIL-1RI	0.7973	0.9387	0.0930	0.2183	0.1579	0.3524
sIL-1RII	0.9755	1.0000	0.5566	0.7403	0.3439	0.5951
sIL-2Ra	0.7318	0.9387	0.4104	0.5848	0.5144	0.7202
sIL-4R	0.3061	0.8701	**0.0098 ****	**0.0483 ***	0.0656	0.1966
sIL-6R	0.2119	0.7469	0.9668	0.8866	0.1022	0.2777
sRAGE						
sTNFRI	0.8547	0.9387	**0.0005 *****	**0.0050 ****	**0.0119 ***	0.0785
sTNFRII	0.1012	0.4935	**0.0039 ****	**0.0222 ***	**0.0237 ***	0.1369
sVEGFR1	0.3286	0.8701	0.9988	0.8866	0.3125	0.5775
sVEGFR2	0.2428	0.7711	0.0781	0.1948		
sVEGFR3	0.4512	0.9079	0.5798	0.7463	0.5757	0.7823
EPO	**0.0335 ***	0.2755	0.2157	0.3912	0.1602	0.3524

Table 5. Un-adjusted and adjusted (false discovery rate; FDR) p-values for serum cytokines

Table 6

Soleus (protein)

Analyte	Sprint/ Sedentary		Endurance/ Sedentary		Voluntary wheel running/ Sedentary	
	Un-adjusted p-value	Adjusted p-value (FDR)	Un-adjusted p-value	Adjusted p-value (FDR)	Un-adjusted p-value	Adjusted p-value (FDR)
G-CSF						
Eotaxin-1/CCL11	0.5651	0.8798	0.1151	0.1165	**0.0001** ***	**0.0002** ***
GM-CSF	0.3088	0.5577	0.5771	0.4482		
IFN-β1						
IFN-γ	**0.0408** *	0.1962	**0.0134** *	**0.0238** *	**0.0001** ***	**0.0002** ***
IL-1α	**0.0478** *	0.1962	**0.0005** ***	**0.0028** **	**0.0001** ***	**0.0002** ***
IL-1β	**0.0297** *	0.1962	**0.0007** ***	**0.0033** **	0.8656	0.5159
IL-2	0.0656	0.2116	**0.0121** *	**0.0238** *	**0.0001** ***	**0.0002** ***
IL-3						
IL-4	0.9554	0.9833	0.7401	0.5118		
IL-5	0.0574	0.1994	0.9874	0.6299	0.4007	0.2761
IL-6	**0.0441** *	0.1962	**0.0021** **	**0.0072** **	**0.0001** ***	**0.0002** ***
IL-7						
IL-9	0.1663	0.3775	**0.0001** ***	**0.0009** ***	**0.0001** ***	**0.0002** ***
IL-10	**0.0382** *	0.1962	0.8224	0.5551	0.9959	0.5376
IL-11						
IL-12 (p40)	**0.0017** **	**0.0384** *	**0.0001** ***	**0.0009** ***	**0.0005** ***	**0.0007** ***
IL-12 (p70)						
IL-13						
IL-15	0.0703	0.2116	**0.0023** **	**0.0072** **	**0.0270** *	**0.0271** *
IL-16	0.8010	0.9767	0.1337	0.1263	**0.0001** ***	**0.0002** ***
IL-17A						
IL-17A/F						
IL-17F						
IL-20	0.6955	0.9236	0.1014	0.1129	**0.0266** *	**0.0271** *
IL-21						
IL-22	**0.0414** *	0.1962	0.2239	0.2048	**0.0027** **	**0.0035** **
IL-23	0.4408	0.7108	0.6091	0.4544		
IL-27						
IL-28B						
IL-33	0.9867	0.9900	**0.0339** *	**0.0481** *	**0.0451** *	**0.0382** *
IP-10/CXCL10	**0.0171** *	0.1962	**0.0117** *	**0.0238** *	0.9997	0.5376
KC/CXCL1	0.0539	0.1994	**0.0055** **	**0.0156** *	**0.0394** *	**0.0348** *
LIF						
LIX/CXCL5						
MCP-1/CCL2	0.7783	0.9761	0.3025	0.2599	0.9976	0.5376
M-CSF	0.1756	0.3775	0.9884	0.6299	0.1950	0.1433
MIG/CXCL9	0.1754	0.3775	0.1195	0.1168	0.4415	0.2950
MIP-1α/CCL3	0.1255	0.3373	0.0528	0.0680	0.7320	0.4612
MIP-1β/CCL4						
MIP-2/CXCL2	0.4107	0.6868	**0.0003** ***	**0.0021** **	0.8335	0.5105

Table 6 – continued

Soleus (protein)

Analyte	Sprint/ Sedentary		Endurance/ Sedentary		Voluntary wheel running/ Sedentary	
	Un-adjusted p-value	Adjusted p-value (FDR)	Un-adjusted p-value	Adjusted p-value (FDR)	Un-adjusted p-value	Adjusted p-value (FDR)
RANTES/CCL5	**0.0454 ***	0.1962	**0.0325 ***	**0.0481 ***	**0.0004 *****	**0.0006 *****
TNF-α						
VEGF	**0.0012 ****	**0.0384 ***	**0.0009 *****	**0.0036 ****	**0.0001 *****	**0.0002 *****
Exodus-2/CCL21	0.1696	0.3775	**0.0178 ***	**0.028 ***	0.1478	0.1124
Fractalkine/CX3CL1					**0.0043 ****	**0.0053 ****
MDC/CCL22	0.6107	0.9001	0.4004	0.3339	0.2480	0.1764
MCP-5/CCL12	0.1270	0.3373	**0.0143 ***	**0.0238 ***	**0.0370 ***	**0.0348 ***
MIP-3α/CCL20	0.2723	0.5345	**0.0126 ***	**0.0238 ***	**0.0001 *****	**0.0002 *****
MIP-3β/CCL19	0.6213	0.9001	0.9999	0.6299	**0.0051 ****	**0.0059 ****
TARC/CCL17						
TIMP-1	0.9289	0.9833	0.6882	0.5003	**0.0001 *****	**0.0002 *****
sCD30	0.8683	0.9833	0.2715	0.2405		
sgp130	0.9033	0.9833	0.1075	0.1129	**0.0386 ***	**0.0348 ***
sIL-1RI	0.6579	0.9001	0.4672	0.3784	**0.0008 *****	**0.0011 ****
sIL-1RII	0.9583	0.9833	0.0957	0.1129	0.1016	0.0800
sIL-2Ra						
sIL-4R						
sIL-6R	0.9339	0.9833	0.5849	0.4482	0.9665	0.5376
sRAGE	0.3387	0.5882	0.1041	0.1129	**0.0001 *****	**0.0002 *****
sTNFRI	0.3044	0.5577	**0.0066 ****	**0.017 ***	0.0828	0.0676
sTNFRII	0.7341	0.9470	0.0564	0.0695	**0.0001 *****	**0.0002 *****
sVEGFR1	0.8220	0.9767	**0.0139 ***	**0.0238 ***	**0.0001 *****	**0.0002 *****
sVEGFR2	**0.0188 ***	0.1962	**0.0001 *****	**0.0009 *****	**0.0106 ***	**0.0117 ***
sVEGFR3	0.6402	0.9001	0.7103	0.5034	0.5825	0.3778
EPO	0.2547	0.5227	**0.0446 ***	0.0602		

Table 6. Un-adjusted and adjusted (false discovery rate; FDR) p-values for cytokines in soleus muscle

Table 7

Plantaris (protein)

Analyte	Sprint/ Sedentary		Endurance/ Sedentary		Voluntary wheel running/ Sedentary	
	Un-adjusted p-value	Adjusted p-value (FDR)	Un-adjusted p-value	Adjusted p-value (FDR)	Un-adjusted p-value	Adjusted p-value (FDR)
G-CSF						
Eotaxin-1/CCL11	0.6784	0.8957	0.9650	1.0000	**0.0050** **	**0.0066** **
GM-CSF	0.3871	0.7955	0.5189	1.0000	0.2970	0.2414
IFN-β1						
IFN-γ	0.2919	0.7955	0.9988	1.0000	**0.0012** **	**0.0023** **
IL-1α	0.6456	0.8957	0.9869	1.0000	**0.0017** **	**0.0029** **
IL-1β	0.3687	0.7955	**0.0181** *	0.3231	0.1910	0.1656
IL-2	0.5327	0.8740	0.9979	1.0000	**0.0013** **	**0.0023** **
IL-3						
IL-4	0.3977	0.7955	0.9947	1.0000	**0.0019** **	**0.0030** **
IL-5	0.4091	0.7955	0.2137	1.0000	0.0608	0.0638
IL-6	0.5963	0.8957	0.9777	1.0000	**0.0006** ***	**0.0014** **
IL-7	0.8920	0.9784	0.6170	1.0000		
IL-9	0.6094	0.8957	0.8781	1.0000	**0.0001** ***	**0.0004** ***
IL-10	0.7113	0.8957	0.9880	1.0000	0.6462	0.4653
IL-11						
IL-12 (p40)	0.3385	0.7955	0.7491	1.0000	**0.0001** ***	**0.0004** ***
IL-12 (p70)						
IL-13	0.3068	0.7955	0.7279	1.0000	0.1020	0.1028
IL-15	**0.0374** *	0.6143	0.3561	1.0000	**0.0002** ***	**0.0006** ***
IL-16	0.6156	0.8957	0.9985	1.0000	0.7976	0.5273
IL-17A	0.2961	0.7955	0.8916	1.0000		
IL-17A/F						
IL-17F						
IL-20	0.9407	1.0000	0.5478	1.0000	0.9999	0.5727
IL-21						
IL-22	0.5315	0.8740	0.1887	1.0000	**0.0001** ***	**0.0004** ***
IL-23	0.1043	0.7955	0.1811	1.0000		
IL-27	0.3590	0.7955	0.8409	1.0000		
IL-28B	0.0782	0.7955	0.2264	1.0000		
IL-33	0.4253	0.7974	0.8678	1.0000	0.1971	0.1656
IP-10/CXCL10	0.2034	0.7955	0.9713	1.0000	**0.0001** ***	**0.0004** ***
KC/CXCL1	0.1453	0.7955	0.9997	1.0000	**0.0004** ***	**0.0010** **
LIF						
LIX/CXCL5	0.2763	0.7955	0.8310	1.0000		
MCP-1/CCL2	0.6894	0.8957	0.8797	1.0000	0.9694	0.5683
M-CSF	0.3396	0.7955	0.8444	1.0000	**0.0003** ***	**0.0008** ***
MIG/CXCL9	0.8945	0.9784	0.9999	1.0000	**0.0001** ***	**0.0004** ***
MIP-1α/CCL3	0.1403	0.7955	**0.0002** ***	**0.0107** *	**0.0031** **	**0.0045** **
MIP-1β/CCL4						
MIP-2/CXCL2	0.2469	0.7955	0.9120	1.0000	0.0575	0.0630

Table 7 – continued

Plantaris (protein)

Analyte	Sprint/ Sedentary		Endurance/ Sedentary		Voluntary wheel running/ Sedentary	
	Un-adjusted p-value	Adjusted p-value (FDR)	Un-adjusted p-value	Adjusted p-value (FDR)	Un-adjusted p-value	Adjusted p-value (FDR)
RANTES/CCL5	0.3809	0.7955	0.2969	1.0000	**0.0010** **	**0.0021** **
TNF-α						
VEGF	**0.0005** ***	**0.0263** *	**0.0057** **	0.1526	**0.0358** *	**0.0410** *
Exodus-2/CCL21	0.8292	0.9464	0.2388	1.0000	**0.0158** *	**0.0199** *
Fractalkine/CX3CL1			0.9999	1.0000		
MDC/CCL22	0.7866	0.9177	0.9897	1.0000	0.1522	0.1370
MCP-5/CCL12	0.4725	0.8554	0.4658	1.0000	0.9679	0.5683
MIP-3α/CCL20	0.5248	0.8740	0.7869	1.0000	**0.0001** ***	**0.0004** ***
MIP-3β/CCL19	0.9822	1.0000	0.6362	1.0000	0.6717	0.4702
TARC/CCL17						
TIMP-1	0.9955	1.0000	0.9809	1.0000	**0.0243** *	**0.0292** *
sCD30	0.6660	0.8957	0.8600	1.0000	0.8342	0.5273
sgp130	0.6167	0.8957	0.2059	1.0000	0.1325	0.1284
sIL-1RI	0.3228	0.7955	0.9762	1.0000	**0.0032** **	**0.0045** **
sIL-1RII	**0.0468** *	0.6143	0.8282	1.0000	0.8370	0.5273
sIL-2Ra						
sIL-4R						
sIL-6R	**0.0048** **	0.1260	0.2630	1.0000	0.6915	0.4710
sRAGE	0.2022	0.7955	0.5269	1.0000	**0.0001** ***	**0.0004** ***
sTNFRI	0.7507	0.8957	0.8913	1.0000	0.3584	0.2737
sTNFRII	0.7392	0.8957	0.8782	1.0000	0.9698	0.5683
sVEGFR1	0.2953	0.7955	0.1043	1.0000	0.1412	0.1318
sVEGFR2	0.7196	0.8957	0.1527	1.0000	0.5676	0.4207
sVEGFR3	0.2636	0.7955	0.3285	1.0000	0.3393	0.2672
EPO	0.1810	0.7955	0.8614	1.0000		

Table 7. Un-adjusted and adjusted (false discovery rate; FDR) p-values for cytokines in plantaris muscle

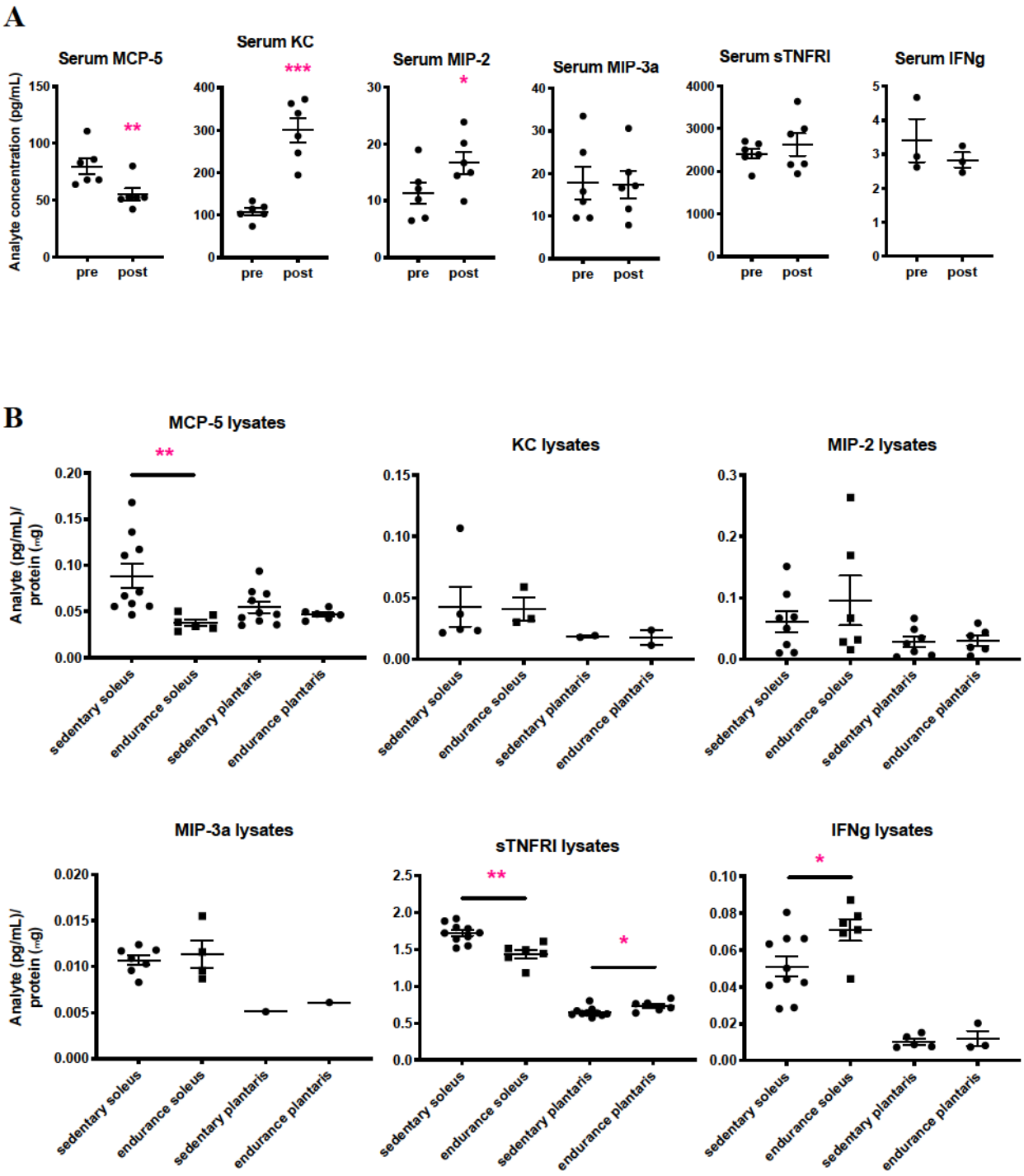

Figure 1. Measurements of six cytokines in a second independent cohort of mice subjected to an endurance run using conventional ELISA method. (A) ELISA quantification of MCP-5/CCL12, MIP-3α/CCL20, KC/CXCL1, MIP-2/CXCL2, IFN-γ, and sTNFRI in pre- and post-exercise serum. (B) ELISA quantification of MCP-5/CCL12, MIP-3α/CCL20, KC/CXCL1, MIP-2/CXCL2, IFN-γ, and sTNFRI in sedentary and exercised soleus and plantaris muscle lysates.

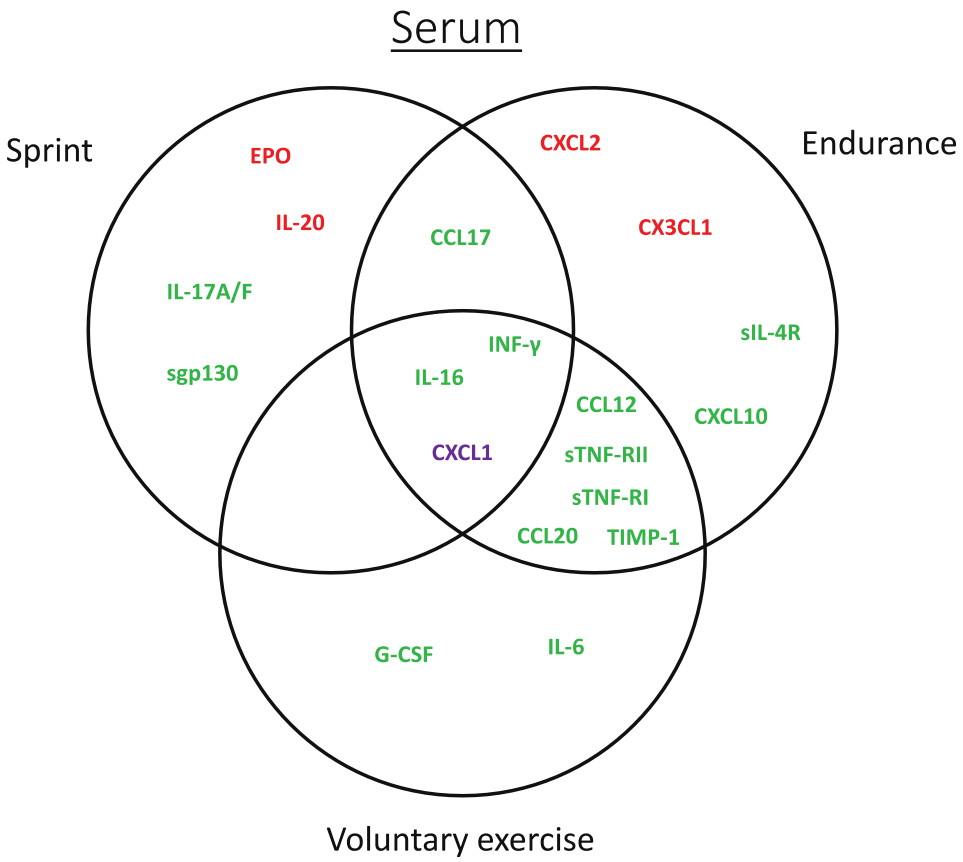

Figure 2. Venn diagram of cytokines altered by sprint, endurance run, or voluntary wheel running in serum. Upregulated cytokines are highlighted in red. Downregulated cytokines are highlighted in green. Cytokines that are upregulated in one exercise paradigm but downregulated in another are highlighted in purple.

Changes in cytokine levels in soleus and plantaris in response to different exercise regimes

In oxidative soleus muscle, an even greater proportion of the detected cytokines was altered by acute and chronic exercise relative to the sedentary control group (**Table 4**). The protein levels of eleven (24%), twenty-one (47%), and twenty-six (62%) cytokines were significantly changed in response to a single bout of sprint, endurance run, and 1-week voluntary wheel running, respectively. Again, we observed a much greater overlap between a single bout of endurance run and 1-week voluntary wheel running (**Fig. 3A**). However, the direction of change (up or downregulated) among the overlapping cytokines was different depending on the types of physical

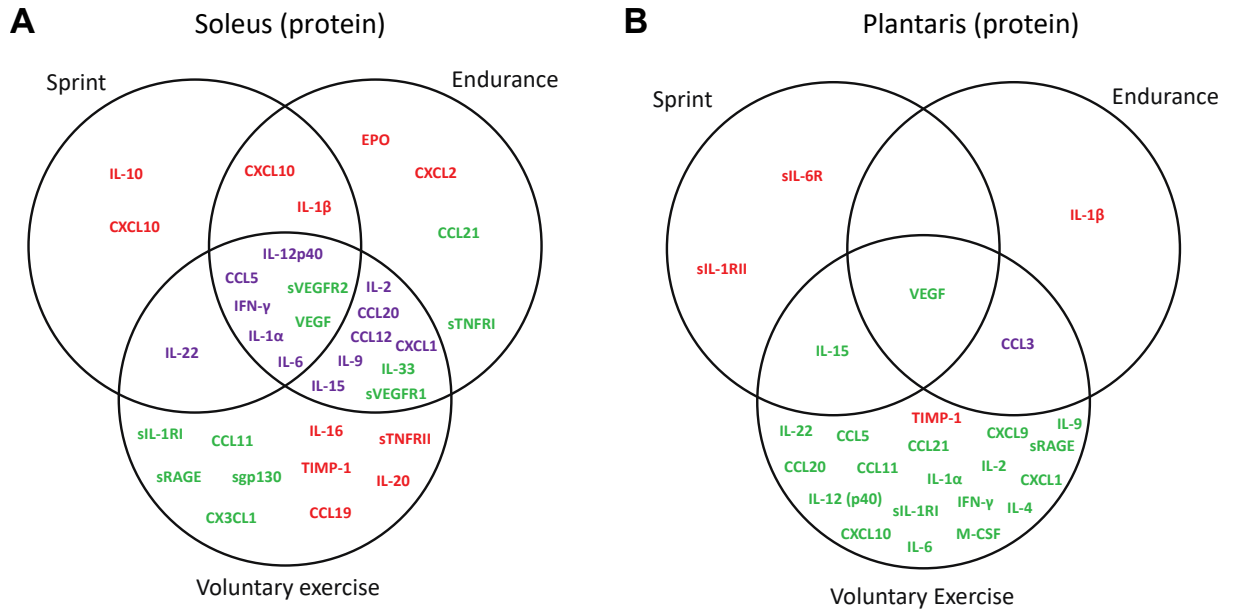

Figure 3. Venn diagram of cytokines altered by sprint, endurance run, or voluntary wheel running in soleus and plantaris muscles. Upregulated cytokines are highlighted in red. Downregulated cytokines are highlighted in green. Cytokines that are upregulated in one exercise paradigm but downregulated in another are highlighted in purple.

activity (**Table 4** and **Fig. 3A**). Despite significant overlap, different types of physical activity clearly altered different sets of cytokines in soleus muscle (**Fig. 3A**). Of the 34 cytokines whose levels changed in soleus muscle by acute or chronic exercise, 11 were upregulated, 11 were downregulated, and 12 were either up or downregulated depending on the types of physical activity.

A very different cytokine profile was seen for the glycolytic (plantaris) muscle when compared to the oxidative (soleus) muscle. Relative to the sedentary control group, the protein levels of four (8%), three (6%), and twenty-two (50%) cytokines were significantly changed in plantaris muscle in response to a single bout of sprint, endurance run, and 1-week voluntary wheel running, respectively (**Table 4**). In striking contrast to the soleus muscle, only 3-4 cytokines were altered by a single bout of sprint or endurance run in the plantaris muscle (**Fig. 3B**). The majority

of the cytokine changes in plantaris were seen in mice subjected to 1-week of voluntary wheel running. Minimal (1-2 cytokines) overlap was observed in plantaris for the three different types of exercise. Of the 25 cytokines altered in plantaris muscle by acute or chronic exercise, 4 were upregulated, 20 were downregulated, and 1 was either up or downregulated depending on the types of physical activity.

Overlap of cytokine changes in serum, soleus, and plantaris in response to each type of exercise

Next, we asked how many of the systemic changes in circulating serum cytokines paralleled the local protein changes in soleus and plantaris. This would help address which among the systemic cytokine changes in blood is directly due to the expression and secretion from skeletal muscle. Surprisingly, for a single bout of sprint, no overlap in cytokine profiles was seen between serum, soleus, and plantaris muscles (**Fig. 4A**). Different sets of cytokines were apparently altered in oxidative (soleus) and glycolytic (plantaris) muscles, with the majority of changes seen in soleus muscle fibers. Combined, a total of 21 cytokines were altered by sprint, with 13 upregulated, 7 downregulated, and 1 with opposite changes between serum and soleus muscle.

For a single bout of endurance run, the majority of the cytokine changes were seen in serum and soleus muscle (**Fig. 4B**). However, no overlap (common to all three) was seen between serum, soleus, and plantaris. Although seven cytokine changes showed overlap between serum and soleus muscle, the direction of change (up or downregulated) was different for three of the cytokines (**Fig. 4B**). Combined, a total of 28 cytokines were altered by a single bout of endurance run, with 13 upregulated, 12 downregulated, and 3 with opposite changes between serum and soleus muscle.

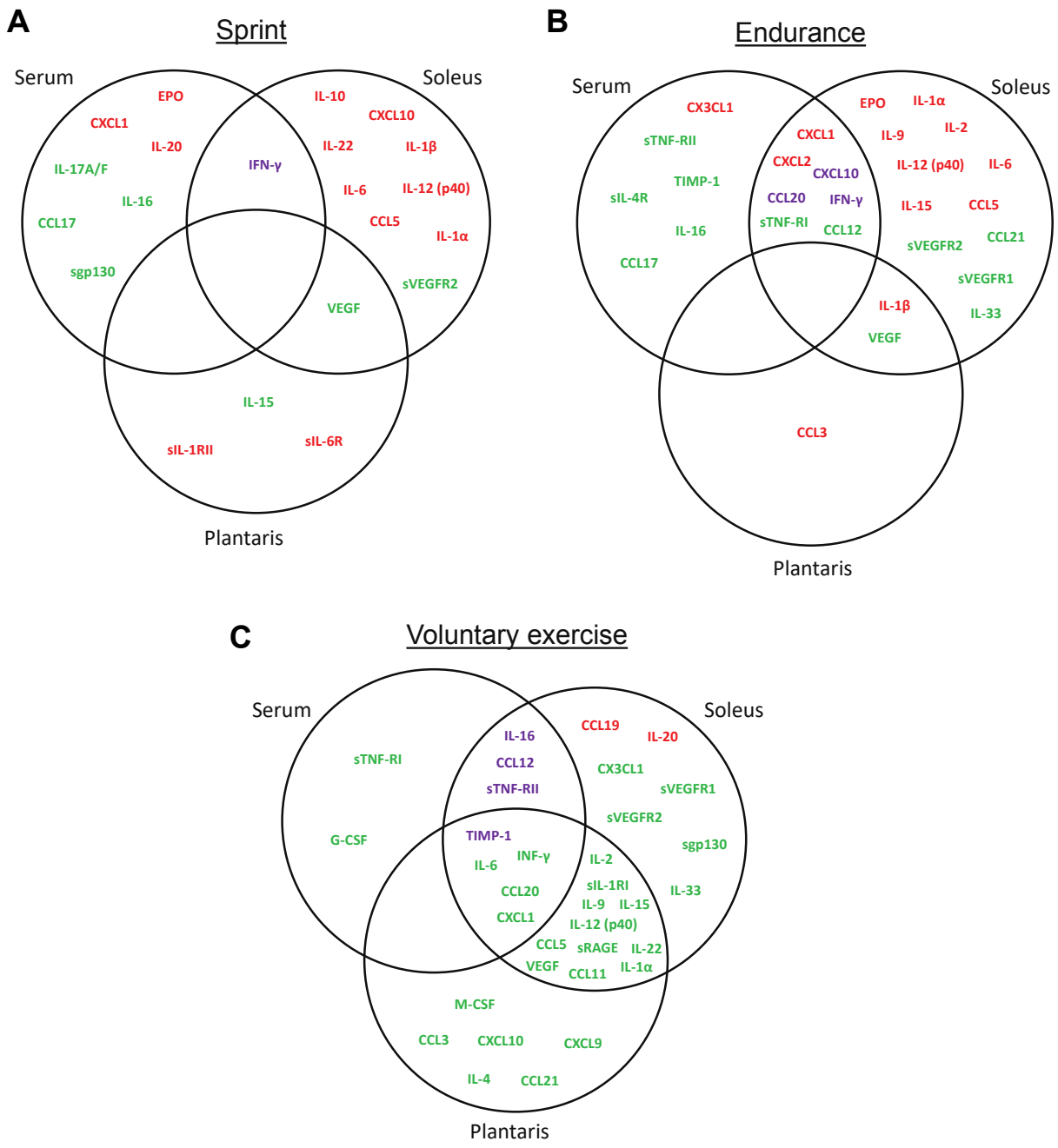

Figure 4. Venn diagram of cytokines altered by sprint, endurance run, or voluntary wheel running in serum and in soleus and plantaris muscles. Upregulated cytokines are highlighted in red. Downregulated cytokines are highlighted in green. Cytokines that are upregulated in one tissue exercise paradigm but downregulated in another are highlighted in purple.

Of the three different types of exercise, the greatest number of cytokines changes were seen in the 1-week voluntary wheel running group relative to the sedentary control group (**Fig. 4C**). Large numbers of cytokine changes showed overlap between serum and soleus or plantaris, as well as between oxidative (soleus) and glycolytic (plantaris) fibers. Interestingly, most of the cytokine changes induced by voluntary wheel running were in the "downregulated" direction (**Fig. 4C**; highlighted in green); in contrast, a large fraction of the cytokine changes seen in sprint and endurance run were in the "upregulated" direction (**Fig. 4A and B**; highlighted in red). Combined, a total of 34 cytokines were altered by 1-week voluntary wheel running, with 2 upregulated, 28 downregulated, 4 with opposite changes between different tissues.

Changes in cytokine mRNA levels in plantaris and soleus in response to different exercise regimes

We next examined changes in cytokine mRNA levels in oxidative (soleus) and glycolytic (plantaris) muscles in response to the three different types of exercise. We used the QuantiGene Plex assays to simultaneously measure the mRNA levels of 63 cytokines (**Tables 8 and 9**). With the exception of CXCL9 transcript, we were able to detect the mRNA of 62 cytokines. Relative to the sedentary control group, the mRNA levels of six (10%), eight (13%), and fourteen (22%) cytokines were significantly changed in soleus in response to sprint, endurance run, and voluntary wheel running, respectively. In plantaris muscle, however, the mRNA levels of five (8%), thirteen (21%), and five (8%) cytokines were significantly changed in response to sprint, endurance, and voluntary wheel running, respectively. Surprisingly, most of the mRNA changes in soleus and plantaris show relatively little overlap between the three types of physical activity (**Fig. 5A and B**). In soleus muscle, 10 cytokine mRNA were upregulated, 7 downregulated, and 3 changed in

Table 8

Accesion #	Gene	Soleus Muscle (mRNA) Sprint/Sedentary (Fold change)	Endurance/sedentary (Fold change)	Voluntary wheel running/sedentary (Fold change)
NM_009971	G-CSF/Csf-3	0.71 ± 0.13	0.45 ± 0.14	0.87 ± 0.18
NM_009969	GM-CSF/Csf-2	1.40 ± 0.18	1.10 ± 0.16	0.92 ± 0.21
NM_010510	IFN-β1	1.50 ± 0.23	1.27 ± 0.19	1.06 ± 0.26
NM_008337	IFN-γ	1.33 ± 0.21	1.25 ± 0.23	0.92 ± 0.20
NM_010554	IL-1α	1.42 ± 0.37	2.18 ± 0.54	0.98 ± 0.15
NM_008361	IL-1β	1.28 ± 0.12	1.02 ± 0.17	1.37 ± 0.13
NM_008366	IL-2	1.40 ± 0.45	2.33 ± 1.3	0.59 ± 0.11
NM_010556	IL-3	1.60 ± 0.19	1.25 ± 0.19	0.98 ± 0.19
NM_021283	IL-4	1.35 ± 0.20	1.05 ± 0.21	0.80 ± 0.19
NM_010558	IL-5	1.34 ± 0.21	1.20 ± 0.20	0.95 ± 0.23
NM_031168	IL-6	1.53 ± 0.25	1.38 ± 0.20	1.28 ± 0.28
NM_008371	IL-7	1.50 ± 0.23	1.29 ± 0.14	0.93 ± 0.20
NM_008373	IL-9	1.22 ± 0.10	1.13 ± 0.13	0.79 ± 0.17
NM_010548	IL-10	1.34 ± 0.19	1.35 ± 0.33	0.95 ± 0.09
NM_008350	IL-11	1.22 ± 0.18	1.03 ± 0.12	0.95 ± 0.16
NM_008352	IL-12 (p40)/ IL-12B	1.47 ± 0.16	1.19 ± 0.18	*** 1.54 ± 0.15**
NM_008351	IL-12 (p70)	1.17 ± 0.16	1.09 ± 0.20	0.96 ± 0.19
NM_008355	IL-13	1.39 ± 0.20	1.35 ± 0.38	0.87 ± 0.18
NM_008357	IL-15	1.07 ± 0.06	0.90 ± 0.07	***** 0.59 ± 0.04**
NM_010551	IL-16	1.05 ± 0.06	**** 0.67 ± 0.04**	0.86 ± 0.06
NM_010552	IL-17A/CTLA8	1.47 ± 0.20	1.26 ± 0.18	1.06 ± 0.24
NM_021380	IL-20	0.99 ± 0.11	*** 0.57 ± 0.13**	**** 0.53 ± 0.10**
NM_021782	IL-21	1.29 ± 0.18	1.06 ± 0.13	0.96 ± 0.22
NM_016971	IL-22	1.52 ± 0.27	1.20 ± 0.19	1.07 ± 0.30
NM_031252	IL-23	1.52 ± 0.27	1.33 ± 0.19	1.03 ± 0.25
NM_145636	IL-27	1.25 ± 0.10	1.07 ± 0.14	0.90 ± 0.11
NM_177396	IL-28B/IFNl3	1.29 ± 0.16	0.94 ± 0.11	0.78 ± 0.17
NM_029594	IL-31	1.45 ± 0.26	1.15 ± 0.15	1.02 ± 0.23
NM_133775	IL-33	1.16 ± 0.08	*** 1.31 ± 0.11**	0.94 ± 0.06
NM_021274	IP-10/CXCL10	1.10 ± 0.17	1.53 ± 0.22	*** 2.57 ± 0.72**
NM_008176	KC/CXCL1	***** 1.74 ± 0.11**	1.36 ± 0.15	0.94 ± 0.10
NM_008501	LIF	1.26 ± 0.18	0.95 ± 0.10	1.00 ± 0.16
NM_009141	LIX/CXCL5	1.68 ± 0.35	1.46 ± 0.21	1.63 ± 0.36
NM_011333	MCP-1/CCL2	1.24 ± 0.11	1.21 ± 0.09	*** 2.59 ± 0.81**
NM_007778	M-CSF/Csf-1	0.97 ± 0.05	****0.67 ± 0.03**	0.81 ± 0.09
NM_008599	MIG/CXCL9	--	--	--
NM_011337	MIP-1α/CCL3	1.45 ± 0.20	1.06 ± 0.17	1.02 ± 0.21
NM_013652	MIP-1β/CCL4	1.25 ± 0.13	1.00 ± 0.17	1.02 ± 0.13
NM_009140	MIP-2/CXCL2	1.56 ± 0.25	1.31 ± 0.21	1.16 ± 0.30
NM_013653	RANTES/CCL5	0.91 ± 0.07	0.71 ± 0.18	***** 2.22 ± 0.30**
NM_013693	TNF-α	1.16 ± 0.21	0.91 ± 0.14	1.09 ± 0.18
NM_001287056	VEGF-A	0.97 ± 0.11	0.85 ± 0.03	*****0.41 ± 0.03**
NM_002989	Exodus-2/CCL21	1.09 ± 0.16	1.20 ± 0.07	0.78 ± 0.10
NM_009142	Fractalkine/CX3CL1	1.03 ± 0.12	0.83 ± 0.08	1.25 ± 0.11
NM_009137	MDC/CCL22	1.34 ± 0.20	1.25 ± 0.31	1.41 ± 0.27
NM_011331	MCP-5/CCL12	1.32 ± 0.21	1.00 ± 0.11	*** 1.64 ± 0.19**
NM_016960	MIP-3α/CCL20	1.36 ± 0.20	1.07 ± 0.12	1.01 ± 0.21

Table 8 – continued

		Soleus Muscle (mRNA)		
Accesion #	Gene	Sprint/Sedentary (Fold change)	Endurance/sedentary (Fold change)	Voluntary wheel running/sedentary (Fold change)
NM_011888	MIP-3β/CCL19	1.23 ± 0.09	1.00 ± 0.15	0.77 ± 0.11
NM_011332	TARC/CCL17	1.38 ± 0.16	1.05 ± 0.13	1.17 ± 0.22
NM_011593	TIMP-1	0.84 ± 0.12	0.75 ± 0.05	***8.37 ± 2.16
NM_009401	CD30/ Tnfrsf8	1.36 ± 0.26	1.39 ± 0.25	1.14 ± 0.28
NM_010560	gp130/ IL-6ST	** 1.13 ± 0.03	* 0.88 ± 0.03	*** 0.64 ± 0.03
NM_008362	IL-1RI	1.08 ± 0.06	1.12 ± 0.03	*** 0.71 ± 0.02
NM_010555	IL-1RII	1.40 ± 0.14	1.27 ± 0.11	0.92 ± 0.13
NM_008367	IL-2Ra	* 1.53 ± 0.14	1.22 ± 0.13	0.68 ± 0.13
NM_001008700	IL-4R	* 1.39 ± 0.14	** 1.48 ± 0.08	1.18 ± 0.12
NM_010559	IL-6R	*1.30 ± 0.10	*1.31 ± 0.07	**0.62 ± 0.06
NM_007425	RAGE / Ager	1.12 ± 0.11	1.13 ± 0.12	1.15 ± 0.13
NM_011609	TNF-RI / Tnfrsf1a	1.16 ± 0.07	0.93 ± 0.03	0.88 ± 0.04
NM_011610	TNF-RII / Tnfrsf1b	1.27 ± 0.12	1.21 ± 0.08	1.26 ± 0.09
NM_010228	VEGFR1 / Flt1	* 1.27 ± 0.09	1.10 ± 0.04	***0.52 ± 0.06
NM_010612	VEGFR2 / Kdr	0.87 ± 0.06	***0.55 ± 0.03	***0.50 ± 0.04
NM_008029	VEGFR3 / Flt4	1.10 ± 0.10	1.13 ± 0.06	0.81 ± 0.07
	# of cytokine changed	6	8	14
	% of cytokine changed	10%	13%	22%

Table 8. Summary of cytokine mRNA levels in soleus muscle in response to sprint, endurance run, or voluntary wheel running for 1 week. All values are normalized to the control sedentary group and shown as fold change ± S.E. Those cytokines whose mRNA that are not detected are indicated by "--". N=10 mice per group. *p< 0.05; **p<0.01; ***p<0.001.

Table 9

		Plantaris Muscle (mRNA)		
Accesion #	Gene	Sprint/Sedentary (Fold change)	Endurance/sedentary (Fold change)	Voluntary wheel running/sedentary (Fold change)
NM_009971	G-CSF/Csf-3	1.10 ± 0.29	--	0.91 ± 0.22
NM_009969	GM-CSF/Csf-2	1.13 ± 0.12	0.72 ± 0.05	0.80 ± 0.08
NM_010510	IFN-β1	1.09 ± 0.16	0.82 ± 0.07	0.87 ± 0.08
NM_008337	IFN-γ	0.93 ± 0.10	0.73 ± 0.06	0.81 ± 0.10
NM_010554	IL-1α	1.37 ± 0.18	0.58 ± 0.05	0.94 ± 0.17
NM_008361	IL-1β	1.14 ± 0.15	0.73 ± 0.07	0.89 ± 0.11
NM_008366	IL-2	1.24 ± 0.30	0.74 ± 0.13	1.24 ± 0.37
NM_010556	IL-3	1.14 ± 0.13	0.97 ± 0.08	0.91 ± 0.21
NM_021283	IL-4	**2.31 ± 0.42	1.37 ± 0.22	1.55 ± 0.24
NM_010558	IL-5	1.00 ± 0.16	0.71 ± 0.07	0.77 ± 0.08
NM_031168	IL-6	0.91 ± 0.10	0.73 ± 0.06	0.81 ± 0.11
NM_008371	IL-7	1.05 ± 0.12	0.94 ± 0.13	0.85 ± 0.10
NM_008373	IL-9	1.32 ± 0.15	0.71 ± 0.07	0.84 ± 0.13
NM_010548	IL-10	1.08 ± 0.08	0.73 ± 0.06	0.82 ± 0.19
NM_008350	IL-11	1.14 ± 0.11	0.89 ± 0.06	0.89 ± 0.08
NM_008352	IL-12 (p40)/ IL-12B	1.24 ± 0.17	0.82 ± 0.06	1.02 ± 0.17
NM_008351	IL-12 (p70)	1.04 ± 0.10	* 0.71 ± 0.06	0.75 ± 0.07
NM_008355	IL-13	1.01 ± 0.13	0.79 ± 0.11	0.87 ± 0.23
NM_008357	IL-15	1.09 ± 0.07	1.04 ± 0.04	1.16 ± 0.05
NM_010551	IL-16	1.10 ± 0.08	0.83 ± 0.15	0.95 ± 0.07
NM_010552	IL-17A/CTLA8	1.00 ± 0.14	0.87 ± 0.06	0.78 ± 0.09
NM_021380	IL-20	0.97 ± 0.07	***0.55 ± 0.06	* 0.75 ± 0.06
NM_021782	IL-21	1.26 ± 0.19	0.81 ± 0.08	0.90 ± 0.12
NM_016971	IL-22	1.12 ± 0.14	0.69 ± 0.07	0.78 ± 0.11
NM_031252	IL-23	0.96 ± 0.12	0.80 ± 0.07	0.82 ± 0.08
NM_145636	IL-27	1.30 ± 0.07	* 0.90 ± 0.08	1.08 ± 0.17
NM_177396	IL-28B/IFNl3	1.08 ± 0.12	0.67 ± 0.05	0.76 ± 0.12
NM_029594	IL-31	0.96 ± 0.14	0.71 ± 0.05	0.73 ± 0.07
NM_133775	IL-33	1.27 ± 0.10	1.29 ± 0.10	0.91 ± 0.08
NM_021274	IP-10/CXCL10	0.72 ± 0.08	0.64 ± 0.15	0.76 ± 0.11
NM_008176	KC/CXCL1	***2.65 ± 0.45	1.45 ± 0.18	0.99 ± 0.12
NM_008501	LIF	0.95 ± 0.07	**0.64 ± 0.04	0.81 ± 0.06
NM_009141	LIX/CXCL5	1.35 ± 0.16	1.02 ± 0.06	1.09 ± 0.13
NM_011333	MCP-1/CCL2	1.21 ± 0.27	1.12 ± 0.18	1.37 ± 0.23
NM_007778	M-CSF/Csf-1	0.96 ± 0.04	***0.58 ± 0.03	0.94 ± 0.06
NM_008599	MIG/CXCL9	--	--	--
NM_011337	MIP-1α/CCL3	0.95 ± 0.12	0.74 ± 0.07	0.78 ± 0.08
NM_013652	MIP-1β/CCL4	1.12 ± 0.15	* 0.62 ± 0.10	0.90 ± 0.06
NM_009140	MIP-2/CXCL2	1.11 ± 0.16	0.90 ± 0.09	0.93 ± 0.10
NM_013653	RANTES/CCL5	0.88 ± 0.14	0.55 ± 0.09	1.18 ± 0.21
NM_013693	TNF-α	1.11 ± 0.16	0.81 ± 0.04	** 1.63 ± 0.17
NM_001287056	VEGF-A	* 0.85 ± 0.06	* 0.87 ± 0.02	***0.76 ± 0.02
NM_002989	Exodus-2/CCL21	1.03 ± 0.06	0.79 ± 0.10	* 0.73 ± 0.07
NM_009142	Fractalkine/CX3CL1	0.93 ± 0.07	** 0.70 ± 0.03	1.01 ± 0.08
NM_009137	MDC/CCL22	1.17 ± 0.15	0.91 ± 0.08	1.31 ± 0.22
NM_011331	MCP-5/CCL12	1.05 ± 0.12	0.74 ± 0.05	0.92 ± 0.09
NM_016960	MIP-3α/CCL20	1.05 ± 0.12	0.76 ± 0.08	0.87 ± 0.09

Table 9 – continued

		Plantaris Muscle (mRNA)		
Accesion #	Gene	Sprint/Sedentary (Fold change)	Endurance/sedentary (Fold change)	Voluntary wheel running/sedentary (Fold change)
NM_011888	MIP-3β/CCL19	1.10 ± 0.10	0.79 ± 0.04	0.77 ± 0.07
NM_011332	TARC/CCL17	1.16 ± 0.14	0.60 ± 0.06	0.83 ± 0.09
NM_011593	TIMP-1	0.88 ± 0.14	*** 0.46 ± 0.05**	*****2.3 ± 0.23**
NM_009401	CD30/ Tnfrsf8	1.04 ± 0.13	0.67 ± 0.04	0.91 ± 0.10
NM_010560	gp130/ IL-6ST	1.05 ± 0.03	**** 0.87 ± 0.02**	0.91 ± 0.03
NM_008362	IL-1RI	1.03 ± 0.05	0.95 ± 0.05	0.95 ± 0.06
NM_010555	IL-1RII	1.05 ± 0.05	0.90 ± 0.07	0.88 ± 0.08
NM_008367	IL-2Ra	*** 1.30 ± 0.11**	1.01 ± 0.05	0.78 ± 0.07
NM_001008700	IL-4R	1.08 ± 0.07	1.14 ± 0.05	0.94 ± 0.05
NM_010559	IL-6R	1.16 ± 0.11	**** 1.37 ± 0.05**	0.87 ± 0.05
NM_007425	RAGE / Ager	1.25 ± 0.10	0.91 ± 0.07	0.96 ± 0.10
NM_011609	TNF-RI / Tnfrsf1a	1.06 ± 0.04	**** 0.86 ± 0.03**	1.04 ± 0.02
NM_011610	TNF-RII / Tnfrsf1b	1.16 ± 0.05	0.95 ± 0.04	1.01 ± 0.04
NM_010228	VEGFR1 / Flt1	1.14 ± 0.08	0.99 ± 0.03	0.84 ± 0.03
NM_010612	VEGFR2 / Kdr	**** 0.77 ± 0.05**	*****0.43 ± 0.02**	0.95 ± 0.04
NM_008029	VEGFR3 / Flt4	1.03 ± 0.05	0.96 ± 0.05	0.98 ± 0.04
	# of cytokine changed	5	13	5
	% of cytokine changed	8%	21%	8%

Table 9. Summary of cytokine mRNA levels in plantaris muscle in response to sprint, endurance run, or voluntary wheel running for 1 week. All values are normalized to the control sedentary group and shown as fold change ± S.E. Those cytokines whose mRNA that are not detected are indicated by "--". N=10 mice per group. *p< 0.05; **p<0.01; ***p<0.001.

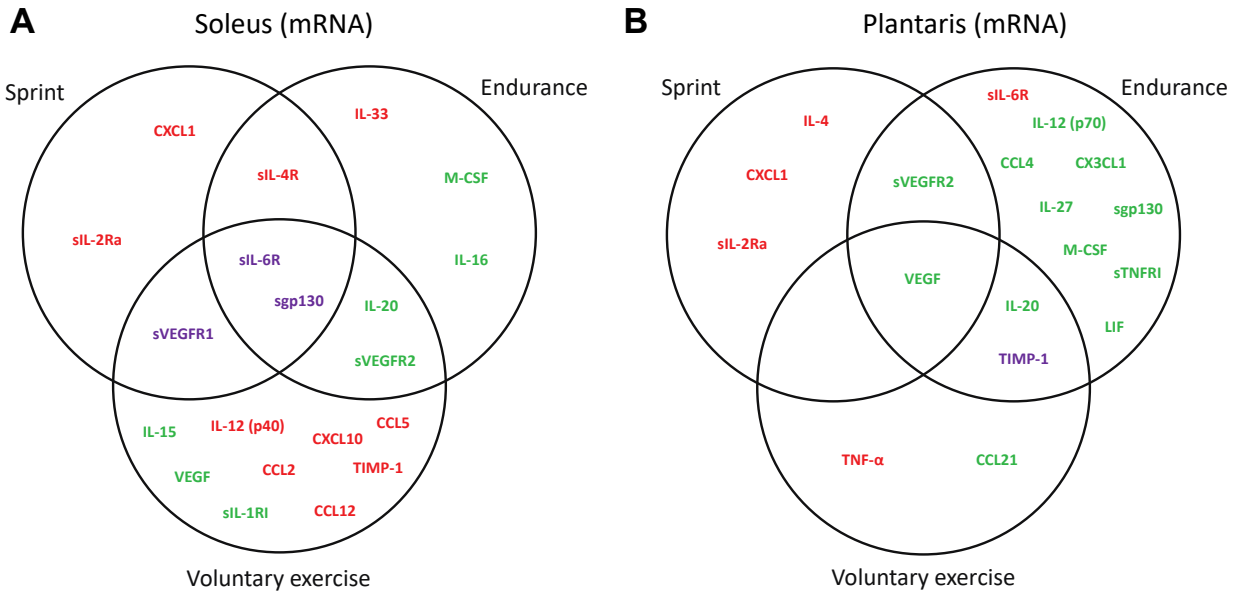

Figure 5. Venn diagram of cytokine mRNA altered by sprint, endurance run, or voluntary wheel running in soleus and plantaris muscles. Upregulated cytokines are highlighted in red. Downregulated cytokines are highlighted in green. Cytokines that are upregulated in one exercise paradigm but downregulated in another are highlighted in purple.

the opposing directions depending on the types of exercise. In plantaris muscle, 5 cytokine mRNA were upregulated, 12 downregulated, and 1 changed in the opposite direction between endurance and chronic wheel running.

Concordance between changes in cytokine mRNA and protein levels in muscle in response to exercise

Next, we addressed the issue of concordance between changes in cytokine mRNA and protein expression in soleus and plantaris muscles. In oxidative (soleus) muscle, parallel reductions in transcript and protein were observed for IL-15, VEGF, sIL1RI, sVEGFR1, sVEGFR2, and sgp130, whereas parallel increases were only observed for CCL12 and TIMP-1. In glycolytic (plantaris) muscle, parallel reductions in transcript and protein were observed for VEGF and

CCL21, whereas a parallel increase was only observed for TIMP-1. Essentially, the majority of the cytokine changes reported here showed discordance between transcript and protein levels (comparing **Tables 4, 8, and 9**).

Expression of cytokines in adipose and liver in response to exercise whose changes in serum were not matched by changes in muscle

Given that the changes in a subset of serum cytokines were not matched by the corresponding changes in their protein levels in muscle, we addressed whether this could be due to secondary adaptive changes in their expression in non-muscle tissues. Acute and chronic exercise can alter systemic metabolism in response to energetic demands, and we have previously shown that different metabolic states alters circulating cytokine levels (43). Thus, we determined the expression of cytokine transcripts in liver and two major fat depots (visceral and subcutaneous white adipose tissues), major metabolic organs known to produce and secrete a wide array of cytokines and chemokines in response to different physiological stimuli. We focused our analyses only on those cytokines whose altered serum levels were not accounted for by changes in protein levels in skeletal muscle in response to exercise. As shown in **Fig. 6**, depending on the types of exercise, expression of cytokine transcripts could be either up- or down-regulated in the liver and/or adipose tissues. With a couple exceptions, most of these changes in mRNA paralleled the

Figure 6. Quantitative real-time PCR analysis of select cytokine transcripts in liver and adipose tissues in response to acute and chronic exercise. Relative mRNA expression of different cytokines in liver, visceral (epididymal) and subcutaneous (inguinal) fat depots. We only focus our analysis on those cytokines whose altered circulating levels were not matched by the corresponding changes in protein levels in skeletal muscle. All mRNA expression values were normalized to 36B4. These values were then normalized to the sedentary condition and the data are shown as average $\pm$ S.E. All *p*-values were calculated using an unpaired *t*-test with Welch's correction (comparing the exercise condition to the sedentary condition). *< 0.05; ** $p < 0.01$; *** $p < 0.001$. **(figure on the following page)**

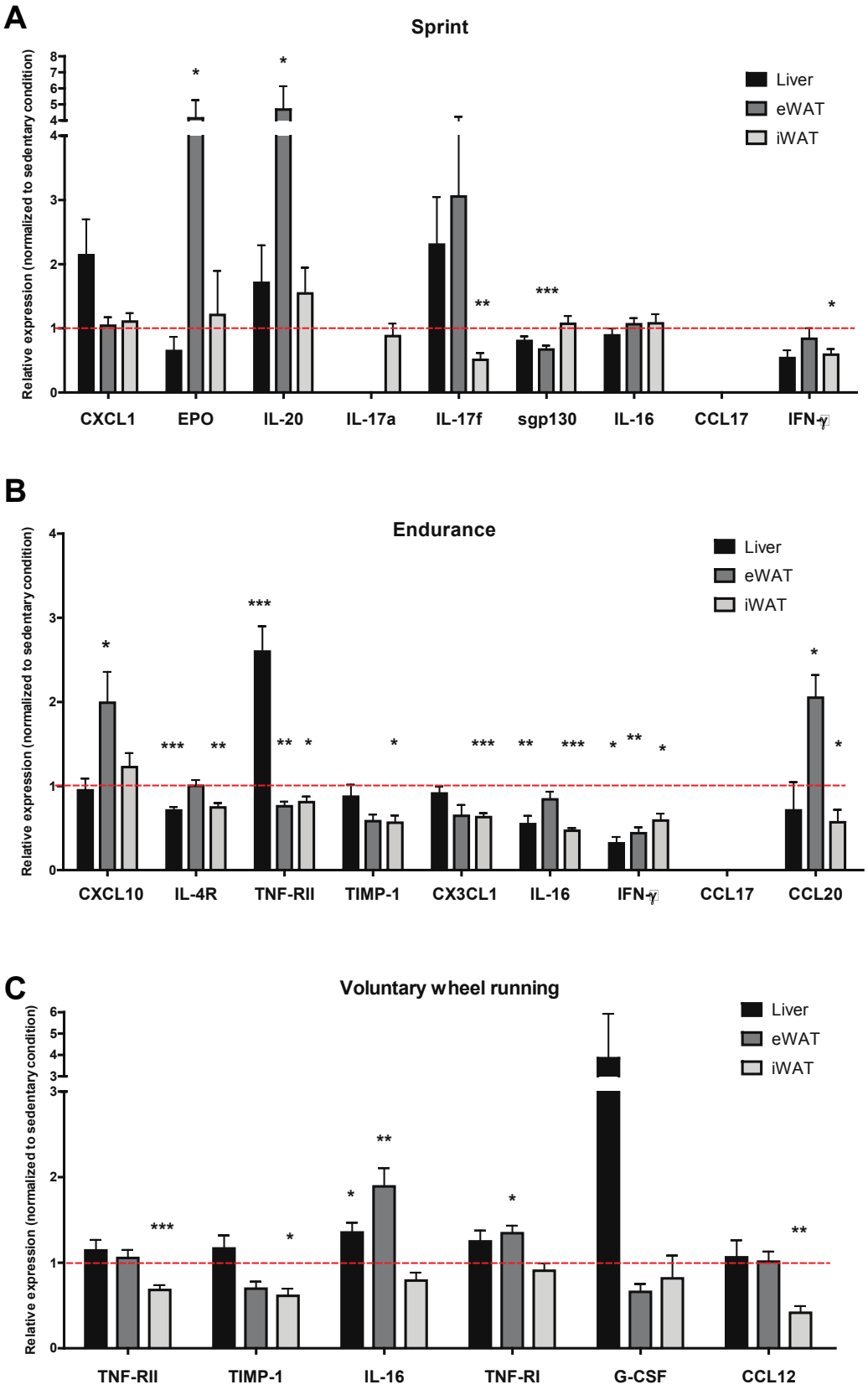
A
Sprint
Relative expression (normalized to sedentary condition)
Liver
eWAT
iWAT
CXCL1
EPO
IL-20
IL-17a
IL-17f
sgp130
IL-16
CCL17
IFN-γ
B
Endurance
Relative expression (normalized to sedentary condition)
Liver
eWAT
iWAT
CXCL10
IL-4R
TNF-RII
TIMP-1
CX3CL1
IL-16
IFN-γ
CCL17
CCL20
C
Voluntary wheel running
Relative expression (normalized to sedentary condition)
Liver
eWAT
iWAT
TNF-RII
TIMP-1
IL-16
TNF-RI
G-CSF
CCL12

cytokine changes seen in circulation. For example, for a single bout of sprint, increased serum EPO and IL-20 levels were paralleled by increased mRNA expression in visceral white adipose tissue, whereas reduced serum IL-17F, sgp130, and INF-γ levels were paralleled by reduction in mRNA expression in either visceral or subcutaneous adipose tissue. For a single bout of endurance run, reduced serum sIL-4R, sTNF-RII, TIMP-1, IL-16, INF-γ, and CCL20 levels were paralleled by reduced mRNA expression in liver and/or adipose tissue. For voluntary wheel running, reduction in serum sTNF-RII, TIMP-1, and CCL12 levels were paralleled by reduced mRNA expression in subcutaneous adipose tissue. These results suggest that changes in a subset of circulating cytokines could, at least in part, be accounted for by the corresponding changes in transcript levels in liver and/or adipose tissues.

DISCUSSION

Here, we undertook an antibody-based profiling approach to determine the extent by which exercise modulates local cytokine levels in glycolytic and oxidative muscle fibers, as well as their systemic circulating levels, in response to three different types of physical activity—an acute sprint and endurance run, or chronic exercise in the form of voluntary wheel running. We chose to focus on cytokine family members as potential myokines given their well-known pleiotropic functions that could potentially link exercise to myriad physiological effects that include immunity (48), inflammation (6), metabolism (43), food intake (32, 49), and autophagy (50).

All the significant changes in cytokine mRNA and protein levels are summarized in **Table 10**. From our antibody-based profiling studies of exercise-regulated cytokines, several notable observations are highlighted. a) Chronic exercise in the form of wheel running consistently induced more cytokine changes than an acute single bout of sprint or endurance run. This is

Table 10

	Serum Protein			Soleus Protein			Soleus mRNA			Plantaris Protein			Plantaris mRNA		
Analyte	**S**	**E**	**VWR**	**S**	**E**	**VWR**	**S**	**E**	**VWR**	**S**	**E**	**VWR**	**S**	**E**	**VWR**
G-CSF			↓												
Eotaxin-1/CCL11						↓						↓			
GM-CSF															
IFN-β1															
IFN-γ	↓	↓	↓	↑	↑	↓						↓			
IL-1α				↑	↑	↓						↓			
IL-1β				↑	↑						↑				
IL-2					↑	↓						↓			
IL-3															
IL-4												↓	↑		
IL-5															
IL-6			↓	↑	↑	↓						↓			
IL-7															
IL-9					↑	↓						↓			
IL-10				↑											
IL-11															
IL-12 (p40)				↑	↑	↓			↑			↓			
IL-12 (p70)														↓	
IL-13															
IL-15					↑	↓			↓	↓		↓			
IL-16	↓	↓	↓			↑		↓							
IL-17A															
IL-17A/F	↓														
IL-17F															
IL-20	↑					↑		↓	↓					↓	↓
IL-21															
IL-22				↑		↓						↓			
IL-23															
IL-27														↓	
IL-28B															
IL-33					↓	↓		↑							
IP-10/CXCL10		↓		↑	↑				↑			↓			
KC/CXCL1	↑	↑	↓		↑	↓	↑					↓	↑		
LIF														↓	
LIX/CXCL5															
MCP-1/CCL2									↑						
M-CSF								↓				↓		↓	
MIG/CXCL9												↓			
MIP-1α/CCL3											↑	↓			
MIP-1β/CCL4														↓	
MIP-2/CXCL2		↑			↑										
RANTES/CCL5				↑	↑	↓			↑			↓			
TNF-α															↑
VEGF				↓	↓	↓			↓	↓	↓	↓	↓	↓	↓
Exodus-2/CCL21					↓							↓			↓

Table 10 - continued

	Serum Protein			Soleus Protein			Soleus mRNA			Plantaris Protein			Plantaris mRNA		
Analyte	**S**	**E**	**VWR**	**S**	**E**	**VWR**	**S**	**E**	**VWR**	**S**	**E**	**VWR**	**S**	**E**	**VWR**
Fractalkine/ CX3CL1		↑				↓								↓	
MDC/CCL22															
MCP-5/CCL12		↓	↓		↓	↑			↑						
MIP-3α/CCL20		↓	↓		↑	↓						↓			
MIP-3β/CCL19						↑									
TARC/CCL17	↓	↓													
TIMP-1		↓	↓			↑			↑			↑		↓	↑
sCD30															
sgp130	↓					↓	↑	↓	↓					↓	
sIL-1RI						↓			↓			↓			
sIL-1RII										↑					
sIL-2Ra							↑						↑		
sIL-4R		↓					↑	↑							
sIL-6R							↑	↑	↓	↑				↑	
sRAGE						↓						↓			
sTNFRI		↓	↓		↓									↓	
sTNFRII		↓	↓			↑									
sVEGFR1					↓	↓	↑		↓						
sVEGFR2				↓	↓	↓		↓	↓				↓	↓	
sVEGFR3															
EPO	↑				↑										

Table 10. Summary of all the statistically significant changes in cytokine mRNA and protein levels in response to sprint (S), endurance run (E), and voluntary wheel running (VWR).

perhaps not surprising as repeated bouts of exercise lead to skeletal muscle adaptation (51). b) Acute and chronic exercise appear to alter distinct sets of cytokines in serum and skeletal muscle, with varying degrees of overlap depending on the type of physical activity. This presumably reflects differences in skeletal muscle adaptation to repeated voluntary wheel running versus a stress-like response to an acute bout of exercise. c) There is more overlap in cytokine profile between a single bout of endurance exercise and chronic wheel running, particularly in serum and oxidative soleus muscle. This suggests that exercise intensity affects the nature of the cytokine response, as endurance and chronic wheel running represent low-intensity exercise whereas an

exhaustive sprint reflects high-intensity exercise. d) We observed more exercise-regulated cytokine changes in skeletal muscle than in serum. This could reflect a higher local concentration of cytokines and hence our greater ability to reliably detect their differences. The circulating plasma levels of most cytokines are in the nanogram and picogram per milliliter range. Due to the dilution effect of plasma, only relatively large changes in cytokine secretion into circulation by skeletal muscle in response to exercise would be detected. Alternatively, some exercise-regulated cytokines act locally within skeletal muscle and are not secreted into circulation. e) Interestingly, between muscle fiber types, we observed significantly more cytokine changes in oxidative soleus compared to glycolytic plantaris muscles irrespective of the types of exercise (sprint, endurance, wheel running). With some exceptions (52), in most human exercise studies, gene and protein expression analyses were performed on quadriceps muscle biopsies consisting of mixed fiber types. As such, cytokine response to exercise in different muscle fiber types in humans is largely unknown. Our study thus highlighted the utility of animal models in addressing questions difficult to answer in human-based exercise studies. f) In oxidative soleus muscle, we observed significant overlaps in cytokine profiles in response to sprint, endurance run, and chronic wheel running. In striking contrast, only minimal overlaps in cytokine profiles were observed in glycolytic plantaris muscle. Thus, not only are more cytokines changed in soleus compared to plantaris, but also those changes seen in soleus show greater overlap between different types of physical activity. These types of unexpected insights relevant to skeletal muscle physiology illustrate the advantage of assessing gene and protein expression in different muscle fiber types. g) In a single bout of exhaustive sprint and endurance run, we observed significantly more cytokines being upregulated than downregulated in serum and in muscle. This may reflect normal physiological stress responses associated with acute exercise. In marked contrast, chronic voluntary wheel running

predominantly resulted in cytokine downregulation in serum and muscle. These differences likely reflect skeletal muscle adaptation to chronic exercise and may be linked to general improvements in inflammatory profiles associated with regular exercise.

IL-6 is the first and most widely studied exercise-regulated cytokine (53). As expected based on previous studies in humans, we observed a significant increase in IL-6 protein level in mouse skeletal muscle in response to a single bout of sprint or endurance exercise (**Table 4**). Interestingly, only oxidative (soleus), but not glycolytic (plantaris), muscle fibers show increased IL-6 protein level in response to sprint or endurance run. One week of voluntary wheel running, however, resulted in reduced IL-6 in both soleus and plantaris, as well as in serum. This reduction presumably reflects skeletal muscle adaptation to repeated bouts of exercise. In healthy humans subjected to 10 weeks of endurance training, contraction-induced IL-6 expression was reduced (54). Intriguingly, neither sprint nor endurance run acutely raised the circulating level of IL-6 in serum (**Table 3**). This could be due to exercise intensity, or insufficient quantities of IL-6 being secreted into systemic circulation to acutely raise its serum level. While most human studies reported increase plasma IL-6 levels after high intensity exercise, some studies did not observe a similar increase in plasma IL-6 after a lower intensity exercise (37). It has been noted that circulating levels of cytokines can vary widely between individuals subjected to different types of exercise (28).

Intriguingly, most of the secreted cytokine receptors (10 out of 13) profiled are altered by exercise. These include sgp130, sRAGE, sIL-1RI, sIL-1RII, sIL-4R, sIL-6R, sTNF-RI, sTNF-RII, sVEGFR1, and sVEGFR2. The soluble form of cytokine receptors in plasma can be generated by multiple mechanisms that include ectodomain shedding by zinc metalloproteinases (e.g., TACE/ADAM17 and ADAM19), as well as by alternative mRNA splicing (42). Protease-

mediated release of receptor ectodomain has been demonstrated for TNF-RI, TNF-RII, IL-1RII, IL-4R, and IL-6R, whereas the soluble forms of gp130, RAGE, VEGFR1, and VEGFR2 are generated by alternative mRNA splicing (42, 55). While previous studies have looked at soluble IL-6R levels in response to exercise in humans (56, 57), our current study represents the first attempt to quantify changes in multiple secreted cytokine receptors in response to exercise. Our results suggest that soluble cytokine receptors could be generated by potentially novel exercise-regulated proteolytic and alternative mRNA splicing mechanisms. In principle, these soluble receptors could influence cytokine signaling by functioning as receptor agonists or antagonists.

Interestingly, there is a subset of 17 circulating cytokines whose changes in serum were not matched by their corresponding changes in muscle. Presumably, these cytokines (EPO, IL-20, IL-17A/F, sgp130, sIL-4R, CCL17, G-CSF, CX3CL1, CXCL1, IL-16, TIMP-1, sTNF-RII, sTNF-RI, IFN-γ, CXCL10, CCL20, and CCL12) are produced and secreted by non-muscle tissues. These changes could be attributed to several potential mechanisms that are dependent or independent of contracting skeletal muscle. Primary cytokines, and other potential myokines, that are secreted into circulation by contracting skeletal muscle could convey a signal to other non-muscle tissues to alter the expression and secretion of secondary cytokines. Liver and adipose tissues are also known to produce and secrete a variety of different cytokines. Given the energetics demands of contracting skeletal muscle, indirect metabolic changes in liver and adipose tissue induced by exercise could potentially also alter the expression and secretion of secondary cytokines. In support, we indeed observed parallel changes in cytokine expression in liver and/or adipose tissue in response to exercise that could, at least in part, account for their changes in circulation but not in skeletal muscle. Thus, our data highlighted the primary cytokine response of skeletal muscle

and the secondary cytokine response in non-muscle tissues resulting from potential exercise-mediated tissue crosstalk.

When skeletal muscles isolated from the same mice were subjected to quantitative mRNA analysis, we found only minimal concordance between cytokine mRNA and protein levels, irrespective of exercise regimen. These observations suggest the importance of posttranscriptional regulation of cytokine expression and secretion in contracting skeletal muscle *in vivo*. Some of these posttranscriptional mechanisms could involve exercise-regulated stabilization of cytokine mRNA transcripts and/or microRNA (miRNA) mediated regulation of mRNA translation (28). Given that posttranscriptional control of cytokine/myokine expression in response to exercise is largely unexplored, our data provided a basis and impetus to further explore these underappreciated mechanisms in the context of physical activity.

Of the 66 cytokines profiled, a surprisingly large fraction is altered by acute and/or short-term exercise. Most of these altered cytokines are shown for the first time to be regulated by exercise *in vivo*. In recent studies, Scheler et al. profiled 23 different cytokines in cultured human myotubes using similar bead-based multiplex approach and showed that 11 cytokines are regulated by electrical pulse stimulation (27); these include IL-8, CXCL1, IL-6, LIF, IL-4, IL-13, IL17A, IL-1β, G-CSF, TNF, and CCL2. Raschke et al. used an antibody array to profile 179 peptides (covering different classes of secretory proteins in addition to cytokines), and identified 23 novel exercise regulated cytokines in electrical pulse stimulated human myotubes (26); these include IL-1α, IL-3, IL-10, IL-16, IL-22, IL-28A, IL-29, IL-31, IFN-γ, TPO, RAGE, CCL1, CCL4, CCL15, CCL17, CCL18, CCL21, CCL23, CCL24, CCL26, CXCL6, CXCL9, and CXCL13. Of the known exercise-regulated cytokines reported in cultured human myotubes (26, 27), we were able to confirm the majority of them *in vivo*, in particular those cytokines that were included in our

multiplex assay. This suggests that many of the cytokine responses we observed are most likely due to changes in the expression and secretion of cytokines from skeletal myotubes. Our results validate the use of rodent exercise models to study cytokine/myokine response in humans. Excluding these recently described exercise-regulated cytokines in cultured human myotubes, our *in vivo* mouse studies—involving three different exercise regimens and two different muscle fiber types—identified an additional 22 novel exercise-regulated cytokines/myokines not previously reported. These include IL-9, IL-12 (p40), IL-20, IL-33, M-CSF, CXCL10, CXCL2, CCL5, CCL3, CCL12, CCL19, CCL20, EPO, TIMP-1, sgp130, sIL-1RI, sIL-1RII, sIL-6R, sTNF-RI, sTNF-RII, sVEGFR1, and sVEGFR2. Of these novel exercise-regulated myokines, a subset (IL-20, CXCL2, CXCL10, CCL12, CCL20, sTNF-RI, sTNF-RII, and TIMP) can be considered "exercise factors" based on the definition that they are produced by skeletal muscle in response to exercise and are secreted into the circulation (11).

Most of the exercise-regulated cytokines we uncovered play myriad roles in the immune and non-immune systems. Many cytokine functions are physiological context-dependent and their effects are cell-type specific (38); their excessive production or suppression are often causally linked to disease. In the context of exercise, the levels of a surprisingly large number of cytokines are changed either locally within skeletal muscle or systemically. It appears that both the pro- and anti-inflammatory cytokines are altered by acute and chronic exercise in rodents (**Table 10**) and in humans (58). It has been suggested that the beneficial local and systemic effects of chronic exercise are due to exercise-induced hormesis, whereby a low level of stress upregulates existing cellular and molecular pathways that improve whole-body physiology (e.g., metabolism and immunity) (58, 59). Thus, it may be a specific combination of cytokines (with diverse and opposing functions) whose direction, magnitude, and duration of change underlie exercise-induced

hormesis. In this context, it is worth noting that chronic exercise with running wheel induced more cytokine changes than either an acute low-intensity (endurance) or high-intensity (sprint) exercise. While this is beyond the scope of the present study, future investigations using genetic gain- or loss-of-function mouse models of select cytokines are clearly needed to further pinpoint the biological effects of muscle-derived cytokines/myokines in muscle and non-muscle tissues.

Several limitations and caveats are noted in the present studies. First, we did not analyze all the known cytokines discovered to date. This is limited by cost and the availability of cytokine-specific multiplex reagents. Second, we did not use an *in vitro* exercise model (e.g., EPS-stimulated myotubes) to directly show that the cytokine changes we see in soleus and plantaris muscle fibers are indeed derived from skeletal myotubes and not from other potential cell types such as satellite cells, endothelial cells, fibroblastic cells, and resident immune cells. It is known that eccentric or resistance exercise, or prolonged running (e.g., marathon), in humans result in muscle damage, leading to the influx of inflammatory leukocytes that can be the source of cytokines upregulated in muscle [extensively reviewed in (60)]. While we cannot rule out this possibility, the type and duration of exercise the mice were subjected to in our study generally do not cause significant muscle damage. Indeed, when obese mice were subjected to endurance interval training, significantly less inflammation and macrophage infiltration were observed in skeletal muscle (61). Since our *in vivo* study confirmed a majority of the exercise-regulated cytokines in cultured human myotubes (26, 27), we presume the novel exercise-regulated cytokines found in the present study are likely to be derived from myotubes. Third, we only measured transcript, and not protein, levels of a select set of cytokines in liver and adipose tissues. Thus, whether changes in mRNA translate into changes in protein levels remain to be determined. Fourth, we did not directly demonstrate the release of cytokines from exercised muscle into

circulation. While this may be technically challenging to perform in mice, *in situ* cytokine flux analysis will provide further insights into how different muscle fiber types modulate the production and secretion of cytokines in response to different exercise. Fifth, although mice run only during the dark cycle (62), one potential caveat of the voluntary exercise group was that the mice had access to the running wheel until the morning before they were sacrificed. However, when we examined the cytokine profiles, the number and type of cytokine changes were significantly different between acute (sprint and endurance run) and chronic (wheel running) exercise groups despite some overlaps (**Fig. 2 and 3**), suggesting that we could discriminate between the two exercise effects. Sixth, the pre-exercise values of some cytokines in the voluntary wheel running group were significantly higher than the pre-exercise values for the sprint and endurance groups. The reason for this is unknown. While all mice were handled identically, the serum samples from the wheel running group were not analyzed at the same time as the sprint and endurance groups. However, samples that were directly compared to one another or used for normalization were always analyzed on the same plate; specifically, serum samples from the pre- and post- sprint and endurance groups were run together while the samples from the pre- and post- wheel running were run together. Our analyses focused on the changes in cytokine levels in each pre- and post-exercise condition. We do not directly compare serum data between exercise regimens. Thus, the differences in absolute values between exercise conditions should not affect the interpretation of our data. Despite these limitations, our current studies reveal important insights concerning exercise regulation of local and systemic cytokine levels.

In summary, our current cytokine profiling study in mice, along with other published studies on exercise-regulated myokines in humans and animal models, indicate that physical activity can significantly alter the skeletal muscle secretome. Many myokines/cytokines have

pleiotropic functions, and some may have opposite effects depending on biological and physiological contexts. Given this complexity, we speculate that a right combination, magnitude, and direction of myokine changes induced by regular exercise, rather than one or two dominant secretory proteins, are likely responsible for the multi-organ effects and health benefits of exercise. The inherent systems-level response to physical activity may pose a major challenge to produce an "exercise pill" that can mimic and recapitulate all the local and systemic physiological and adaptive processes induced and suppressed by regular exercise.

REFERENCES

1. Lee, I. M., Shiroma, E. J., Lobelo, F., Puska, P., Blair, S. N., Katzmarzyk, P. T., and Lancet Physical Activity Series Working, G. (2012) Effect of physical inactivity on major non-communicable diseases worldwide: an analysis of burden of disease and life expectancy. *Lancet* 380, 219-229
2. Booth, F. W., Roberts, C. K., Thyfault, J. P., Ruegsegger, G. N., and Toedebusch, R. G. (2017) Role of Inactivity in Chronic Diseases: Evolutionary Insight and Pathophysiological Mechanisms. *Physiol Rev* 97, 1351-1402
3. Li, S., Zhao, J. H., Luan, J., Ekelund, U., Luben, R. N., Khaw, K. T., Wareham, N. J., and Loos, R. J. (2010) Physical activity attenuates the genetic predisposition to obesity in 20,000 men and women from EPIC-Norfolk prospective population study. *PLoS Med* 7
4. Goodyear, L. J., and Kahn, B. B. (1998) Exercise, glucose transport, and insulin sensitivity. *Annu Rev Med* 49, 235-261
5. Zierath, J. R., and Wallberg-Henriksson, H. (2015) Looking Ahead Perspective: Where Will the Future of Exercise Biology Take Us? *Cell Metab* 22, 25-30
6. Pedersen, B. K. (2017) Anti-inflammatory effects of exercise: role in diabetes and cardiovascular disease. *Eur J Clin Invest* 47, 600-611
7. Hawley, J. A., Hargreaves, M., Joyner, M. J., and Zierath, J. R. (2014) Integrative biology of exercise. *Cell* 159, 738-749
8. Neufer, P. D., Bamman, M. M., Muoio, D. M., Bouchard, C., Cooper, D. M., Goodpaster, B. H., Booth, F. W., Kohrt, W. M., Gerszten, R. E., Mattson, M. P., Hepple, R. T., Kraus, W. E., Reid, M. B., Bodine, S. C., Jakicic, J. M., Fleg, J. L., Williams, J. P., Joseph, L., Evans, M., Maruvada, P., Rodgers, M., Roary, M., Boyce, A. T., Drugan, J. K., Koenig, J. I., Ingraham, R. H., Krotoski, D., Garcia-Cazarin, M., McGowan, J. A., and Laughlin, M. R. (2015) Understanding the Cellular and Molecular Mechanisms of Physical Activity-Induced Health Benefits. *Cell Metab* 22, 4-11
9. Pedersen, B. K. (2009) Edward F. Adolph distinguished lecture: muscle as an endocrine organ: IL-6 and other myokines. *J Appl Physiol* 107, 1006-1014
10. Pedersen, B. K., and Febbraio, M. A. (2012) Muscles, exercise and obesity: skeletal muscle as a secretory organ. *Nat Rev Endocrinol* 8, 457-465
11. Catoire, M., and Kersten, S. (2015) The search for exercise factors in humans. *FASEB J* 29, 1615-1628
12. Hartwig, S., Raschke, S., Knebel, B., Scheler, M., Irmler, M., Passlack, W., Muller, S., Hanisch, F. G., Franz, T., Li, X., Dicken, H. D., Eckardt, K., Beckers, J., de Angelis, M. H., Weigert, C., Haring, H. U., Al-Hasani, H., Ouwens, D. M., Eckel, J., Kotzka, J., and Lehr, S. (2014) Secretome profiling of primary human skeletal muscle cells. *Biochim Biophys Acta* 1844, 1011-1017
13. Deshmukh, A. S., Cox, J., Jensen, L. J., Meissner, F., and Mann, M. (2015) Secretome Analysis of Lipid-Induced Insulin Resistance in Skeletal Muscle Cells by a Combined Experimental and Bioinformatics Workflow. *J Proteome Res* 14, 4885-4895
14. Chan, C. Y., Masui, O., Krakovska, O., Belozerov, V. E., Voisin, S., Ghanny, S., Chen, J., Moyez, D., Zhu, P., Evans, K. R., McDermott, J. C., and Siu, K. W. (2011) Identification of differentially regulated secretome components during skeletal myogenesis. *Mol Cell Proteomics* 10, M110 004804
15. Henningsen, J., Rigbolt, K. T., Blagoev, B., Pedersen, B. K., and Kratchmarova, I. (2010) Dynamics of the skeletal muscle secretome during myoblast differentiation. *Mol Cell Proteomics* 9, 2482-2496
16. Yoon, J. H., Kim, D., Jang, J. H., Ghim, J., Park, S., Song, P., Kwon, Y., Kim, J., Hwang, D., Bae, Y. S., Suh, P. G., Berggren, P. O., and Ryu, S. H. (2015) Proteomic analysis of the palmitate-induced myotube secretome reveals involvement of the annexin A1-formyl peptide receptor 2 (FPR2) pathway in insulin resistance. *Mol Cell Proteomics* 14, 882-892
17. Yoon, J. H., Song, P., Jang, J. H., Kim, D. K., Choi, S., Kim, J., Ghim, J., Kim, D., Park, S., Lee, H., Kwak, D., Yea, K., Hwang, D., Suh, P. G., and Ryu, S. H. (2011) Proteomic analysis of tumor

necrosis factor-alpha (TNF-alpha)-induced L6 myotube secretome reveals novel TNF-alpha-dependent myokines in diabetic skeletal muscle. *J Proteome Res* 10, 5315-5325
18. Yoon, J. H., Yea, K., Kim, J., Choi, Y. S., Park, S., Lee, H., Lee, C. S., Suh, P. G., and Ryu, S. H. (2009) Comparative proteomic analysis of the insulin-induced L6 myotube secretome. *Proteomics* 9, 51-60
19. Norheim, F., Raastad, T., Thiede, B., Rustan, A. C., Drevon, C. A., and Haugen, F. (2011) Proteomic identification of secreted proteins from human skeletal muscle cells and expression in response to strength training. *Am J Physiol Endocrinol Metab* 301, E1013-1021
20. Ostrowski, K., Rohde, T., Zacho, M., Asp, S., and Pedersen, B. K. (1998) Evidence that interleukin-6 is produced in human skeletal muscle during prolonged running. *J Physiol* 508 (Pt 3), 949-953
21. Steensberg, A., van Hall, G., Osada, T., Sacchetti, M., Saltin, B., and Klarlund Pedersen, B. (2000) Production of interleukin-6 in contracting human skeletal muscles can account for the exercise-induced increase in plasma interleukin-6. *J Physiol* 529 Pt 1, 237-242
22. Haugen, F., Norheim, F., Lian, H., Wensaas, A. J., Dueland, S., Berg, O., Funderud, A., Skalhegg, B. S., Raastad, T., and Drevon, C. A. (2010) IL-7 is expressed and secreted by human skeletal muscle cells. *Am J Physiol Cell Physiol* 298, C807-816
23. Quinn, L. S., Anderson, B. G., Strait-Bodey, L., Stroud, A. M., and Argiles, J. M. (2009) Oversecretion of interleukin-15 from skeletal muscle reduces adiposity. *Am J Physiol Endocrinol Metab* 296, E191-202
24. Broholm, C., Laye, M. J., Brandt, C., Vadalasetty, R., Pilegaard, H., Pedersen, B. K., and Scheele, C. (2011) LIF is a contraction-induced myokine stimulating human myocyte proliferation. *J Appl Physiol* 111, 251-259
25. Hoier, B., Olsen, K., Nyberg, M., Bangsbo, J., and Hellsten, Y. (2010) Contraction-induced secretion of VEGF from skeletal muscle cells is mediated by adenosine. *American journal of physiology. Heart and circulatory physiology* 299, H857-862
26. Raschke, S., Eckardt, K., Bjorklund Holven, K., Jensen, J., and Eckel, J. (2013) Identification and validation of novel contraction-regulated myokines released from primary human skeletal muscle cells. *PLoS One* 8, e62008
27. Scheler, M., Irmler, M., Lehr, S., Hartwig, S., Staiger, H., Al-Hasani, H., Beckers, J., de Angelis, M. H., Haring, H. U., and Weigert, C. (2013) Cytokine response of primary human myotubes in an in vitro exercise model. *Am J Physiol Cell Physiol* 305, C877-886
28. Peake, J. M., Della Gatta, P., Suzuki, K., and Nieman, D. C. (2015) Cytokine expression and secretion by skeletal muscle cells: regulatory mechanisms and exercise effects. *Exerc Immunol Rev* 21, 8-25
29. Akira, S., Hirano, T., Taga, T., and Kishimoto, T. (1990) Biology of multifunctional cytokines: IL 6 and related molecules (IL 1 and TNF). *FASEB J* 4, 2860-2867
30. Dinarello, C. A. (2007) Historical insights into cytokines. *Eur J Immunol* 37 Suppl 1, S34-45
31. Buchanan, J. B., and Johnson, R. W. (2007) Regulation of food intake by inflammatory cytokines in the brain. *Neuroendocrinology* 86, 183-190
32. Zorrilla, E. P., Sanchez-Alavez, M., Sugama, S., Brennan, M., Fernandez, R., Bartfai, T., and Conti, B. (2007) Interleukin-18 controls energy homeostasis by suppressing appetite and feed efficiency. *Proc Natl Acad Sci U S A* 104, 11097-11102
33. Luheshi, G. N., Gardner, J. D., Rushforth, D. A., Loudon, A. S., and Rothwell, N. J. (1999) Leptin actions on food intake and body temperature are mediated by IL-1. *Proc Natl Acad Sci U S A* 96, 7047-7052
34. Pourteymour, S., Eckardt, K., Holen, T., Langleite, T., Lee, S., Jensen, J., Birkeland, K. I., Drevon, C. A., and Hjorth, M. (2017) Global mRNA sequencing of human skeletal muscle: Search for novel exercise-regulated myokines. *Mol Metab* 6, 352-365
35. Lundberg, T. R., Fernandez-Gonzalo, R., Tesch, P. A., Rullman, E., and Gustafsson, T. (2016) Aerobic exercise augments muscle transcriptome profile of resistance exercise. *Am J Physiol Regul Integr Comp Physiol* 310, R1279-1287

36. Catoire, M., Mensink, M., Boekschoten, M. V., Hangelbroek, R., Muller, M., Schrauwen, P., and Kersten, S. (2012) Pronounced effects of acute endurance exercise on gene expression in resting and exercising human skeletal muscle. *PLoS One* 7, e51066
37. Catoire, M., Mensink, M., Kalkhoven, E., Schrauwen, P., and Kersten, S. (2014) Identification of human exercise-induced myokines using secretome analysis. *Physiol Genomics* 46, 256-267
38. Borish, L. C., and Steinke, J. W. (2003) 2. Cytokines and chemokines. *J Allergy Clin Immunol* 111, S460-475
39. Dupont, N. C., Wang, K., Wadhwa, P. D., Culhane, J. F., and Nelson, E. L. (2005) Validation and comparison of luminex multiplex cytokine analysis kits with ELISA: determinations of a panel of nine cytokines in clinical sample culture supernatants. *Journal of reproductive immunology* 66, 175-191
40. Tighe, P., Negm, O., Todd, I., and Fairclough, L. (2013) Utility, reliability and reproducibility of immunoassay multiplex kits. *Methods* 61, 23-29
41. Moncunill, G., Aponte, J. J., Nhabomba, A. J., and Dobano, C. (2013) Performance of multiplex commercial kits to quantify cytokine and chemokine responses in culture supernatants from Plasmodium falciparum stimulations. *PLoS One* 8, e52587
42. Levine, S. J. (2008) Molecular mechanisms of soluble cytokine receptor generation. *J Biol Chem* 283, 14177-14181
43. Petersen, P. S., Lei, X., Seldin, M. M., Rodriguez, S., Byerly, M. S., Wolfe, A., Whitlock, S., and Wong, G. W. (2014) Dynamic and extensive metabolic state-dependent regulation of cytokine expression and circulating levels. *Am J Physiol Regul Integr Comp Physiol* 307, R1458-1470
44. Collins, M. L., Irvine, B., Tyner, D., Fine, E., Zayati, C., Chang, C., Horn, T., Ahle, D., Detmer, J., Shen, L. P., Kolberg, J., Bushnell, S., Urdea, M. S., and Ho, D. D. (1997) A branched DNA signal amplification assay for quantification of nucleic acid targets below 100 molecules/ml. *Nucleic Acids Res* 25, 2979-2984
45. Flagella, M., Bui, S., Zheng, Z., Nguyen, C. T., Zhang, A., Pastor, L., Ma, Y., Yang, W., Crawford, K. L., McMaster, G. K., Witney, F., and Luo, Y. (2006) A multiplex branched DNA assay for parallel quantitative gene expression profiling. *Anal Biochem* 352, 50-60
46. Canales, R. D., Luo, Y., Willey, J. C., Austermiller, B., Barbacioru, C. C., Boysen, C., Hunkapiller, K., Jensen, R. V., Knight, C. R., Lee, K. Y., Ma, Y., Maqsodi, B., Papallo, A., Peters, E. H., Poulter, K., Ruppel, P. L., Samaha, R. R., Shi, L., Yang, W., Zhang, L., and Goodsaid, F. M. (2006) Evaluation of DNA microarray results with quantitative gene expression platforms. *Nat Biotechnol* 24, 1115-1122
47. Schmittgen, T. D., and Livak, K. J. (2008) Analyzing real-time PCR data by the comparative C(T) method. *Nat Protoc* 3, 1101-1108
48. Lin, Y. S., Jan, M. S., and Chen, H. I. (1993) The effect of chronic and acute exercise on immunity in rats. *Int J Sports Med* 14, 86-92
49. Reed, J. A., Clegg, D. J., Smith, K. B., Tolod-Richer, E. G., Matter, E. K., Picard, L. S., and Seeley, R. J. (2005) GM-CSF action in the CNS decreases food intake and body weight. *J Clin Invest* 115, 3035-3044
50. He, C., Bassik, M. C., Moresi, V., Sun, K., Wei, Y., Zou, Z., An, Z., Loh, J., Fisher, J., Sun, Q., Korsmeyer, S., Packer, M., May, H. I., Hill, J. A., Virgin, H. W., Gilpin, C., Xiao, G., Bassel-Duby, R., Scherer, P. E., and Levine, B. (2012) Exercise-induced BCL2-regulated autophagy is required for muscle glucose homeostasis. *Nature* 481, 511-515
51. Egan, B., and Zierath, J. R. (2013) Exercise metabolism and the molecular regulation of skeletal muscle adaptation. *Cell Metab* 17, 162-184
52. Hiscock, N., Chan, M. H., Bisucci, T., Darby, I. A., and Febbraio, M. A. (2004) Skeletal myocytes are a source of interleukin-6 mRNA expression and protein release during contraction: evidence of fiber type specificity. *FASEB J* 18, 992-994
53. Pedersen, B. K., and Febbraio, M. A. (2008) Muscle as an endocrine organ: focus on muscle-derived interleukin-6. *Physiol Rev* 88, 1379-1406

54. Fischer, C. P., Plomgaard, P., Hansen, A. K., Pilegaard, H., Saltin, B., and Pedersen, B. K. (2004) Endurance training reduces the contraction-induced interleukin-6 mRNA expression in human skeletal muscle. *Am J Physiol Endocrinol Metab* 287, E1189-1194
55. Malherbe, P., Richards, J. G., Gaillard, H., Thompson, A., Diener, C., Schuler, A., and Huber, G. (1999) cDNA cloning of a novel secreted isoform of the human receptor for advanced glycation end products and characterization of cells co-expressing cell-surface scavenger receptors and Swedish mutant amyloid precursor protein. *Brain Res Mol Brain Res* 71, 159-170
56. Gray, S. R., Clifford, M., Lancaster, R., Leggate, M., Davies, M., and Nimmo, M. A. (2009) The response of circulating levels of the interleukin-6/interleukin-6 receptor complex to exercise in young men. *Cytokine* 47, 98-102
57. Leggate, M., Nowell, M. A., Jones, S. A., and Nimmo, M. A. (2010) The response of interleukin-6 and soluble interleukin-6 receptor isoforms following intermittent high intensity and continuous moderate intensity cycling. *Cell Stress Chaperones* 15, 827-833
58. Pedersen, B. K., and Hoffman-Goetz, L. (2000) Exercise and the immune system: regulation, integration, and adaptation. *Physiol Rev* 80, 1055-1081
59. Peake, J. M., Markworth, J. F., Nosaka, K., Raastad, T., Wadley, G. D., and Coffey, V. G. (2015) Modulating exercise-induced hormesis: Does less equal more? *J Appl Physiol (1985)* 119, 172-189
60. Paulsen, G., Mikkelsen, U. R., Raastad, T., and Peake, J. M. (2012) Leucocytes, cytokines and satellite cells: what role do they play in muscle damage and regeneration following eccentric exercise? *Exerc Immunol Rev* 18, 42-97
61. Samaan, M. C., Marcinko, K., Sikkema, S., Fullerton, M. D., Ziafazeli, T., Khan, M. I., and Steinberg, G. R. (2014) Endurance interval training in obese mice reduces muscle inflammation and macrophage content independently of weight loss. *Physiol Rep* 2
62. Bains, R. S., Wells, S., Sillito, R. R., Armstrong, J. D., Cater, H. L., Banks, G., and Nolan, P. M. (2018) Assessing mouse behaviour throughout the light/dark cycle using automated in-cage analysis tools. *J Neurosci Methods* 300, 37-47

CHAPTER 3:

Myonectin deletion promotes adipose fat storage and reduces liver steatosis*

*Text and figures in this chapter were published in *FASEB* in 2019:

Little, H. C., Rodriguez, S., Lei, X., Tan, S. Y., Stewart, A. N., Sahagun, A., Sarver, D. C., and Wong, G. W. (2019) Myonectin deletion promotes adipose fat storage and reduces liver steatosis. *FASEB J.* [Epub ahead of print]

ABSTRACT

We recently described myonectin (also known as CTRP15 and erythroferrone) as a novel skeletal muscle-derived myokine with metabolic functions. Here, we use a genetic mouse model to determine myonectin's requirement for metabolic homeostasis. Female myonectin-deficient mice had larger gonadal fat pad, developed mild insulin resistance when fed a high-fat diet and had reduced food intake following a fast, but were otherwise indistinguishable from wild-type littermates. Male mice lacking myonectin, however, had reduced physical activity when fed *ad-libitum* and in the postprandial state, but not during a fast. When stressed with a high-fat diet, myonectin knockout male mice had significantly elevated very-low-density lipoprotein (VLDL)-triglyceride and strikingly impaired lipid clearance from circulation following an oral lipid load. Fat distribution between adipose and liver was also altered in myonectin-deficient male mice fed a high-fat diet. Greater fat storage resulted in significantly enlarged adipocytes and was associated with increased postprandial lipoprotein lipase activity in adipose tissue. Parallel to this was a striking reduction in liver steatosis due to significantly reduced triglyceride accumulation. Liver metabolite profiling revealed additional significant changes in bile acids and one-carbon metabolism pathways. Combined, our data affirm the physiological importance of myonectin in regulating local and systemic lipid metabolism.

INTRODUCTION

Skeletal muscle takes up the majority of circulating postprandial glucose and plays a vital role in maintaining whole-body energy balance (1, 2). Impaired insulin responsiveness in skeletal muscle is mechanistically linked to type 2 diabetes (3, 4). As a major metabolic organ, skeletal muscle is believed to communicate with other organs and tissues via secreted hormones to

influence whole-body metabolism. The discovery that skeletal muscle dynamically secretes a variety of myokines—proteins that stimulate muscle and non-muscle tissues to regulate various biological processes—has provided a novel and critical conceptual framework to understand skeletal muscle's role in coordinating integrated physiology (5, 6).

Of the hundreds of proteins secreted by skeletal muscle (7-9), only a few have been functionally characterized; these include myostatin (10-12), IL-6 (13), fibroblast growth factor 21 (FGF21) (14, 15), insulin-like 6 (INSL6) (16), follistatin-like 1 (FSTL1) (17), leukemia inhibitory factor (LIF) (18), IL-7 (19), IL-15 (20), musclin (21, 22), and irisin (23). These myokines either act locally within skeletal muscle as autocrine/paracrine factors or circulate in blood as endocrine factors, linking skeletal muscle to the regulation of physiological processes in non-muscle tissues (6, 11, 13, 14, 23-27).

We recently described myonectin/CTRP15 as a novel myokine expressed predominantly by skeletal muscle (28) and determined that exercise can upregulate its expression and circulating level (28, 29). Myonectin is a member of the C1q/TNF-related proteins (CTRPs) with a signature C-terminal globular C1q domain (28, 30-35). Since our initial identification and characterizations of myonectin (28, 36) it has also been referred to as erythroferrone, a secreted protein induced in erythroblasts that links stress erythropoiesis to iron mobilization in liver in response to blood loss (37, 38).

Using genetic gain- or loss-of-function mouse models, we and others provided *in vivo* evidence for the important metabolic and cardiovascular functions of several CTRP family members (29, 33, 39-59). Unlike other family members, myonectin is the only CTRP whose basal expression is primarily restricted to skeletal muscle. Several lines of evidence suggest that myonectin is a physiologically relevant metabolic regulator (28, 36). First, overnight fasting

reduces and re-feeding increases myonectin mRNA and serum levels. Second, and similar to re-feeding, a bolus of glucose or emulsified lipid administered to overnight-fasted mice increases circulating myonectin (28). The addition of glucose, amino acids, or free fatty acids to cultured myotubes also upregulates myonectin expression, suggesting that nutrient uptake and metabolism by muscle cells is sufficient to induce production of this protein. Third, the expression and circulating levels of myonectin are significantly reduced in diet-induced obese and insulin-resistant mice (28). Fourth, infusion of recombinant myonectin into mice reduces circulating free fatty acid levels by promoting free fatty acid uptake (28). Fifth, myonectin suppresses liver autophagy (36), an intracellular recycling pathway activated in the fasted state and inhibited in the fed state. Finally, circulating level of myonectin is associated with insulin resistance and type 2 diabetes in humans (60, 61). The caveat of our previous functional studies, however, is the reliance on recombinant protein infusion in mice and the use of established muscle and adipocyte cell lines (28, 36); it is unclear whether myonectin/erythroferrone is required for metabolic homeostasis in a physiological context (62). Therefore, we aimed to determine the physiological function of myonectin using a genetic loss-of-function mouse model. Our data provide evidence that myonectin does indeed have a role in regulating lipid metabolism in the context of metabolic stress induced by high-fat feeding, and that this effect is sex-dependent.

MATERIALS AND METHODS

Animals

Myonectin (Erfe/Fam132b+/-) heterozygous mice were obtained from the Mutant Mouse Regional Resource Center (MMRRC) at UC Davis (strain B6;129S5-*Fam132b*^{tm1Lex}/Mmucd, ID MMRRC:032289-UCD). Mice were generated by Lexicon Pharmaceuticals (63). We maintained

the mice on the C57BL/6N genetic background for >6 generations. PCR genotyping strategy was provided by MMRRC. Genotyping primers for the myonectin wildtype (WT) allele were: forward, 5'-GTCAGCCTTACCTGCCCAG-3'; and reverse, 5'-GACGTGAATCTC AGTCTGGC-3'; yielding a WT PCR product of 216 bp. Primers for the KO allele were: forward, 5'-GCAGCG CATCGCCTTCTATC-3'; and reverse, 5'-GACCGTCACTGAGGTTCCAC-3'; yielding a KO PCR product of 390 bp. To confirm loss of *myonectin* mRNA from KO mice, quantitative PCR was performed on muscle samples using two independent sets of myonectin-specific primers: Primer set # 1, forward, 5'-TGCTTGGATGCTGTT CGTCAA-3' and reverse, 5'-CAGATGGGATAAAGGGGCCTG-3'; primer set # 2, forward, 5'-GCGAGAGA GCCATCTGGAGCACTG-3' and reverse, 5'-GGTCCCTTTCTTGGCTGCTCGGTG-3'. All mice were housed in polycarbonate cages with *ad-libitum* access to water and food in a temperature-controlled room with 12-hour (h) light–dark cycles. Mice were fed either a high-fat diet (HFD, 60% calories from fat, Research Diets, D12492) or a matched control low-fat diet (LFD, 10% calories from fat, Research Diets, D12450B) throughout the study beginning at 5-6 weeks of age. Body weights of WT and myonectin-KO mice were measured weekly. At the end of the study, mice were euthanized 2 h after food removal in the morning or after an overnight fast followed by 2 h of *ad-libitum* re-feeding. Tissues were dissected, weighed, and snap-frozen in liquid nitrogen for RNA and protein extraction or prepared for histology. Additional tissues were stored at −80°C. All animal experiments were approved by the Animal Care and Use Committee of the Johns Hopkins University School of Medicine.

Mouse body composition analysis

Body composition of myonectin-KO mice and WT littermates was determined using a quantitative nuclear magnetic resonance (NMR) instrument (Echo-MRI-100, Echo Medical Systems LLC, Waco, TX) at the Johns Hopkins University School of Medicine mouse phenotyping core facility. Echo-magnetic resonance imaging analyses measured total fat mass, lean mass, and water content.

Indirect calorimetry

Indirect calorimetry was performed as previously described (54). In brief, WT and myonectin-KO mice were used for simultaneous assessments of daily body weight change, food intake (corrected for spillage), physical activity, and whole-body metabolic profile in an open-flow indirect calorimeter (CLAMS, Columbus Instruments, Columbus, OH). Data were collected for three to four consecutive days to confirm that mice were acclimated to calorimetry chambers (indicated by stable body weights, food intakes, and diurnal metabolic patterns), and data from the following day(s) were analyzed. Rates of oxygen consumption (VO_2) and carbon dioxide production (VCO_2) in each chamber were measured throughout the studies. Respiratory exchange ratio (RER, VCO_2/VO_2) was calculated by CLAMS software (version 4.02) to estimate relative oxidation of carbohydrates (RER = 1.0) versus fats (RER = 0.7), not accounting for protein oxidation. Energy expenditure (EE) was calculated as $EE = VO_2 \times [3.815 + (1.232 \times RER)]$. VO_2, VCO_2, and EE data were normalized to lean mass. Physical activity was measured by infrared beam breaks in the metabolic chamber. Average metabolic values were calculated per subject and averaged across subjects for statistical analysis.

Mouse serum and blood chemistry analysis

Blood samples were collected by tail bleeds using capillary blood collection tubes (Microvette CB 300; Sarstedt, Newton, NC). Blood samples were allowed to clot on ice then centrifuged for 10 min at 10,000 x g to collect serum. Serum TG and cholesterol levels were measured using an Infinity kit (Thermo Fisher Scientific, Middletown, VA). Non-esterified free fatty acids were measured using a NEFA-HR (2) kit (Wako Chemicals, Richmond, VA). β-hydroxybutyrate was measured using a LiquiColor assay (Stanbio). Assays were performed according to the manufacturer's protocol.

ELISA

Insulin (Millipore), ANGPTL3 (Thermo) and ANGPTL4 (Aviva Systems Biology) levels were measured in serum according to the manufacturer's protocol.

Glucose and insulin tolerance tests

For glucose tolerance tests (GTTs), mice were fasted overnight (~15 h) and subsequently intraperitoneally injected or orally gavaged with a glucose solution in saline at a dose of 1 g glucose/kg body weight. Blood was collected from the tail vein into capillary blood collection tubes before injection and 15 minutes (min) post-injection for assessment of insulin levels. Serum was isolated from blood and stored at -80°C until analysis. Tail vein blood glucose levels at the indicated time points were monitored with a glucometer (NovaMax Plus, Billerica, MA). For insulin tolerance tests (ITTs), mice were intraperitoneally injected with recombinant human insulin (Gibco) diluted in saline after a 2-h fast at a dose of 1-1.5 units insulin/kg body weight. Food was removed between 9:00 AM and 10:00 AM. Tail vein blood glucose was monitored with a glucometer at the indicated time points.

Lipid tolerance test

After an overnight fast (~15 h), mice were orally gavaged with 20% emulsified intralipid (soybean oil, Sigma) at a dose of 10 μL/g body weight. Blood was collected from the tail vein into capillary blood collection tubes before gavage and 1, 2, 3, and 4 h post-gavage. Serum was isolated from blood samples and assayed for triglyceride (TG) and non-esterified fatty acids (NEFA) using commercially available kits according to the manufacturer's protocol.

Hepatic VLDL-TG secretion

Mice were fasted for 4 h, beginning 2 h into the light cycle. Poloxamer 407 diluted in saline was intraperitoneally injected at a dose of 1 mg/g body weight to inhibit LPL activity. Blood was collected from the tail vein into capillary blood collection tubes before injection and at 1, 2, 4, and 8 h post-injection. Serum was isolated from blood and assayed for TG using a colorimetric kit.

Intestinal lipid absorption and secretion

Overnight fasted mice (~15 h) were intraperitoneally injected with poloxamer 407 diluted in saline at a dose of 1 mg/g body weight to inhibit LPL activity. After 1 h, mice were orally gavaged with 20% emulsified intralipid (10 μL/g body weight). Blood was collected from the tail vein into capillary blood collection tubes before gavage and at 1, 2, 3, and 4 h post-gavage. Serum was isolated from blood samples and assayed for TG using a colorimetric kit.

Blood and tissue collection

Mice were anesthetized with isoflurane and blood was collected from the retro-orbital plexus through heparin-coated capillary tubes (Fisher). Blood samples were allowed to clot on ice then centrifuged for 10 min at 10,000 x g. Separated serum was aliquoted and stored at -80°C. Organs were excised and weighed, then flash frozen in liquid nitrogen before being stored at -80°C.

Complete blood count analysis

A complete blood count on blood samples was performed at the Pathology Phenotyping Core at the Johns Hopkins University School of Medicine. Blood samples were collected from the femoral vein using EDTA-coated blood collection tubes (Sarstedt) and analyzed using Procyte Dx analyzer (IDEXX laboratories).

Serum lipoprotein analysis

Lipoprotein analyses were performed at the Metabolism core at the Baylor College of Medicine. 300 μL of serum were pooled from 10 mice of each genotype (30 μL per mouse). Pooled serum samples from WT and KO mice were subjected to fractionation using fast protein liquid chromatography (FPLC), followed by quantification of TG and cholesterol levels in each fraction.

Heparin releasable LPL activity in serum

Mice were fasted overnight (~13 h) and given free access to food for 2 h. The experiment was conducted as previously described (64). Mice were briefly anesthetized with isoflurane and retro-orbitally injected with heparin sodium salt (Sigma) diluted in saline at a dose of 300 U/kg body weight. Blood was collected from the tail vein into capillary blood collection tubes before

injection and 5 min post-injection. Serum was isolated from blood samples. Pre-heparin serum was used to measure serum TG levels. Total lipase activity was measured using a commercial kit (BioVision) in post-heparin serum.

Mouse histology

Adipose and liver tissues from littermate-matched WT and myonectin-KO mice were fixed in 10% formalin at 4°C overnight. Fixed tissues were embedded in paraffin, sectioned, and stained with hematoxylin and eosin (H&E) at the Histology Reference Laboratory at the Johns Hopkins University School of Medicine.

Adipocyte cell size analysis

Adipocyte size was measured using the "MRI Adipocyte Tools" macro in the ImageJ software. All cells in one field of view at 100X magnification per tissue section per mouse were analyzed from a total of 5 WT and 5 KO littermate-matched mice for visceral (gonadal) white adipose tissue and 4 WT and 5 KO littermate-matched mice for subcutaneous (inguinal) white adipose tissue. On average, 230 cells were measured for each sample.

Extraction and quantification of mouse hepatic lipid contents

50-80 mg of frozen liver tissue was homogenized in 500 μL ultra-pure water. 200 μL lysate were transferred to a new tube and 1 mL of 2:1 chloroform:methanol was added. After thorough mixing, samples were spun at 1,700 rpm for 5 min at 4°C. The lower chloroform phase was transferred to a new tube and dried in a speed vacuum. Extracted lipids were resuspended in 5% Triton x100 in saline. Samples were assayed for TG and cholesterol using commercially available

colorimetric kits (Thermo Scientific). Protein content was measured in the original water lysate using BCA assay (Thermo), and lipid levels were normalized to total protein.

Western blotting

Frozen tissue samples were homogenized in RIPA buffer (50 mM Tris-HCl, pH 7.4; 150 mM NaCl; 1 mM EDTA; 1% Triton X-100; 0.25% deoxycholate) supplemented with a protease inhibitor cocktail (Sigma) and a phosphatase inhibitor cocktail (Roche). Protein content was measured using BCA assay. Samples for Western blotting were diluted in SDS loading dye (final concentration: 50 mM Tris-HCl, pH 7.4, 2% SDS, 6% glycerol, 1% 2-mercaptoethanol, and 0.01% bromphenol blue) and denatured at 95°C for 10 min. 10-20 μg total protein were loaded into each lane of a 10% polyacrylamide gel (BioRad) and separated by electrophoresis. The BioRad Trans-Blot Turbo semi-dry system was used to transfer protein onto PVDF membranes. Blots were blocked in 5% non-fat milk in PBST then exposed to primary antibodies overnight at 4°C. After washing, blots were exposed to secondary antibodies conjugated to HRP for 1 h then developed in ECL (Amersham ECL select). Bands were visualized with MultiImage III FluorChem Q (Alpha Innotech) and quantified using Alphaview Software (Alpha Innotech). All primary antibodies were diluted 1:1000 in PBST + 0.02% sodium azide and all secondary antibodies were diluted 1:5,000 in 5% non-fat milk in PBST. Antibodies used: LPL (GeneTex, GTX101125), Hsc70 (Santa Cruz, sc-7298), perilipin 2 (Thermo, PA1-16972), mouse IgG-HRP (Cell Signaling, 7076), and rabbit IgG-HRP (Cell Signaling, 7074).

Liver metabolomics analysis

Metabolite quantifications of WT (n=10) and myonectin-KO (n=10) liver samples were performed by Metabolon (Morrisville, NC) using their metabolomics platform. Sample processing, compound identification by tandem mass spectrometry, metabolite quantification and data normalization, data extraction, and curation were all performed according to the standard protocol of Metabolon.

Stimulated adipose tissue lipolysis

Mice were fasted for 5 h beginning at 9:30 AM. The β_3-adrenergic receptor agonist, CL 316-243 (Santa Cruz), was diluted in saline and intraperitoneally injected at a dose of 1 mg/kg body weight. Blood was collected from the tail vein into capillary blood collection tubes before injection and at 15 min post-injection. Blood glucose was monitored with a glucometer before and at 15 min after CL 316-243 injection. Serum was separated from blood and assayed for NEFA and glycerol using calorimetric kits (Wako and Sigma, respectively).

Tissue LPL activity

Tissue LPL activity was measured as previously described (65). Briefly, frozen tissue samples were pulverized in liquid nitrogen using a mortar and pestle. Approximately 50 mg pulverized tissue were incubated in Krebs-Ringer solution containing BSA and heparin. After clarifying, the supernatant was used to measure LPL activity using a commercial kit (Roar Biomedical). Activity was normalized to tissue weight.

Quantitative real-time PCR analysis

RNA was isolated from tissues using TRIzol reagent (Invitrogen) according to the manufacturer's protocol and treated with DNAse I (New England Biolabs) to remove genomic DNA. For each sample, 1-2 μg total RNA were reverse transcribed using random primers and the GoScript reverse transcription system from Promega. Quantitative real-time PCR was performed on a CFX connect system using iTaq Universal SYBR Green PCR master mix (BioRad). Gene expression was first normalized to *36b4* [also known as acidic ribosomal phosphoprotein P0 (*Rplp0*)] to generate a ΔC_t value, and then $\Delta\Delta C_t$ was obtained by normalizing data to mean ΔC_t of the control group (66). Primers used are listed in **Table 1**.

Maximal exercise capacity

Maximal sprint and endurance exercise tests were performed as we described previously (67). Briefly, 12-week-old mice fed a standard chow diet were first subjected to the endurance exercise test. Mice were acclimated to the treadmill for three days before the experiment and the exercise test was carried out on the fourth day. Blood glucose and lactate values were measured before and after exercise using glucose and lactate meters (Nova Biomedical). Blood was collected from the tail vein into capillary blood collection tubes before and after exercise, and silver nitrate sticks were used to cauterize the wound. Mice were run in multiple groups beginning at 9:30 AM until exhaustion. After 2.5 weeks of recovery, mice were subjected to the sprint exercise test. A day before the experiment, mice were re-acclimated to the treadmill using the same protocol as the original day-3 acclimation. For the sprint exercise experiment, mice were run in multiple groups beginning at 8:30 AM until exhaustion. As with the endurance test, blood, glucose, and lactate were collected before and after exercise. The experimenter was blinded with respect to genotype during all exercise tests.

Table 1

Gene	Alias	Forward primer (5' to 3')	Reverse primer (5' to 3')
Rplp0	36B4	AGATTCGGGATATGCTGTTGGC	TCGGGTCCTAGACCAGTGTTC
myonectin (primer set # 1)		TGCTTGGATGCTGTTCGTCAA	CAGATGGGATAAAGGGGCCTG
myonectin (primer set # 2)		GCGAGAGAGCCATCTGGAGCACTG	GGTCCCTTTCTTGGCTGCTCGGTG
Abca1		GCTGCAGGAATCCAGAGAAT	CATGCACAAGGTCCTGAGAA
Abcg5		AGGGCCTCACATCAACAGAG	GCTGACGCTGTAGGACACAT
Abcg8		CTGTGGAATGGGACTGTACTTC	GTTGGACTGACCACTGTAGGT
Acaca	ACC1	TGACAGACTGATCGCAGAGAAAG	TGGAGAGCCCCACACACA
Acacb	ACC2	GGGCTCCCTGGATGACAAC	GCTCTTCCGGGAGGAGTTCT
Acadl	LCAD	TCTTTTCCTCGGAGCATGACA	GACCTCTCTACTCACTTCTCCAG
Acadm	MCAD	AGGGTTTAGTTTTGAGTTGACGG	CCCCGCTTTTGTCATATTCCG
Acox1		AGATTGGTAGAAATTGCTGCAAA	ACGCCACTTCCTTGCTCTTC
Alas1		TCGCCGATGCCCATTCTTATC	GGCCCCAACTTCCATCATCT
Angptl3		GAGGAGCAGCTAACCAACTTAAT	TCTGCATGTGCTGTTGACTTAAT
Angptl4		CCAAGACCATGACCTCCGTG	CGTTGCCGTGGGATAGAGTG
Angptl8		CTGACCCTGCTCTTTCACGG	GCTCTGTCATAGAGGCCCAG
Apoa1		AAGAGGATGTGGAGCTCTACC	TTCTCGCCAAGTGTCTTCAGG
Apoa4		CAGTGAGGAGCCCAGGATGTT	TCTACAGCCTCCTTGGCATT
Apoa5		TCCTCGCAGTGTTCGCAAG	CGAAGCTGCCTTTCAGGTTCT
Apoc2		AGGTTCCGGCTTGATGAGAA	AGTGGGTTGGCAGGCTTTAT
Apoc3		TACAGGGCTACATGGAACAAGC	CAGGGATCTGAAGTGATTGTCC
Apoe		CTGACAGGATGCCTAGCCG	CGCAGGTAATCCCAGAAGC
Atg12		TGGCCTCGGAACAGTTGTTTA	GGGCAAAGGACTGATTCACAT
Atg5		TGTGCTTCGAGATGTGTGGTT	ACCAACGTCAAATAGCTGACTC
Atg7		CCTGCACAACACCAACACAC	CACCTGACTTTATGGCTTCCC
Bdh1		TGACACCCGTCGGACCTAC	TTCTCAGTCGGTCACTCTTCA
Cav1		GGACATCTCTACACTGTTCCCA	CGCGTCATACACTTGCTTCT
Cd36		ATGGGCTGTGATCGGAACTG	AGCCAGGACTGCACCAATAAC
Cebpa		CAAGAACAGCAACGAGTACCG	GTCACTGGTCAACTCCAGCAC
Cpt1a		CACCAACGGGCTCATCTTCTA	CAAAATGACCTAGCCTTCTATCGAA
Cyp27a1		CCAGGCACAGGAGAGTACG	GGGCAAGTGCAGCACATAG
Cyp7a1		GGGATTGCTGTGGTAGTGAGC	GGTATGGAATCAACCCGTTGTC
Cyp7b1		GGAGCCACGACCCTAGATG	TGCCAAGATAAGGAAGCCAAC
Cyp8b1		CCTCTGGACAAGGGTTTTGTG	GCACCGTGAAGACATCCCC
Dgat1		GCCTTACTGGTTGAGTCTATCAC	GCACCACAGGTTGACATCC
Dgat2		GCGCTACTTCCGAGACTACTT	GGGCCTTATGCCAGGAAACT
Fabp1		ATGAACTTCTCCGGCAAGTACC	GGTCCTCGGGCAGACCTAT
Fabp4		ATCAGCGTAAATGGGGATTTGG	GTCTGCGGTGATTTCATCGAA
Fasn	FAS	GGAGGTGGTGATAGCCGGTAT	TGGGTAATCCATAGAGCCCAG
G6pc		CGACTCGCTATCTCCAAGTGA	GTTGAACCAGTCTCCGACCA
Gpam	GPAT1	CAACACCATCCCCGACATC	GTGACCTTCGATTATGCGATCA
Gpat3		GGCCTTCGGATTATCCCTGG	CTTGGGGGCTCCTTTCTGAA
Gpihbp1		AGGGCTGTCCTCCTGATCTTG	GGGTCCGCATCACCATCTT
Hamp	hepcidin	GCAGAAGAGAAGGAAGAGAGACACC	TGTAGAGAGGTCAGGATGTGGCTC
Hfe		CGGGCTGCCTTTGTTTGAG	CTGGCTTGAGGTTTGCTCC
Hmgcr		CTTGTGGAATGCCTTGTGATTG	AGCCGAAGCAGCACATGAT
Hmox1		AAGCCGAGAATGCTGAGTTCA	GCCGTGTAGATATGGTACAAGGA
Hnf4a		CACGCGGAGGTCAAGCTAC	CCCAGAGATGGGAGAGGTGAT
Lcat		GTAACCACACACGGCCTGTC	TCTTACGGTAGCACATCCAGTT
Ldlr		TCAGACGAACAAGGCTGTCC	CCATCTAGGCAATCTCGGTCTC
Lipc	hepatic lipase	CCCTGGCATACCAGCACTAC	CTCCGAGAAAACTTCGCAGATT
Lipe	HSL	GCTGGGCTGTCAAGCACTGT	GTAACTGGGTAGGCTGCCAT
Lpl		GGGAGTTTGGCTCCAGAGTTT	TGTGTCTTCAGGGGTCCTTAG
Lrp1		GACCAGGTGTTGGACACAGATG	AGTCGTTGTCTCCGTCACACTTC

Table 1 – continued

Gene	Alias	Forward primer (5' to 3')	Reverse primer (5' to 3')
Mgll	monoglyceride lipase	CGGACTTCCAAGTTTTTGTCAGA	GCAGCCACTAGGATGGAGATG
Mlxipl	ChREBP	AGATGGAGAACCGACGTATCA	ACTGAGCGTGCTGACAAGTC
mt-Co2		GCCGACTAAATCAAGCAACA	CAATGGGCATAAAGCTATGG
mt-Cytb		CATTTATTATCGCGGCCCTA	TGTTGGGTTGTTTGATCCTG
Mylip		AGGAGATCAACTCCACCTTCTG	ATCTGCAGACCGGACAGG
Nr1h4	FXR	GCTTGATGTGCTACAAAAGCTG	CGTGGTGATGGTTGAATGTCC
Pck1	PEPCK	CTGCATAACGGTCTGGACTTC	CAGCAACTGCCCGTACTCC
Pcsk9		TTGCAGCAGCTGGGAACTT	CCGACTGTGATGACCTCTGGA
Pnpla2	ATGL	TGTGGCCTCATTCCTCCTAC	TCGTGGATGTTGGTGGAGCT
Pparg		TCGCTGATGCACTGCCTATG	GAGAGGTCCACAGAGCTGATT
Ppargc1a	PGC1-α	GGAGCCGTGACCACTGACA	TGGTTTGCTGCATGGTTCTG
Sdc1		CTTTGTCACGGCAGACACCTT	GACAGAGGTAAAAGCAGTCTCG
Slc27a1	FATP1	CTGGGACTTCCGTGGACCT	TCTTGCAGACGATACGCAGAA
Slc27a5	FATP5	GTTCTCCCGTCCAAGACCATT	GCTCCGTACAGAGTGTAGCAAG
Slc40a1	ferroportin	TGGAACTCTATGGAAACAGCCT	TGGCATTCTTATCCACCCAGT
Sqle		ATAAGAAATGCGGGGATGTCAC	ATATCCGAGAAGGCAGCGAAC
Srebf1		GGAGCCATGGATTGCACATT	GGCCCGGGAAGTCACTGT
Srebf2		GCGTTCTGGAGACCATGGA	ACAAAGTTGCTCTGAAAACAAATCA
Vldlr		GAGCCCCTGAAGGAATGCC	CCTATAACTAGGTCTTTGCAGATATGG

Table 1. Primers used for quantitative real-time PCR analyses

Recovery after endurance exercise

Mice used in this experiment were fed a standard chow diet. Mice were acclimated to the treadmill as previously described, but with the addition of a fourth acclimation day in which mice ran on the treadmill at 14 m/min for 5 min at a 10° incline (67). The endurance exercise run was performed on the fifth day when the mice were 11 weeks of age. Mice were fasted for 2 h in the morning before exercise. The run was conducted as previously described (68): 60 min at a speed of 14 m/min at a 10° incline. A shock grid at the back of the treadmill encouraged mice to continue running by administering a mild shock each time they stepped off the belt. If any mice met the pre-determined criteria for exhaustion before the end of the run, they were removed from the treadmill and their data were omitted from analysis (67). The experimenter was blinded with respect to genotype during the treadmill run. Blood glucose and lactate values were measured at the indicated time points using glucose and lactate meters (Nova Biomedical). One cohort of mice received a

glucose gavage within 5 min of the end of the run (0.5 mg glucose/g body weight dissolved in saline). All mice were allowed to recover in their cages with free access to water but no food. After 2 h of recovery following the end of the run, mice were euthanized. Blood and tissues were collected as described above.

Tissue glycogen measurement

Tissue glycogen was measured using a protocol adapted from the NIH-funded Mouse Metabolic Phenotyping Centers (https://mmpc.org/shared/protocols.aspx). Frozen whole liver and gastrocnemius muscle were pulverized in liquid nitrogen. Approximately 25 mg liver tissue or 50 mg muscle were homogenized in 400 µL 0.9 N perchloric acid. Samples were clarified by centrifuging at 10,000 x g for 10 min at 4°C and transferring the supernatant to a new tube. 50 µL supernatant were transferred to each of two reaction tubes, along with 25 µL 1M potassium bicarbonate and 125 µL 0.4 M sodium acetate buffer (pH 4.8) with or without 5 mg/mL amyloglucosidase (Sigma). Reactions were incubated for 2 h at 40°C on a heat block. After 2 h, reactions were neutralized with NaOH then vortexed and centrifuged for 3 min at 10,000 x g at room temperature. Twenty µL of supernatant from each reaction was used to measure glucose using an Amplex Red glucose assay kit (Invitrogen) according to the manufacturer's protocol. Amyloglucosidase hydrolyzes glycogen into free glucose monomers. For each tissue sample, the amount of glucose in the condition without amyloglucosidase (measuring free glucose) was subtracted from the amount of glucose in the condition with amyloglucosidase (measuring free glucose + glucose from glycogen) to yield the amount of glucose from glycogen only. This value was then normalized to tissue weight.

Statistical analysis

Comparisons between two groups of data were performed using two-tailed Student's t-tests with Welch's correction and 95% confidence intervals. For experiments with two independent variables, a 2-way ANOVA was conducted and the Bonferroni method was used for multiple comparisons. Graphpad Prism 7 software was used to conduct analyses. Values were considered significant at $P < 0.05$. All data are presented as mean ± SEM. * $P < 0.05$, ** $P < 0.01$, *** $P < 0.001$.

RESULTS

Myonectin-deficient mouse model

We used a whole-body knockout (KO) mouse model to assess the metabolic function of myonectin *in vivo*. To create a myonectin-null allele, exons 2 through 7 of the myonectin gene were replaced with a neomycin cassette (**Fig. 1A**). Using one set of primers that targeted the WT myonectin gene and another set that targeted the neomycin cassette, we could distinguish between WT, heterozygous, and homozygous null mice (**Fig. 1B**). To verify that myonectin was not expressed in the KO mice, we measured myonectin mRNA levels in the skeletal muscle—the tissue with the highest expression in WT mice (28)—by quantitative PCR. Using two independent primer sets, we confirmed the absence of myonectin transcript (**Fig. 1C**). In the absence of a reliable antibody that can recognize endogenous myonectin without cross-reactivity, we did not quantify myonectin protein level in WT and KO mice. Myonectin KO mice were viable, fertile, born at the expected Mendelian ratio, and exhibited no gross developmental abnormalities.

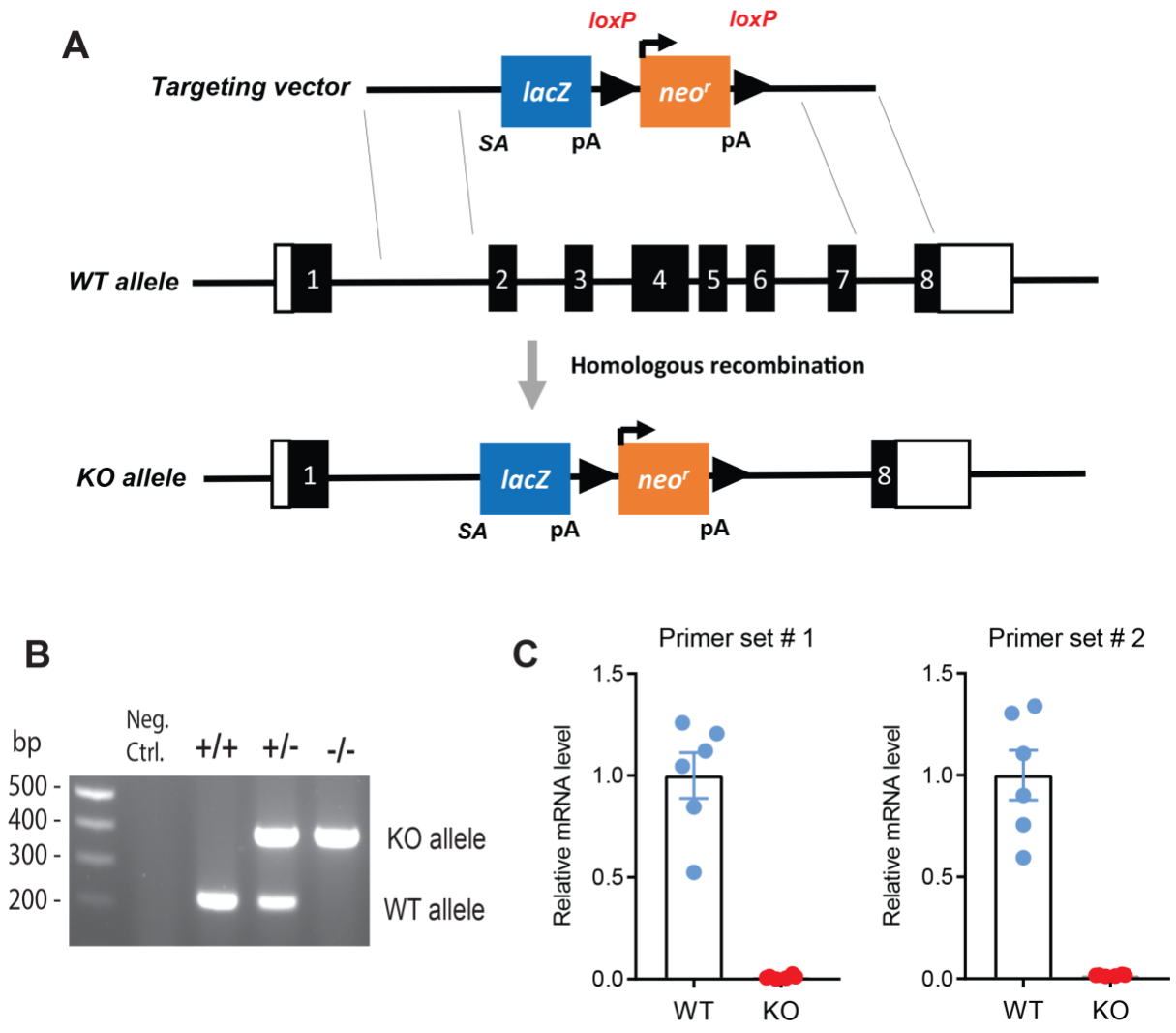

Figure 1. Myonectin-deficient mouse model. (A) Schematic of the gene targeting strategy used to generate myonectin-knockout (KO) mice. The majority of the myonectin gene (exons 2-7) was replaced with a neomycin resistance gene and lacZ reporter cassette. SA, splice acceptor; pA, polyadenylation signal. (B) PCR genotyping showing successful production of wildtype (+/+), heterozygous (Het; +/-), and homozygous KO (-/-) mice. (C) The absence of myonectin transcript in the mouse gastrocnemius muscle was confirmed by quantitative PCR using two independent primer pairs. Primer set #1 targets exon 2 and 3, yielding a PCR product size of 143 bp. Primer set #2 targets exon 4 and 6, yielding a PCR product size of 381 bp. WT n=6 and KO n=6 female mice.

Myonectin is not required for the physiological response to exercise

Under basal conditions, myonectin is primarily produced in skeletal muscle and its expression can be further induced by exercise (28, 29). We therefore first tested whether it is

required for the physiological response to exercise. During both maximal sprint and endurance exercise on a treadmill, loss of myonectin had no impact on total running distance and the post-exercise serum levels of glucose, lactate, non-esterified free fatty acids, triglyceride, and ketone (β-hydroxybutyrate) levels in female WT and KO mice (**Table 2**). However, we did observe significantly higher pre-exercise serum ketones (β-hydroxybutyrate) in KO female mice relative to WT littermate controls. For male mice, with the exception of post-sprint exercise serum triglyceride levels that were significantly lower in the KO animals, no significant genotypic differences were noted in exercise parameters (**Table 2**). In the post-exercise recovery phase (with or without glucose gavage post-exercise), myonectin deficiency did not significantly affect the ability of KO animals to replenish their skeletal muscle or liver glycogen stores (**Table 3**). These results indicate that myonectin is not required for physiologic response and adaptation to an acute bout of exercise.

Myonectin knockout mice fed a control low-fat diet show no overt metabolic phenotypes

Given its potential role as a postprandial metabolic regulator (28, 36), we tested whether myonectin is necessary for metabolic homeostasis under basal conditions. Male and female WT and KO mice were fed a control low-fat diet (LFD) for 12 weeks, beginning at 6 weeks of age. Neither sex displayed genotypic differences in body weight over time or in body composition (**Fig. 2A-B**). Organ weights (heart, kidney, spleen, liver, and adipose tissue) were also not different between genotypes of either sex (**Table 4**). Indirect calorimetry revealed no differences in *ad-libitum* food intake, metabolic rate, or energy expenditure between WT and KO mice of either sex (**Tables 5 and 6**). However, *ad-libitum* fed female KO mice had a higher respiratory exchange ratio (RER) in the dark cycle and lower physical activity in the light cycle.

	Female mice			Male mice		
	WT	KO	*P*-value	WT	KO	*P*-value
Endurance exercise capacity						
N	14	15		9	14	
Time to exhaustion (min)	116.1 ± 5.253	125.0 ± 4.317	0.2052	99.1 ± 7.172	101.5 ± 3.694	0.7714
Running distance (m)	1770 ± 117.5	1968 ± 101.6	0.2135	1406 ± 141.2	1447 ± 75.8	0.8031
Pre-exercise glucose (mg/dL)	161.9 ± 4.655	157.9 ± 3.933	0.5253	190.2 ± 6.357	183.3 ± 3.758	0.3640
Post-exercise glucose (mg/dL)	148.5 ± 11.27	128.9 ± 6.84	0.1508	175.1 ± 17.39	161.4 ± 8.85	0.4953
Pre-exercise lactate (mM)	2.000 ± 0.0989	1.873 ± 0.1197	0.4219	1.433 ± 0.1424	1.550 ± 0.1763	0.6120
Post-exercise lactate (mM)	5.232 ± 0.3179	5.013 ± 0.3570	0.6508	5.300 ± 0.6388	4.779 ± 0.4960	0.5278
Pre-exercise TG (mg/dL)	56.75 ± 5.872	50.17 ± 4.273	0.3740	53.01 ± 7.726	57.32 ± 6.143	0.6675
Post-exercise TG (mg/dL)	52.00 ± 2.629	53.31 ± 2.485	0.7202	37.13 ± 2.472	43.26 ± 2.363	0.0905
Pre-exercise NEFA (mM)	1.225 ± 0.0940	1.035 ± 0.0652	0.1113	1.196 ± 0.0543	1.172 ± 0.1284	0.8662
Post-exercise NEFA (mM)	2.387 ± 0.1764	2.756 ± 0.1466	0.1196	1.633 ± 0.1979	2.020 ± 0.2182	0.2049
Pre-exercise β-hydroxybutyrate (μM)	**122.4 ± 8.09**	**163.8 ± 17.07 ***	**0.0405**	139.2 ± 10.93	133.0 ± 15.28	0.7445
Post-exercise β-hydroxybutyrate (μM)	545.7 ± 47.10	623.3 ± 52.92	0.2830	377.0 ± 58.62	370.2 ± 44.52	0.9278
Sprint exercise capacity						
N	15	15		9	12	
Time to exhaustion (min)	14.52 ± 0.4734	14.71 ± 0.5862	0.7999	12.90 ± 0.6590	12.97 ± 0.4013	0.9373
Running distance (m)	244.4 ± 13.20	250.6 ± 17.11	0.7764	200.8 ± 17.31	201.2 ± 10.79	0.9851
Pre-exercise glucose (mg/dL)	169.6 ± 5.266	176.1 ± 4.392	0.3491	180.8 ± 4.481	186.1 ± 5.140	0.4461
Post-exercise glucose (mg/dL)	180.8 ± 3.558	176.3 ± 5.092	0.4788	221.9 ± 8.093	209.8 ± 5.042	0.2219
Pre-exercise lactate (mM)	2.270 ± 0.2750	2.027 ± 0.1584	0.4512	1.711 ± 0.1184	1.917 ± 0.1753	0.3440
Post-exercise lactate (mM)	11.02 ± 0.4419	10.29 ± 0.5822	0.3293	8.872 ± 1.116	9.700 ± 0.803	0.5559
Pre-exercise TG (mg/dL)	48.40 ± 4.332	49.07 ± 4.985	0.9203	59.03 ± 4.007	54.92 ± 3.592	0.4559
Post-exercise TG (mg/dL)	46.93 ± 2.458	48.55 ± 2.033	0.6159	**56.55 ± 3.604**	**45.31 ± 2.351 ***	**0.0202**
Pre-exercise NEFA (mM)	1.083 ± 0.1190	0.856 ± 0.1453	0.2368	1.199 ± 0.0983	1.307 ± 0.1314	0.5187
Post-exercise NEFA (mM)	1.012 ± 0.0526	0.919 ± 0.1231	0.4964	0.982 ± 0.1055	0.814 ± 0.0894	0.2403
Pre-exercise β-hydroxybutyrate (μM)	**199.6 ± 13.41**	**244.9 ± 15.74 ***	**0.0371**	161.9 ± 21.62	203.9 ± 33.47	0.3055
Post-exercise β-hydroxybutyrate (μM)	224.0 ± 17.87	239.6 ± 14.98	0.5103	204.8 ± 24.29	224.4 ± 20.16	0.5423

Table 2. Time to exhaustion, total distance run, and blood parameters during an endurance exercise capacity test or a sprint exercise capacity test in chow-fed male and female WT and myonectin-KO mice. Mice were 12 weeks of age for the endurance test and 14.5 weeks of age for the sprint test. Values that are statistically significant (*P<0.05) are bolded and underlined.

	Female mice			Male mice		
	WT	KO	*P*-value	WT	KO	*P*-value
No glucose gavage post exercise						
N	6	5		5	6	
Body weight (g)	18.23 ± 0.3836	18.10 ± 0.8701	0.8934	25.50 ± 0.7668	24.38 ± 0.7631	0.3293
Liver weight (g)	0.7950 ± 0.0193	0.7340 ± 0.0370	0.1928	1.076 ± 0.0367	1.040 ± 0.0357	0.4999
Pre-exercise glucose (mg/dL)	181.5 ± 5.30	187.0 ± 10.70	0.6614	211.8 ± 6.63	201.0 ± 8.67	0.3487
0 min post-exercise glucose (mg/dL)	184.5 ± 6.35	191.6 ± 13.31	0.6478	207.0 ± 13.02	211.3 ± 11.13	0.8064
30 min post-exercise glucose (mg/dL)	158.2 ± 7.85	150.4 ± 11.60	0.5959	159.0 ± 6.46	158.0 ± 6.81	0.9175
60 min post-exercise glucose (mg/dL)	144.7 ± 13.11	154.8 ± 6.84	0.5139	140.8 ± 10.96	163.3 ± 5.90	0.1183
120 min post-exercise glucose (mg/dL)	127.8 ± 5.88	135.2 ± 5.08	0.3682	145.4 ± 12.84	154.2 ± 4.74	0.5496
Pre-exercise lactate (mM)	1.750 ± 0.1057	1.560 ± 0.0980	0.2200	2.400 ± 0.4572	2.033 ± 0.1333	0.4783
0 min post-exercise lactate (mM)	3.950 ± 0.2814	4.300 ± 0.7987	0.6965	4.460 ± 0.1778	4.400 ± 0.3907	0.8928
Muscle glycogen (nmol glucose from glycogen/mg tissue)	9.75 ± 0.5824	10.53 ± 1.3198	0.6115	11.16 ± 1.085	12.37 ± 1.981	0.6097
Liver glycogen (nmol glucose from glycogen/mg tissue)	30.81 ± 7.6927	12.10 ± 0.8849	0.0591	67.37 ± 19.70	78.24 ± 11.16	0.6470
With glucose gavage post exercise						
N	5	6		5	5	
Body weight (g)	19.94 ± 0.3444	20.33 ± 0.8887	0.6932	24.12 ± 0.5417	24.86 ± 0.6823	0.4216
Liver weight (g)	0.8300 ± 0.0319	0.8417 ± 0.0464	0.8409	1.006 ± 0.0279	1.008 ± 0.0323	0.9638
Pre-exercise glucose (mg/dL)	162.2 ± 7.51	160.7 ± 4.82	0.8684	198.2 ± 7.37	192.2 ± 5.21	0.5270
0 min post-exercise glucose (mg/dL)	150.8 ± 17.89	159.5 ± 8.31	0.6754	197.4 ± 12.48	192.0 ± 10.22	0.7467
30 min post-exercise glucose (mg/dL)	137.6 ± 9.48	153.2 ± 4.52	0.1906	179.0 ± 2.19	172.6 ± 8.35	0.4948
60 min post-exercise glucose (mg/dL)	127.7 ± 6.74	129.0 ± 2.00	0.8649	156.0 ± 13.00	154.7 ± 0.67	0.9350
120 min post-exercise glucose (mg/dL)	103.8 ± 12.01	105.5 ± 7.98	0.9094	139.4 ± 7.90	137.8 ± 4.42	0.8652
Pre-exercise lactate (mM)	1.580 ± 0.1068	1.517 ± 0.0601	0.6225	1.540 ± 0.0872	1.740 ± 0.1568	0.3060
0 min post-exercise lactate (mM)	6.520 ± 1.3782	4.433 ± 0.7697	0.2316	2.800 ± 0.1140	4.600 ± 1.1406	0.1901
Muscle glycogen (nmol glucose from glycogen/mg tissue)	9.63 ± 0.5762	10.56 ± 0.2763	0.1976	12.15 ± 0.835	12.91 ± 0.836	0.5347
Liver glycogen (nmol glucose from glycogen/mg tissue)	27.91 ± 4.6121	44.47 ± 9.4856	0.1596	42.61 ± 17.04	47.36 ± 11.02	0.8216

Table 3. Chow-fed Male and female WT and myonectin-KO mice (at 11 weeks of age) were subjected to an endurance run on the treadmill, and blood glucose and lactate values were measured at the indicated timepoints. Half of the mice received a glucose gavage immediately after completing the run. All mice were allowed to recover for 2 h before euthanization.

Similar to the female KO mice, *ad-libitum* fed male KO mice also had significantly lower physical activity in the light cycle and over a 24-hr period. Myonectin is robustly induced upon re-feeding following a fast (36). We therefore challenged the WT and KO mice with a 24-h fast followed by 24-h free access to food while they were in the metabolic cages. No genotypic differences in either sex were observed during the fast (**Tables 5 and 6**). However, in the refeeding phase, female KO

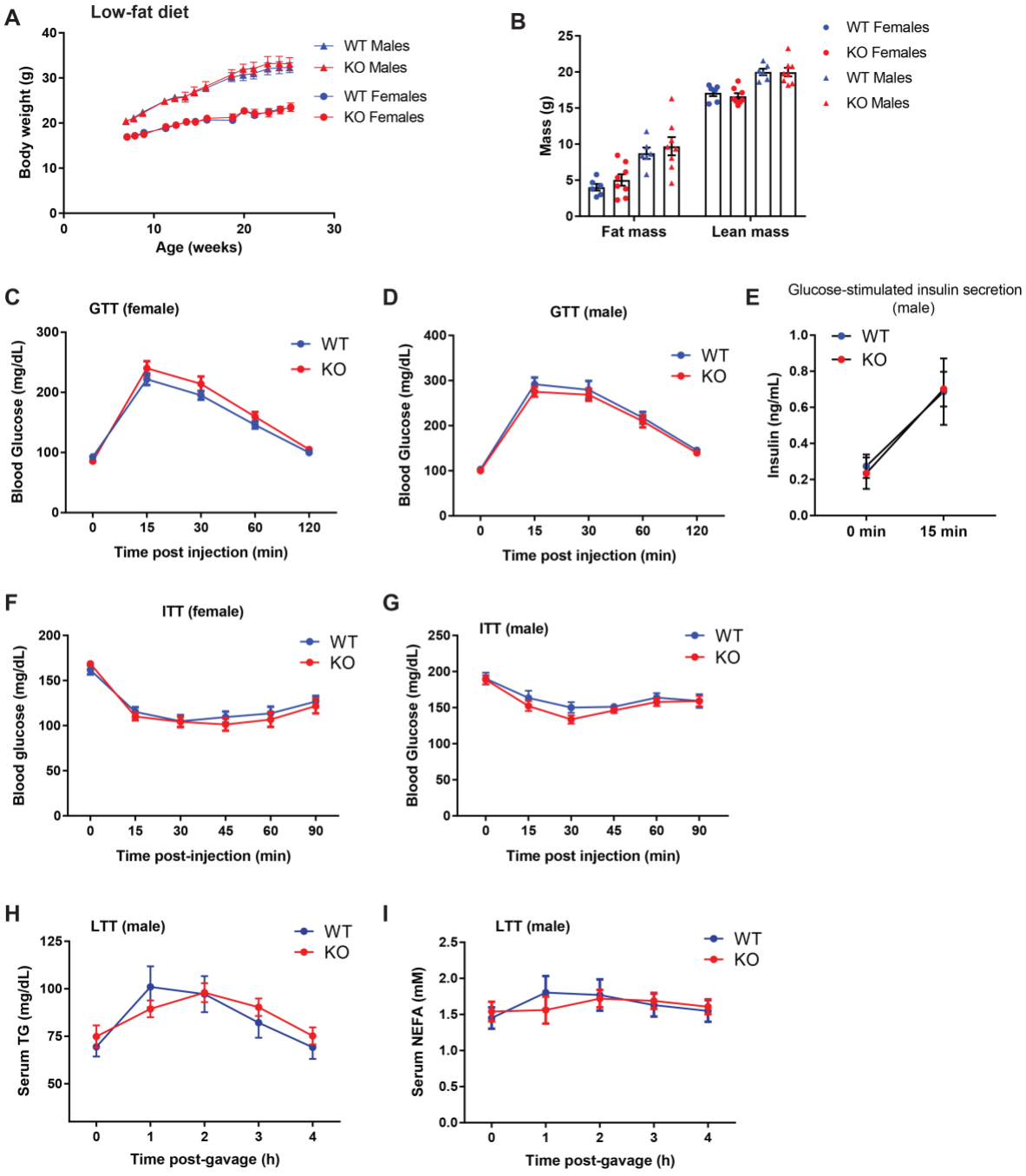

Figure 2. No overt metabolic phenotypes were observed in myonectin-KO mice fed a control low-fat diet. (A) Body weights of female (WT, n=6; KO, n=8) and male (WT, n=6; KO, n=8) mice over time. Mice were weaned at 3.5 weeks of age onto a standard chow diet. At 6 weeks of age, the diet was switched to a control low-fat diet (Research Diets). (B) Body composition analysis of female (WT, n=6; KO, n=8) and male (WT, n=6; KO, n=8) mice at 29 weeks of age. (C-D) Blood glucose levels during glucose tolerance tests (GTT) in female (WT, n=12; KO, n=13) and male (WT, n=12; KO, n=17) mice at 18 weeks of age. (E) Serum insulin levels in male mice at 0 min before glucose injection (WT, n=5; KO, n=5) and at 15 min after glucose injection (WT, n=6, KO, n=9); for some samples, insulin levels were below the threshold of detection. (F-G) Blood glucose levels during insulin tolerance tests (ITT) in female (WT, n=12; KO, n=13)

and male (WT, n=5; KO, n=7) mice at 24 weeks of age. Insulin was injected at a dose of 1 unit/kg body weight for both males and females. (H-I) Serum TG (H) and NEFA (I) levels during lipid tolerance tests (LTT) in male mice (WT, n=12; KO, n=15-16) at 23 weeks of age.

	Female Mice			**Male Mice**		
	WT	KO	*P*-value	WT	KO	*P*-value
Low fat diet						
N	6	5		12	16	
Body weight (g)	26.82 ± 1.096	25.70 ± 0.752	0.4240	35.87 ± 1.095	35.64 ± 1.194	0.8898
Blood glucose (mg/dL)	155.5 ± 4.951	170.2 ± 9.687	0.2251	190.3 ± 5.656	186.3 ± 4.079	0.5703
Liver weight (g)	1.273 ± 0.0943	1.178 ± 0.0658	0.4298	1.648 ± 0.0988	1.608 ± 0.1383	0.8186
eWAT weight (g)	0.3517 ± 0.0393	0.3460 ± 0.0414	0.9232	0.8500 ± 0.0581	0.8200 ± 0.0569	0.7154
iWAT weight (g)	0.2917 ± 0.0329	0.2440 ± 0.0303	0.3141	0.5917 ± 0.0535	0.5753 ± 0.0428	0.8139
Kidney weight (g)	0.1117 ± 0.0040	0.1120 ± 0.0049	0.9593	0.1567 ± 0.0095	0.1514 ± 0.0070	0.6687
Heart weight (g)	0.1517 ± 0.0079	0.1580 ± 0.0097	0.6263	0.2267 ± 0.0196	0.2100 ± 0.0089	0.4638
Spleen weight (g)	0.0983 ± 0.0087	0.1300 ± 0.0147	0.1223	0.0833 ± 0.0068	0.0856 ± 0.0085	0.8349
High fat diet						
N	7	8		12	16	
Body weight (g)	53.06 ± 0.818	55.29 ± 1.725	0.2700	50.98 ± 0.890	51.91 ± 1.065	0.5092
Blood glucose (mg/dL)	198.4 ± 10.00	201.0 ± 9.58	0.8556	196.5 ± 10.62	194.0 ± 6.95	0.8458
Liver weight (g)	1.786 ± 0.1177	1.771 ± 0.1085	0.9294	2.837 ± 0.1359	2.493 ± 0.1302	0.0793
eWAT weight (g)	**2.266 ± 0.1038**	**2.646 ± 0.1096 ***	**0.0256**	**0.806 ± 0.0564**	**1.009 ± 0.0702 ***	**0.0329**
iWAT weight (g)	1.596 ± 0.0695	1.819 ± 0.0784	0.0530	**1.289 ± 0.0485**	**1.445 ± 0.0470 ***	**0.0296**
Kidney weight (g)	0.1429 ± 0.0064	0.1400 ± 0.0044	0.7207	0.2108 ± 0.0060	0.2033 ± 0.0058	0.3771
Heart weight (g)	0.1479 ± 0.0051	0.1500 ± 0.0073	0.8142	0.1808 ± 0.0069	0.1907 ± 0.0090	0.3951
Spleen weight (g)	0.1443 ± 0.0207	0.1338 ± 0.0146	0.6854	0.1200 ± 0.0049	0.1163 ± 0.0069	0.6633

Table 4. Body weight, blood glucose, and organ weights from WT and myonectin-KO mice. All mice were euthanized after 2-4 h food removal in the morning. At the time of sacrifice, LFD-fed males and females were 35 weeks old, and HFD males and females were 39 weeks old. For LFD-fed males, N= 6 WT and 8 KO for kidney and heart weights. Values that are statistically significant (* $P < 0.05$) are bolded and underlined.

mice had lower RER in the light cycle, and male KO mice had significantly reduced physical activity in the dark cycle and over a 24-hr period (**Tables 5 and 6**). Because myonectin is also upregulated after an acute bout of exercise (28), we provided the WT and KO mice with a voluntary running wheel in the metabolic cages in a separate experiment. No major genotypic differences in either sex were observed (**Table 7**).

	Low-fat diet (female)								
	WT	KO	*P*-value	WT	KO	*P*-value	WT	KO	*P*-value
	***Ad-libitum* (dark cycle)**			***Ad-libitum* (light cycle)**			***Ad-libitum* (24 hr)**		
N	6	6		6	6		6	6	
Body weight (g)							23.69 ± 0.71	23.67 ± 0.78	0.9816
Food intake (kcal)	11.34 ± 0.5525	13.30 ± 0.8616	0.0979	4.00 ± 0.3027	3.52 ± 0.4833	0.4293	15.34 ± 0.6757	16.98 ± 0.7156	0.1262
VO2 (mL/kg lean mass/h)	6226 ± 360.15	6211 ± 266.79	0.9751	5078 ± 221.79	5153 ± 47.77	0.7562	5650 ± 239.43	5680 ± 131.95	0.9144
VCO2 (mL/kg lean mass/h)	5980 ± 288.22	6222 ± 229.13	0.5264	4337 ± 213.50	4453 ± 68.20	0.6219	5153 ± 193.94	5333 ± 91.15	0.4282
RER (VCO2/VO2)	**0.9632 ± 0.0100**	**1.0035 ± 0.0139 ***	**0.0424**	0.8533 ± 0.0119	0.8644 ± 0.0120	0.5242	0.9133 ± 0.0087	0.9398 ± 0.0101	0.0750
EE (kcal/kg lean mass/h)	31.12 ± 1.7285	31.36 ± 1.2895	0.9125	24.72 ± 1.1017	25.14 ± 0.2314	0.7194	27.90 ± 1.1485	28.24 ± 0.6070	0.8019
Total activity (beam breaks)	89169 ± 22955	76618 ± 13112	0.6477	**27651 ± 1674**	**20527 ± 1654 ***	**0.0128**	116819 ± 24438	97145 ± 13992	0.5047
Ambulatory activity (counts)	62096 ± 18035	51144 ± 8978	0.6028	**17165 ± 1826**	**11441 ± 1462 ***	**0.0355**	79261 ± 19212	62585 ± 9459	0.4607
	Fasting (dark cycle)			**Fasting (light cycle)**			**Fasting (24 hr)**		
N	5	6		5	6		5	6	
Body weight (g)							20.68 ± 0.84	20.50 ± 0.90	0.8808
Food intake (kcal)	0	0		0	0		0	0	
VO2 (mL/kg lean mass/h)	5658 ± 165.67	5958 ± 312.73	0.4239	4020 ± 259.17	4275 ± 335.13	0.5610	4837 ± 208.50	5108 ± 296.49	0.4736
VCO2 (mL/kg lean mass/h)	4219 ± 141.64	4365 ± 201.45	0.5683	3000 ± 211.40	3130 ± 221.65	0.6798	3607 ± 172.87	3742 ± 196.15	0.6204
RER (VCO2/VO2)	0.7453 ± 0.0074	0.7341 ± 0.0063	0.2791	0.7451 ± 0.0097	0.7342 ± 0.0118	0.4923	0.7453 ± 0.0078	0.7336 ± 0.0067	0.2872
EE (kcal/kg lean mass/h)	26.78 ± 0.8006	28.11 ± 1.4406	0.4467	19.03 ± 1.2461	20.17 ± 1.5478	0.5812	22.90 ± 1.0048	24.10 ± 1.3710	0.4981
Total activity (beam breaks)	96004 ± 13580	92982 ± 17340	0.8939	46965 ± 11932	48531 ± 22673	0.9529	142969 ± 22646	141513 ± 35927	0.9735
Ambulatory activity (counts)	68721 ± 9475	67799 ± 12992	0.9556	32873 ± 8610	34541 ± 17317	0.9336	101594 ± 15363	102340 ± 26904	0.9814
	Re-feed (dark cycle)			**Re-feed (light cycle)**			**Re-feed (24 hr)**		
N	5	6		5	6		5	6	
Body weight (g)							23.17 ± 1.06	22.45 ± 0.79	0.6028
Food intake (kcal)	14.65 ± 0.7735	15.42 ± 2.0633	0.7432	5.50 ± 0.1779	5.13 ± 0.4825	0.5040	20.15 ± 0.9101	20.19 ± 1.6992	0.9856
VO2 (mL/kg lean mass/h)	5347 ± 222.17	5673 ± 110.57	0.2376	4839 ± 148.65	4978 ± 104.46	0.4699	5102 ± 182.80	5340 ± 51.57	0.2694
VCO2 (mL/kg lean mass/h)	5408 ± 213.09	5666 ± 131.89	0.3373	5000 ± 148.67	4944 ± 140.85	0.7922	5211 ± 179.39	5321 ± 53.04	0.5836
RER (VCO2/VO2)	1.0119 ± 0.0089	0.9986 ± 0.0087	0.3115	**1.0338 ± 0.0145**	**0.9925 ± 0.0087 ***	**0.0463**	1.0219 ± 0.0110	0.9965 ± 0.0043	0.0825
EE (kcal/kg lean mass/h)	27.06 ± 1.1056	28.62 ± 0.5768	0.2562	24.62 ± 0.7348	25.08 ± 0.5710	0.6353	25.89 ± 0.9105	26.93 ± 0.2572	0.3237
Total activity (beam breaks)	38270 ± 3078	43979 ± 4778	0.3438	16763 ± 1463	14686 ± 1536	0.3532	55032 ± 4218	58665 ± 5862	0.6276
Ambulatory activity (counts)	23748 ± 4240	27082 ± 2675	0.5276	8759 ± 1978	7406 ± 831	0.5538	32507 ± 6124	34487 ± 3267	0.7848

Table 5. Indirect calorimetry, physical activity, and food intake analysis of female mice fed a control low-fat diet (LFD). At the time of the study, mice were 27 weeks of age. Mice were given 2 days to acclimate to the metabolic cages. "*Ad-libitum*" data were collected on the third day. Mice were denied access to food but had free access to water on day 4 ("fasting" data), and "re-feed" data were collected on day 5 when mice regained free access to food. Values that are statistically significant (*P<0.05) are bolded and underlined

Low-fat diet (male)

	WT	KO	*P-value*	WT	KO	*P-value*	WT	KO	*P-value*
	***Ad-libitum* (dark cycle)**			***Ad-libitum* (light cycle)**			***Ad-libitum* (24 hr)**		
N	6	6		6	6		6	6	
Body weight (g)							33.78 ± 0.93	32.27 ± 1.54	0.4267
Food intake (kcal)	12.10 ± 0.4483	12.19 ± 1.0683	0.9447	4.68 ± 0.5210	4.32 ± 0.2848	0.5692	16.78 ± 0.9393	16.51 ± 1.2516	0.8670
VO2 (mL/kg lean mass/h)	5140 ± 336.81	4764 ± 122.47	0.3327	4507 ± 317.60	4266 ± 87.28	0.4925	4821 ± 327.53	4512 ± 93.37	0.3996
VCO2 (mL/kg lean mass/h)	4979 ± 325.83	4702 ± 169.58	0.4737	4037 ± 276.07	3855 ± 106.02	0.5594	4506 ± 300.88	4274 ± 130.21	0.5038
RER (VCO2/VO2)	0.9691 ± 0.0099	0.9857 ± 0.0141	0.3607	0.8976 ± 0.0157	0.9032 ± 0.0093	0.7630	0.9355 ± 0.0120	0.9463 ± 0.0111	0.5245
EE (kcal/kg lean mass/h)	25.74 ± 1.6833	23.97 ± 0.6710	0.3620	22.17 ± 1.5447	21.02 ± 0.4594	0.5046	23.94 ± 1.6160	22.48 ± 0.5144	0.4205
Total activity (beam breaks)	31086 ± 2573	25107 ± 2927	0.1565	**14819 ± 1041**	**10042 ± 1007 ****	**0.0080**	**45905 ± 2828**	**35148 ± 3672 ***	**0.0443**
Ambulatory activity (counts)	15473 ± 1901	12719 ± 1800	0.3176	6390 ± 910	4123 ± 528	0.0631	21862 ± 2305	16841 ± 2167	0.1436
	Fasting (dark cycle)			**Fasting (light cycle)**			**Fasting (24 hr)**		
N	6	6		6	6		6	6	
Body weight (g)							30.40 ± 1.00	29.26 ± 1.54	0.5519
Food intake (kcal)	0	0		0	0		0	0	
VO2 (mL/kg lean mass/h)	4821 ± 351.50	4499 ± 137.61	0.4240	3773 ± 252.60	3497 ± 141.25	0.3683	4292 ± 299.08	3996 ± 125.83	0.3935
VCO2 (mL/kg lean mass/h)	3560 ± 273.93	3319 ± 101.56	0.4404	2715 ± 185.86	2508 ± 110.25	0.3650	3133 ± 227.98	2912 ± 97.03	0.4025
RER (VCO2/VO2)	0.7376 ± 0.0052	0.7377 ± 0.0017	0.9839	0.7192 ± 0.0037	0.7165 ± 0.0058	0.7110	0.7294 ± 0.0037	0.7284 ± 0.0029	0.8459
EE (kcal/kg lean mass/h)	22.78 ± 1.6772	21.25 ± 0.6499	0.4268	17.74 ± 1.1923	16.43 ± 0.6730	0.3673	20.23 ± 1.4214	18.83 ± 0.5989	0.3950
Total activity (beam breaks)	46032 ± 3459	39156 ± 4027	0.2250	14328 ± 1523	12284 ± 1298	0.3317	60360 ± 3607	51439 ± 4403	0.1493
Ambulatory activity (counts)	26838 ± 2492	22431 ± 2843	0.2713	6571 ± 1026	5685 ± 803	0.5127	33409 ± 2625	28116 ± 3097	0.2223
	Re-feed (dark cycle)			**Re-feed (light cycle)**			**Re-feed (24 hr)**		
N	6	6		6	6		6	6	
Body weight (g)							32.65 ± 1.00	31.51 ± 1.23	0.4913
Food intake (kcal)	16.11 ± 0.7839	15.39 ± 0.7509	0.5229	4.01 ± 0.2276	3.91 ± 0.1932	0.7383	20.12 ± 0.9052	19.29 ± 0.8238	0.5175
VO2 (mL/kg lean mass/h)	5289 ± 306.05	4745 ± 95.61	0.1413	4366 ± 278.17	4085 ± 89.06	0.3716	4848 ± 289.28	4430 ± 90.21	0.2167
VCO2 (mL/kg lean mass/h)	5092 ± 280.39	4618 ± 120.98	0.1657	4179 ± 242.68	3952 ± 104.51	0.4205	4655 ± 257.94	4300 ± 105.02	0.2446
RER (VCO2/VO2)	0.9637 ± 0.0067	0.9725 ± 0.0088	0.4410	0.9595 ± 0.0155	0.9675 ± 0.0137	0.7086	0.9618 ± 0.0099	0.9704 ± 0.0089	0.5320
EE (kcal/kg lean mass/h)	26.45 ± 1.5117	23.79 ± 0.5101	0.1458	21.81 ± 1.3535	20.45 ± 0.4541	0.3787	24.23 ± 1.4185	22.20 ± 0.4674	0.2214
Total activity (beam breaks)	**33740 ± 2923**	**23819 ± 1962 ***	**0.0207**	10661 ± 986	8470 ± 891	0.1307	**44401 ± 3607**	**32289 ± 2359 ***	**0.0212**
Ambulatory activity (counts)	15749 ± 1880	11041 ± 1046	0.0608	4111 ± 452	3088 ± 449	0.1393	**19860 ± 2129**	**14129 ± 1240 ***	**0.0483**

Table 6. Indirect calorimetry, physical activity, and food intake analysis of male mice fed a control low-fat diet (LFD). At the time of the study, mice were 27 weeks of age. Mice were given 2 days to acclimate to the metabolic cages. "*Ad-libitum*" data were collected on the third day. Mice were denied access to food but had free access to water on day 4 ("fasting" data), and "re-feed" data were collected on day 5 when mice regained free access to food. Values that are statistically significant (*P<0.05) are bolded and underlined.

With access to running wheel	Female Mice			Male Mice		
	WT	KO	*P*-value	WT	KO	*P*-value
N	5	5		5	5	
body weight (g)	24.92 ± 0.85	22.93 ± 0.68	0.1064	34.44 ± 1.10	31.97 ± 1.16	0.1612
Food intake (kcal)	16.57 ± 2.316	13.60 ± 1.027	0.2889	15.53 ± 1.032	14.21 ± 0.6769	0.3194
VO2 (mL/kg lean mass/h)	5540 ± 290.24	5967 ± 215.82	0.2747	5010 ± 218.42	4865 ± 158.65	0.6086
VCO2 (mL/kg lean mass/h)	5380 ± 182.51	5511 ± 150.72	0.5962	4639 ± 252.99	4445 ± 99.65	0.5062
RER (VCO2/VO2)	0.9237 ± 0.0362	0.9270 ± 0.0331	0.9478	0.9246 ± 0.0157	0.9153 ± 0.0181	0.7072
EE(kcal/kg lean mass/h)	27.76 ± 1.1344	29.55 ± 0.9034	0.2540	24.83 ± 1.1369	24.04 ± 0.7031	0.5740
Total activity (beam breaks)	98718 ± 8863	97087 ± 17367	0.9361	45503 ± 4999	42172 ± 9876	0.7737
Ambulatory activity (counts)	42468 ± 7579	49323 ± 10918	0.6216	16620 ± 2691	16296 ± 5834	0.9615
Wheel activity (counts)	11553 ± 1989	10975 ± 1499	0.8229	3196 ± 465	2095 ± 893	0.3157
Cumulative wheel activity (counts)	73647 ± 16929	62831 ± 5709	0.5719	15172 ± 1112	14373 ± 2802	0.8012

Table 7. Indirect calorimetry, physical activity, and food intake of myonectin-KO and WT mice (age 30 weeks) with access to a voluntary running wheel. Mice were given 4 days to acclimate to the metabolic cages and become accustomed to using the running wheel. Data were collected on day 5.

To assess whether myonectin deficiency alters carbohydrate metabolism, glucose tolerance tests (GTT) were performed. The rate of glucose uptake in peripheral tissues in response to glucose injection was not different between genotypes of either sex (**Fig. 2C,D**). The magnitude of insulin secretion in response to a rise in blood glucose during GTT did not differ between genotypes in males (**Fig. 2E**). We also performed insulin tolerance tests (ITT) to assess insulin action in peripheral tissue. The rate of glucose disposal in response to a bolus of insulin did not differ between genotypes of either sex (**Fig. 2F,G**). We previously showed that recombinant myonectin infusion promotes lipid uptake in mice (28). To test whether myonectin deficiency affects the ability of mice to handle an acute lipid load, we performed lipid tolerance tests. Overnight-fasted mice were orally gavaged with a bolus of emulsified intralipid, and serum lipid levels were measured over time to assess the rate of lipid uptake and clearance by peripheral tissues. No genotypic differences were observed in the rate of clearance of serum TG or NEFA (**Fig. 2H,I**). Aside from physical activity in the *ad-libitum* fed state or during refeeding, our data indicate that

myonectin is dispensable for whole-body carbohydrate and lipid metabolism under basal conditions.

Minimal impact of myonectin deficiency on carbohydrate metabolism in the context of obesity

We next determined whether myonectin is required for a proper response to metabolic stress. A separate cohort of male and female WT and KO mice was challenged with a high-fat diet (HFD), beginning at 5 weeks of age, to induce obesity and insulin resistance. We performed the same sets of metabolic tests as in the control LFD-fed cohorts to determine whether myonectin deficiency exacerbates or improves the pathophysiological phenotypes associated with diet-induced obesity and insulin resistance. Body weight and body composition did not differ between genotypes of either sex (**Fig. 3A,B**). Despite no difference in overall fat mass, the gonadal fat pad was larger in myonectin-KO female mice relative to WT littermates (**Table 4**). Indirect calorimetry analyses indicated no differences in metabolic rate, physical activity, or energy expenditure between genotypes of either sex under *ad-libitum* fed conditions, or during a 24-h fast and 24-h re-feed (**Tables 8-9**). However, we noted that *ad-libitum* fed female KO mice had significantly reduced food intake in the light cycle (**Table 8**). In the refeeding phase following a fast, female KO mice had reduced food intake and lower RER in the dark cycle; the reduction in food intake was also observed over the 24-hr refeed period. In contrast to female mice, the only difference seen in KO male mice was reduced RER in the light cycle in the *ad-libitum* fed state (**Table 9**). Myonectin-deficient female mice also showed a modest impairment in the rate of glucose uptake in peripheral tissues in response to glucose or insulin injection (**Fig. 3C,F**). Myonectin-deficient male mice, however, were indistinguishable from WT littermates in glucose and insulin tolerance

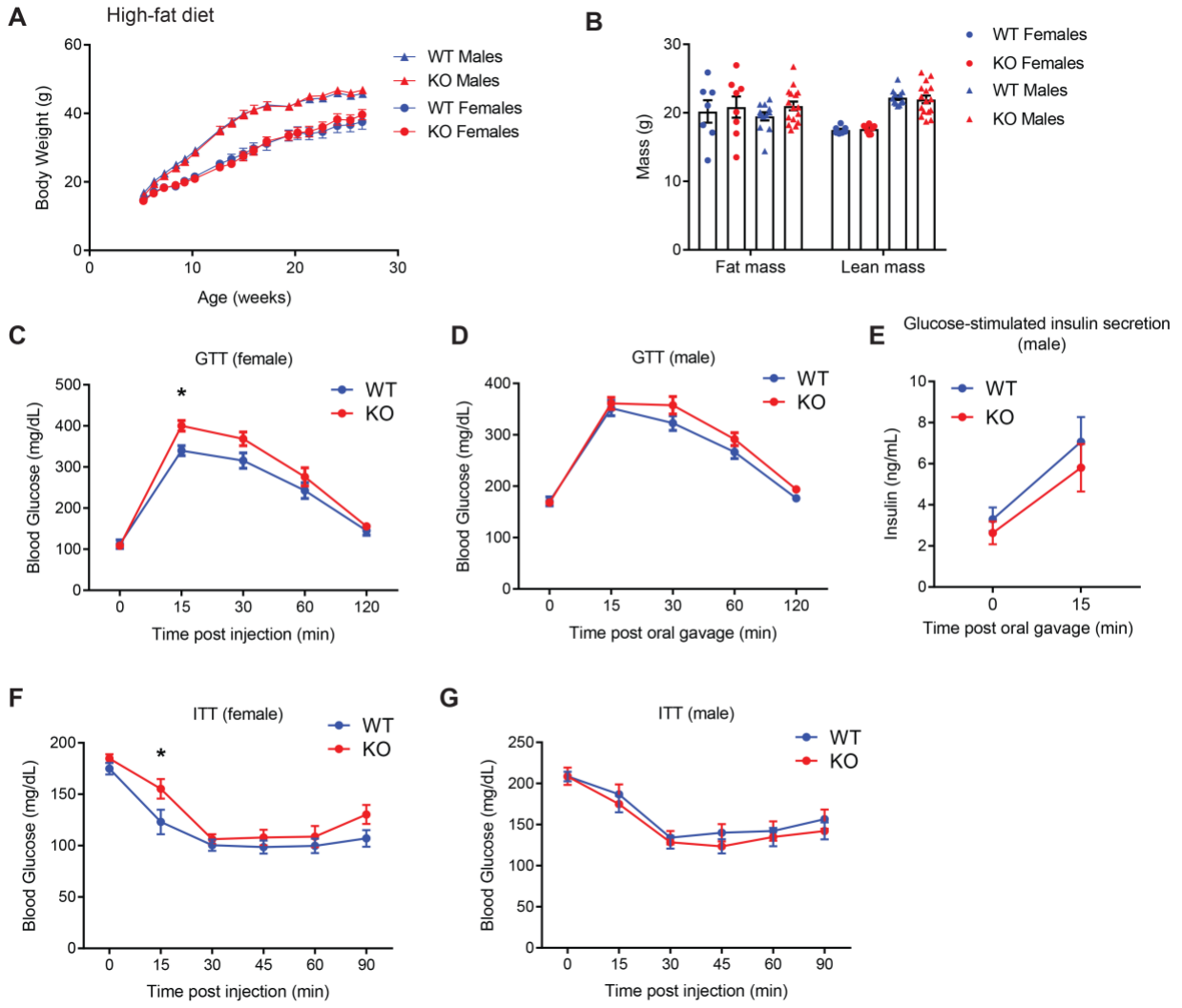

Figure 3. There are no overt carbohydrate metabolism phenotypes in the myonectin-KO mice fed a high-fat diet. (A) Body weights of female (WT, n=8; KO, n=8) and male (WT, n=12-13; KO, n=16) mice over time. Mice were weaned at 3.5 weeks of age onto a standard chow diet. At 5 weeks of age, the diet was switched to a high-fat diet (Research Diets). (B) Body composition analysis of female (WT, n=7; KO, n=8) and male (WT, n=12, KO, n=16) mice at 28 weeks of age. (C) Blood glucose levels during intraperitoneal glucose tolerance tests (ip-GTT) in 18-week-old female mice (WT, n=8; KO, n=8). (D) Blood glucose levels during oral-GTT in 19-week-old male mice (WT, n=12; KO, n=12). (E) Serum insulin levels in male mice at 0 min before glucose gavage (WT, n=11; KO, n=9) and at 15 min after glucose gavage (WT, n=12; KO, n=11); for some samples, insulin levels were below the threshold of detection. (F-G) Blood glucose levels during ITT in female (WT, n=7; KO, n=8) and male mice (WT, n=11; KO, n=15) at 23 weeks of age. Insulin was injected at a dose of 1.2 units/kg body weight for female mice and 1.5 units/kg body weight for male mice. * $P < 0.05$

High-fat diet (female)

	WT	KO	*P*-value	WT	KO	*P*-value	WT	KO	*P*-value
	***Ad-libitum* (dark cycle)**			***Ad-libitum* (light cycle)**			***Ad-libitum* (24 hr)**		
N	6	6		6	6		6	6	
Body weight (g)							39.26 ± 2.16	39.25 ± 2.03	0.9978
Food intake (kcal)	7.78 ± 0.936	6.02 ± 1.133	0.2629	**2.77 ± 0.278**	**1.70 ± 0.346 ***	**0.0419**	10.55 ± 1.118	7.71 ± 1.404	0.1522
VO2 (mL/kg lean mass/h)	5829 ± 241.71	5891 ± 32.68	0.8086	5275 ± 214.59	5244 ± 153.42	0.9072	5550 ± 225.09	5567 ± 74.91	0.9464
VCO2 (mL/kg lean mass/h)	4417 ± 174.41	4366 ± 30.95	0.7821	3981 ± 126.93	3886 ± 103.03	0.5756	4198 ± 147.35	4126 ± 52.17	0.6601
RER (VCO2/VO2)	0.7584 ± 0.0105	0.7412 ± 0.0070	0.2064	0.7561 ± 0.0082	0.7415 ± 0.0046	0.1591	0.7573 ± 0.0088	0.7412 ± 0.0055	0.1582
EE (kcal/kg lean mass/h)	27.68 ± 1.1285	27.85 ± 0.1266	0.8840	25.03 ± 0.9735	24.79 ± 0.7097	0.8482	26.35 ± 1.0355	26.32 ± 0.3409	0.9822
Total activity (beam breaks)	26652 ± 5042	30357 ± 4571	0.5983	13739 ± 2849	14363 ± 2550	0.8736	40391 ± 7665	44720 ± 6227	0.6709
Ambulatory activity (counts)	12799 ± 2466	15179 ± 2289	0.4956	5513 ± 1255	5936 ± 1065	0.8029	18313 ± 3549	21115 ± 2485	0.5340
	Fasting (dark cycle)			**Fasting (light cycle)**			**Fasting (24 hr)**		
N	6	6		6	6		6	6	
Body weight (g)							36.85 ± 2.12	37.01 ± 1.99	0.9586
Food intake (kcal)	0	0		0	0		0	0	
VO2 (mL/kg lean mass/h)	5643 ± 221.60	5644 ± 101.86	0.9970	4585 ± 230.51	4547 ± 157.97	0.8953	5115 ± 212.53	5091 ± 126.55	0.9234
VCO2 (mL/kg lean mass/h)	4027 ± 144.58	3996 ± 70.73	0.8508	3286 ± 154.03	3245 ± 106.04	0.8312	3657 ± 140.15	3617 ± 85.75	0.8125
RER (VCO2/VO2)	0.7142 ± 0.0033	0.7080 ± 0.0019	0.1412	0.7174 ± 0.0033	0.7139 ± 0.0023	0.4137	0.7155 ± 0.0029	0.7107 ± 0.0018	0.1953
EE (kcal/kg lean mass/h)	26.49 ± 1.0231	26.46 ± 0.4750	0.9761	21.54 ± 1.0690	21.35 ± 0.7329	0.8838	24.02 ± 0.9832	23.88 ± 0.5880	0.9035
Total activity (beam breaks)	35897 ± 6045	40484 ± 5337	0.5822	12202 ± 2746	12706 ± 2495	0.8947	48099 ± 8473	53190 ± 7425	0.6612
Ambulatory activity (counts)	19678 ± 3376	22210 ± 2924	0.5834	5290 ± 1297	5383 ± 1143	0.9583	24968 ± 4426	27593 ± 3670	0.6580
	Re-feed (dark cycle)			**Re-feed (light cycle)**			**Re-feed (24 hr)**		
N	6	6		6	6		6	6	
Body weight (g)							37.79 ± 2.06	37.57 ± 1.98	0.9405
Food intake (kcal)	**11.11 ± 0.135**	**9.48 ± 0.561 ***	**0.0423**	3.44 ± 0.386	2.90 ± 0.312	0.3070	**14.55 ± 0.4454**	**12.39 ± 0.5515 ***	**0.0155**
VO2 (mL/kg lean mass/h)	5914 ± 239.53	6071 ± 125.66	0.5772	5201 ± 254.85	5187 ± 174.10	0.9657	5552 ± 239.42	5624 ± 145.89	0.8049
VCO2 (mL/kg lean mass/h)	4506 ± 157.98	4526 ± 81.21	0.9122	3984 ± 165.08	3904 ± 109.04	0.6957	4241 ± 155.71	4211 ± 92.23	0.8723
RER (VCO2/VO2)	**0.7629 ± 0.0054**	**0.7458 ± 0.0040 ***	**0.0311**	0.7675 ± 0.0074	0.7534 ± 0.0053	0.1536	0.7650 ± 0.0060	0.7493 ± 0.0044	0.0629
EE (kcal/kg lean mass/h)	28.11 ± 1.1074	28.74 ± 0.5772	0.6305	24.75 ± 1.1746	24.60 ± 0.7974	0.9179	26.41 ± 1.1045	26.64 ± 0.6687	0.8595
Total activity (beam breaks)	31069 ± 8060	35028 ± 5833	0.6999	12508 ± 2680	11956 ± 2066	0.8739	43577 ± 10661	46984 ± 7839	0.8025
Ambulatory activity (counts)	15373 ± 4644	17250 ± 2722	0.7363	5174 ± 1418	4881 ± 852	0.8636	20547 ± 6036	22131 ± 3547	0.8267

Table 8. Indirect calorimetry, physical activity, and food intake analysis of female mice fed a high-fat diet (HFD). At the time of the study, mice were 30 weeks of age. Mice were given 3 days to acclimate to the metabolic cages. "*Ad-libitum*" data were collected on the fourth day. Mice were denied access to food but had free access to water on day 5 ("fasting" data), and "re-feed" data were collected on day 6 when mice regained free access to food. Values that are statistically significant (*P<0.05) are bolded and underlined.

High-fat diet (Male)									
	WT	KO	*P-value*	WT	KO	*P-value*	WT	KO	*P-value*
	***Ad-libitum* (dark cycle)**			***Ad-libitum* (light cycle)**			***Ad-libitum* (24 hr)**		
N	6	6		6	6		6	6	
Body weight (g)							44.71 ± 1.21	46.41 ± 2.74	0.5898
Food intake (kcal)	11.05 ± 0.485	10.92 ± 0.674	0.8820	3.69 ± 0.415	2.89 ± 0.326	0.1680	14.73 ± 0.5065	13.81 ± 0.7965	0.3621
VO2 (mL/kg lean mass/h)	4896 ± 178.31	5268 ± 157.82	0.1494	4340 ± 179.53	4720 ± 163.00	0.1485	4615 ± 175.50	4992 ± 157.97	0.1426
VCO2 (mL/kg lean mass/h)	3803 ± 136.51	4071 ± 120.76	0.1729	3339 ± 131.94	3561 ± 122.98	0.2469	3569 ± 129.95	3814 ± 120.27	0.1971
RER (VCO2/VO2)	0.7769 ± 0.0044	0.7728 ± 0.0031	0.4642	**0.7697 ± 0.0034**	**0.7545 ± 0.0041 ***	**0.0181**	0.7735 ± 0.0031	0.7641 ± 0.0032	0.0600
EE (kcal/kg lean mass/h)	23.36 ± 0.8468	25.11 ± 0.7497	0.1532	20.67 ± 0.8468	22.39 ± 0.7719	0.1638	22.00 ± 0.8290	23.74 ± 0.7498	0.1516
Total activity (beam breaks)	19968 ± 2233	18985 ± 1879	0.7434	10056 ± 446	9179 ± 1061	0.4721	30024 ± 2392	28164 ± 2693	0.6170
Ambulatory activity (counts)	8471 ± 1549	7870 ± 1280	0.7713	3449 ± 326	2999 ± 614	0.5364	11920 ± 1768	10869 ± 1810	0.6866
	Fasting (dark cycle)			**Fasting (light cycle)**			**Fasting (24 hr)**		
N	6	5		6	5		6	5	
Body weight (g)							41.54 ± 1.21	44.41 ± 2.82	0.3888
Food intake (kcal)	0	0		0	0		0	0	
VO2 (mL/kg lean mass/h)	4666 ± 216.33	4867 ± 194.46	0.5055	3693 ± 133.10	3930 ± 159.85	0.2869	4177 ± 170.75	4396 ± 162.82	0.3770
VCO2 (mL/kg lean mass/h)	3340 ± 147.61	3470 ± 137.69	0.5348	2659 ± 83.47	2806 ± 113.43	0.3308	2998 ± 112.11	3136 ± 113.67	0.4094
RER (VCO2/VO2)	0.7162 ± 0.0027	0.7130 ± 0.0025	0.4004	0.7207 ± 0.0041	0.7139 ± 0.0021	0.1842	0.7182 ± 0.0033	0.7134 ± 0.0020	0.2482
EE (kcal/kg lean mass/h)	21.91 ± 1.0068	22.84 ± 0.9109	0.5107	17.37 ± 0.6102	18.45 ± 0.7493	0.2941	19.63 ± 0.7892	20.63 ± 0.7609	0.3825
Total activity (beam breaks)	17821 ± 1731	22326 ± 3195	0.2595	6245 ± 459	7229 ± 894	0.3654	24066 ± 2046	29555 ± 3826	0.2512
Ambulatory activity (counts)	7579 ± 890	10425 ± 2360	0.3090	1672 ± 215	2318 ± 586	0.3466	9250 ± 1019	12743 ± 2867	0.3028
	Re-feed (dark cycle)			**Re-feed (light cycle)**			**Re-feed (24 hr)**		
N	6	5		6	5		6	5	
Body weight (g)							42.57 ± 1.15	45.43 ± 2.83	0.3890
Food intake (kcal)	11.14 ± 0.977	10.66 ± 0.898	0.7228	4.42 ± 0.318	3.28 ± 0.435	0.0690	15.56 ± 1.108	13.94 ± 0.8541	0.2759
VO2 (mL/kg lean mass/h)	4992 ± 136.64	5113 ± 150.94	0.5682	4295 ± 129.02	4374 ± 122.97	0.6656	4639 ± 128.56	4738 ± 134.79	0.6089
VCO2 (mL/kg lean mass/h)	3764 ± 83.21	3849 ± 107.15	0.5454	3329 ± 75.07	3332 ± 89.30	0.9795	3544 ± 76.37	3587 ± 95.73	0.7344
RER (VCO2/VO2)	0.7546 ± 0.0066	0.7531 ± 0.0031	0.8406	0.7761 ± 0.0079	0.7618 ± 0.0032	0.1406	0.7646 ± 0.0069	0.7572 ± 0.0027	0.3527
EE (kcal/kg lean mass/h)	23.68 ± 0.6204	24.25 ± 0.7067	0.5629	20.48 ± 0.5819	20.79 ± 0.5782	0.7166	22.07 ± 0.5817	22.50 ± 0.6314	0.6292
Total activity (beam breaks)	26584 ± 5071	19906 ± 1166	0.2506	8855 ± 1394	8000 ± 702	0.6000	35440 ± 6372	27905 ± 1726	0.2993
Ambulatory activity (counts)	12476 ± 3090	8073 ± 846	0.2206	3173 ± 826	2498 ± 461	0.4965	15649 ± 3888	10571 ± 1263	0.2603

Table 9. Indirect calorimetry, physical activity, and food intake analysis of male mice fed a high-fat diet (HFD). At the time of the study, mice were 30 weeks of age. Mice were given 3 days to acclimate to the metabolic cages. "*Ad-libitum*" data were collected on the fourth day. Mice were denied access to food but had free access to water on day 5 ("fasting" data), and "re-feed" data were collected on day 6 when mice regained free access to food. Values that are statistically significant (*P<0.05) are bolded and underlined.

tests (**Fig. 3D,G**). The magnitude of insulin secretion in response to glucose injection during the glucose tolerance test did not differ between genotypes in males (**Fig. 3E**). Together, these results indicate that myonectin deficiency has minimal impact on whole body carbohydrate metabolism in the pathophysiological context of diet-induced obesity.

Impact of myonectin deletion on hematologic parameters

Myonectin (also referred to as erythroferrone) plays important roles in linking stress erythropoiesis and hepatic iron mobilization in response to blood loss or anemia by suppressing hepcidin expression in liver (37, 38). Here, under basal non-stressed conditions, myonectin deficiency did not alter any blood parameters, including hemoglobin level, hematocrit, and population counts of lymphoid and myeloid cell types in male mice (**Table 10**), consistent with previous findings (38). Interestingly, under basal conditions when mice were fed a control low-fat diet, female mice lacking myonectin had significantly elevated total white blood cell counts as well as lymphocyte counts (**Table 10**). Although diet-induced obesity can adversely affect multiple cell types in the immune system (69), metabolic stress from a high-fat diet did not alter any of the blood parameters in myonectin-deficient mice of either sex relative to control WT littermates (**Table 10**). Liver hepcidin expression was also indistinguishable between WT and KO mice (**Fig. 4**). Thus, myonectin is not required for iron homeostasis under conditions where stress erythropoiesis is not induced.

Myonectin deletion impairs lipid handling in diet-induced obese male mice

Although HFD-fed female WT and myonectin-KO mice had similar rates of lipid clearance following an oral lipid gavage (**Fig. 5**), male KO mice exhibited significant impairment

	Female Mice			Male Mice		
	WT	KO	*P*-value	WT	KO	*P*-value
Low fat diet						
Sample size (n)	6	6		6	9	
RBC (10^6/μL)	11.89 ± 0.2685	11.97 ± 0.2279	0.8214	12.80 ± 0.3004	12.35 ± 0.1321	0.2129
HGB (g/dL)	17.17 ± 0.3442	17.28 ± 0.3563	0.8186	18.37 ± 0.3756	17.87 ± 0.2309	0.2871
HCT (%)	56.93 ± 1.4317	56.97 ± 1.1575	0.9859	62.42 ± 1.9624	60.06 ± 0.8699	0.3078
MCV (fL)	47.88 ± 0.2868	47.58 ± 0.2442	0.4447	48.70 ± 0.4517	48.59 ± 0.3385	0.8478
MCH (pg)	14.45 ± 0.0563	14.43 ± 0.0615	0.8455	14.35 ± 0.1057	14.48 ± 0.0878	0.3724
MCHC (g/dL)	30.17 ± 0.2216	30.35 ± 0.1996	0.5526	29.48 ± 0.4126	29.76 ± 0.2021	0.5712
RET (10^3/μL)	811.8 ± 91.48	637.6 ± 25.27	0.1182	644.5 ± 43.98	701.1 ± 26.10	0.2984
PLT (10^3/μL)	1037 ± 48.3	691 ± 248.3	0.2583	1069 ± 144.9	1093 ± 109.8	0.8997
WBC (10^3/μL)	**6.718 ± 0.5719**	**9.045 ± 0.5986 ***	**0.0185**	6.637 ± 0.6392	7.682 ± 0.4734	0.2177
NEUT (10^3/μL)	0.9000 ± 0.1218	0.6733 ± 0.0561	0.1346	0.5640 ± 0.0588	0.9922 ± 0.2907	0.1841
LYMPH (10^3/μL)	**5.533 ± 0.5610**	**8.068 ± 0.5548 ****	**0.0093**	5.590 ± 0.6740	6.319 ± 0.4194	0.3884
MONO (10^3/μL)	0.1250 ± 0.0186	0.0933 ± 0.0167	0.2335	0.0450 ± 0.0050	0.0956 ± 0.0267	0.0976
EO (10^3/μL)	0.1517 ± 0.0199	0.2050 ± 0.0257	0.1334	0.0817 ± 0.0101	0.2633 ± 0.1085	0.1333
BASO (10^3/μL)	0.0083 ± 0.0031	0.0050 ± 0.0034	0.4850	0.0033 ± 0.0033	0.0122 ± 0.0022	0.0528
High fat diet						
Sample size (n)	8	8		12	16	
RBC (10^6/μL)	12.02 ± 0.1721	12.21 ± 0.1471	0.4158	11.85 ± 0.2219	11.76 ± 0.1389	0.7460
HGB (g/dL)	17.38 ± 0.2051	17.65 ± 0.2188	0.3747	17.07 ± 0.2577	17.03 ± 0.1895	0.9129
HCT (%)	56.30 ± 0.7725	57.25 ± 0.7043	0.3790	56.26 ± 0.9363	56.26 ± 0.9798	0.9976
MCV (fL)	46.86 ± 0.1936	46.89 ± 0.2787	0.9424	47.51 ± 0.2797	47.81 ± 0.4274	0.5651
MCH (pg)	14.44 ± 0.0680	14.46 ± 0.0885	0.8262	14.42 ± 0.1036	14.48 ± 0.0823	0.6301
MCHC (g/dL)	30.88 ± 0.1634	30.86 ± 0.3111	0.9723	30.35 ± 0.1681	30.32 ± 0.2532	0.9189
RET (10^3/μL)	738.7 ± 39.02	762.1 ± 64.40	0.7615	678.1 ± 27.93	651.8 ± 22.40	0.4697
PLT (10^3/μL)	973 ± 145.9	794 ± 129.5	0.3743	1063 ± 120.9	979 ± 95.0	0.5902
WBC (10^3/μL)	8.653 ± 0.6896	9.700 ± 0.7905	0.3353	10.66 ± 1.0864	9.72 ± 0.5907	0.4594
NEUT (10^3/μL)	0.8988 ± 0.1308	0.8500 ± 0.1179	0.7860	1.175 ± 0.1496	1.135 ± 0.1726	0.8623
LYMPH (10^3/μL)	7.391 ± 0.5727	8.479 ± 0.6326	0.2234	9.093 ± 0.9694	8.201 ± 0.4738	0.4205
MONO (10^3/μL)	0.0725 ± 0.0146	0.0638 ± 0.0110	0.6403	0.1183 ± 0.0148	0.1475 ± 0.0297	0.3884
EO (10^3/μL)	0.2813 ± 0.0702	0.3013 ± 0.0919	0.8653	0.2575 ± 0.0796	0.2194 ± 0.0387	0.6722
BASO (10^3/μL)	0.0088 ± 0.0030	0.0063 ± 0.0018	0.4856	0.0117 ± 0.0021	0.0169 ± 0.0025	0.1239

Table 10. Complete blood count of WT and myonectin-KO mice. At the time of sample collection, LFD-fed mice were 20 weeks of age, HFD-fed females were 22 weeks of age, and HFD-fed males were 26 weeks of age. Platelet counts were omitted from 1 WT and 2 KO LFD-fed females and 2 KO LFD-fed males due to the presence of platelet clumps in the sample. Values that are statistically significant are bolded and underlined. Abbreviation: RBC: red blood cell count, HGB: hemoglobin, HCT: hematocrit, MCV: mean corpuscular (erythrocyte) volume, MCH: mean corpuscular hemoglobin, MCHC: mean corpuscular hemoglobin concentration, RET: reticulocyte count, PLT: platelet count, WBC: white blood cell count, NEUT: neutrophil count, LYMPH: lymphocyte count, MONO: monocyte count, EO: eosinophil count, BASO: basophil count. * $P < 0.05$, ** $P < 0.01$

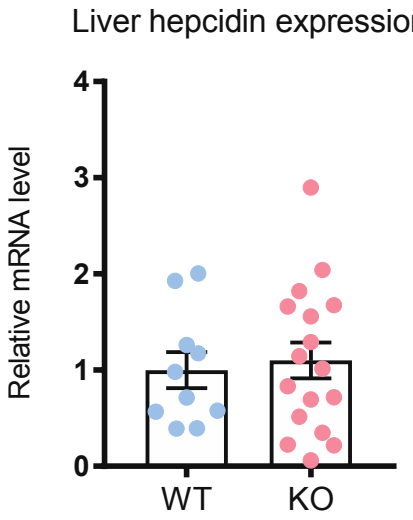

Figure 4. Myonectin WT and KO male mice fed a high-fat diet do not differ in liver hepcidin expression. Hepcidin mRNA expression in livers isolated from high-fat fed male mice sacrificed at 36 weeks of age in a postprandial state (WT, n=10; KO, n=17).

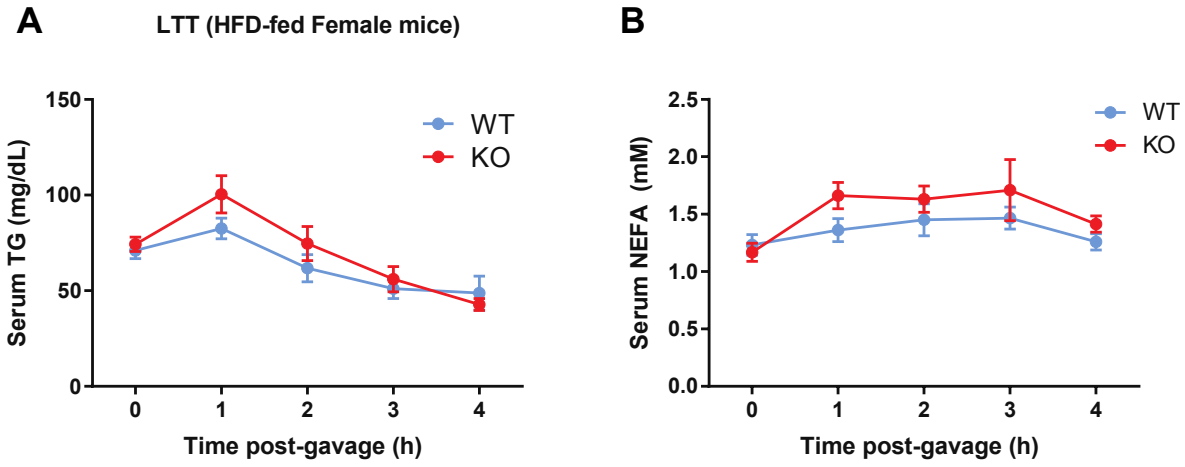

Figure 5. Myonectin WT and KO female mice fed a HFD do not differ in lipid tolerance. Serum triglyceride (TG; A) and non-esterified free fatty acid (NEFA; B) levels in mice during lipid tolerance tests (LTT) in female mice (WT, n=8; KO, n=8) at 24 weeks of age.

in uptake of triglyceride and free fatty acids from the circulation compared to WT littermates (**Fig. 6**). The impaired lipid clearance phenotype following lipid loading was confirmed in two additional independent cohorts of HFD-fed mice. Mice develop insulin resistance after exposure to a high-fat diet for a short period (1-4 weeks), whereas more pronounced differences in body weight gain occur after longer exposure to high-fat feeding (70). Because lipid tolerance was different between WT and KO male mice fed an HFD, we sought to determine whether insulin resistance due to HFD is sufficient to impair lipid disposal in response to oral lipid gavage. In contrast to chronic high-fat feeding, relatively short exposure to an HFD for 4 weeks did not alter lipid tolerance in myonectin-deficient mice compared to WT littermates (**Fig. 7**). This result suggests that excess adiposity from chronic high-fat feeding is necessary to alter lipid handling capacity in myonectin-null animals.

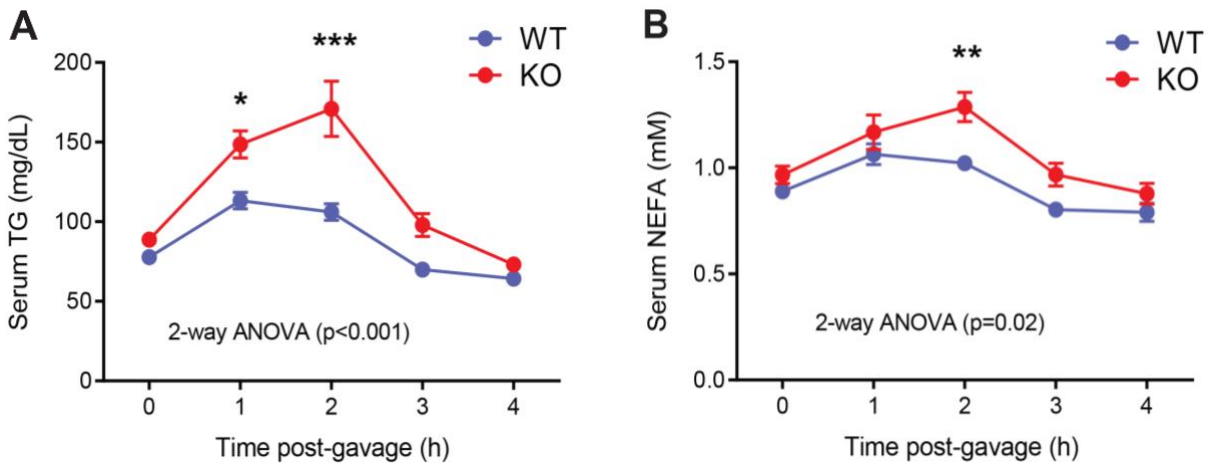

Figure 6. Impaired lipid tolerance in myonectin-KO male mice fed a high-fat diet. (A) Serum triglyceride (TG) and (B) non-esterified free fatty acids (NEFA) during lipid tolerance test (LTT) in male mice (WT, n=12; KO, n=16) at 17 weeks of age. * $P < 0.05$, ** $P < 0.01$, *** $P < 0.001$.

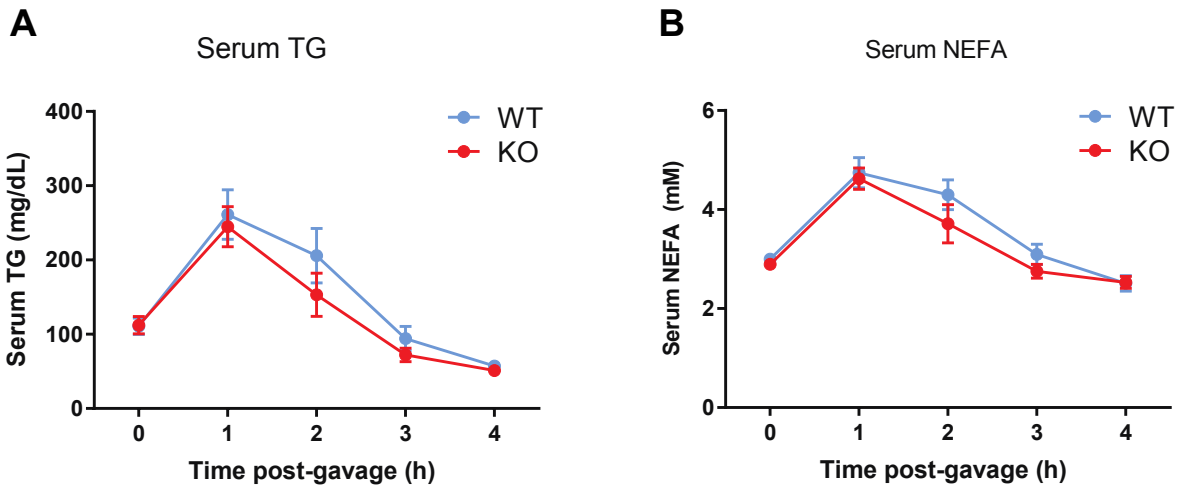

Figure 7. Insulin resistance alone is insufficient to induce impaired lipid clearance phenotype in myonectin-KO male mice fed a high-fat diet for only 4 weeks. Serum triglyceride (TG; A) and non-esterified free fatty acids (NEFA; B) levels in male mice during lipid tolerance tests (LTT) at 9 weeks of age (WT, n=13; KO, n=9).

Impact of myonectin deficiency on metabolic response to high-fat feeding later in life

Diet-induced obese mice in our studies were exposed to HFD beginning at 5 weeks of age, which corresponds to adolescence. To determine whether myonectin is required for metabolic flexibility in adult animals, we exposed another cohort of mice to HFD after they reached 21 weeks of age. After switching from standard chow to HFD for 12 weeks, mice were assessed by several tolerance tests. Body weight and glucose and insulin tolerance did not differ between genotypes of either sex (**Fig. 8A-G**). No differences in lipid tolerance were noted between WT and KO female mice (**Fig. 8H,I**). Male myonectin-KO mice, however, exhibited reduced capacity to clear serum TG from the circulation following an oral lipid gavage (**Fig. 8J,K**). The magnitude of difference between genotypes in lipid tolerance was smaller in this older cohort of myonectin-deficient male mice as compared to younger cohorts (Figure 6). These results indicate that the severity of the lipid tolerance phenotype is contingent upon the age at which mice are exposed to the metabolic stress of high-fat feeding.

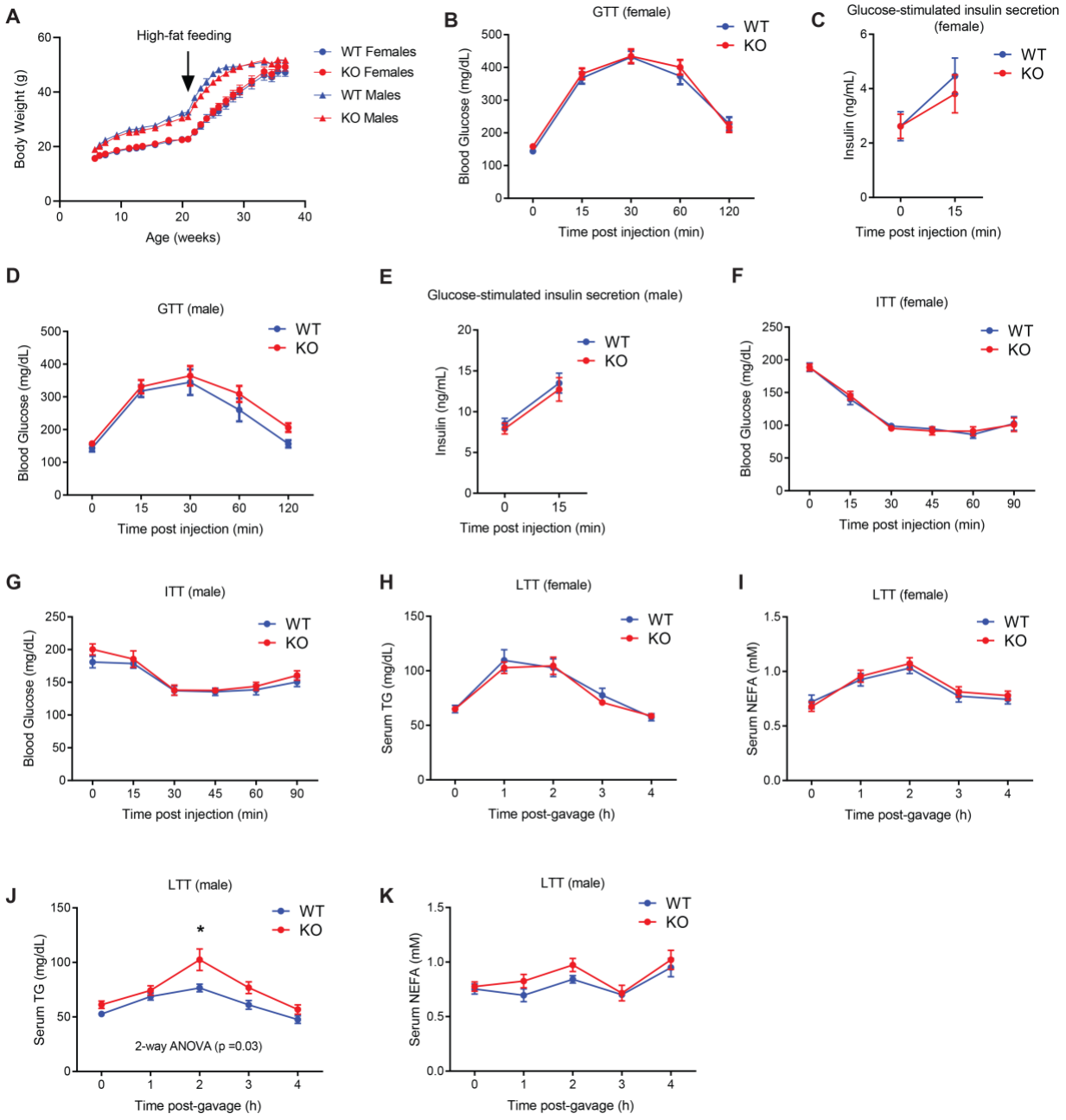

Figure 8. Body weight analysis, and glucose, insulin, and lipid tolerance in WT and myonectin-KO mice exposed to a high-fat diet later in life. Mice were weaned onto a standard chow diet and switched to a high-fat diet at 21 weeks of age. (A) Body weight measurements over time of female (WT, n=14; KO, n=15) and male (WT, n=8; KO, n=14) mice. (B,D) Blood glucose levels during glucose tolerance tests (GTT) in female (WT, n=14; KO, n=15; B) and male (WT, n=8; KO, n=13; D) mice at 36 weeks of age. (C) Serum insulin levels during GTT in female mice at time 0 before glucose injection (WT, n= 10; KO, n=12) and at 15 min after glucose injection (WT, n=14; KO, n=15); for some samples, insulin levels were below the threshold of detection. (E) Serum insulin levels during GTT in male mice at time 0 before glucose injection (WT, n=8 ; KO, n=14) and at 15 min after glucose injection (WT, n=7; KO, n=14); for some samples, insulin levels were below the threshold of detection. (F) Blood glucose levels during insulin tolerance tests (ITT) in female mice at 43 weeks of age (WT, n=13; KO, n=15). (G) Blood glucose levels

during ITT in male mice at 41 weeks of age (WT, n=7; KO, n=13). Insulin was injected at a dose of 1.2 units/kg body weight for female mice and 1.5 units/kg body weight for male mice. (H-I) serum TG (H) and NEFA (I) levels during lipid tolerance tests (LTT) in female mice at 34 weeks of age (WT, n=12-14; KO, n=15). (J-K) serum TG (J) and NEFA (K) levels during LTT in male mice at 34 weeks of age (WT, n=8; KO, n=13-14). * $P < 0.05$

Elevated postprandial VLDL-triglyceride levels in myonectin-deficient male mice

Although myonectin deficiency impairs the capacity to acutely handle orally delivered emulsified intralipid, it is unclear whether myonectin is required for the proper handling of dietary lipids in a postprandial state following physiologically normal *ad-libitum* feeding. To test this, HFD-fed male mice were fasted overnight and then given free access to food for 2 h. Blood samples were taken before and after re-feeding, and serum lipid levels were measured. While fasting serum TG levels were similar between WT and KO mice, postprandial serum TG levels were significantly higher in myonectin-KO mice upon re-feeding following a fast (**Fig. 9A**). Fasting and postprandial serum NEFA and cholesterol levels were not different between genotypes (**Fig. 9B,C**). Food intake did not differ between WT and KO mice (**Table 9**), thus differences in calorie intake cannot explain differences in postprandial serum TG levels. Fractionation of pooled postprandial serum revealed that myonectin-KO male mice had significantly elevated and larger very-low-density lipoprotein (VLDL)-triglyceride particle levels compared to WT males (**Fig. 9D**). Lipoprotein cholesterol profiles showed that the size, but not the amount, of HDL-cholesterol was larger in the myonectin-KO animals (**Fig. 9E**). These data indicate that myonectin is required for proper postprandial handling of dietary triglyceride derived from normal *ad-libitum* feeding of an HFD.

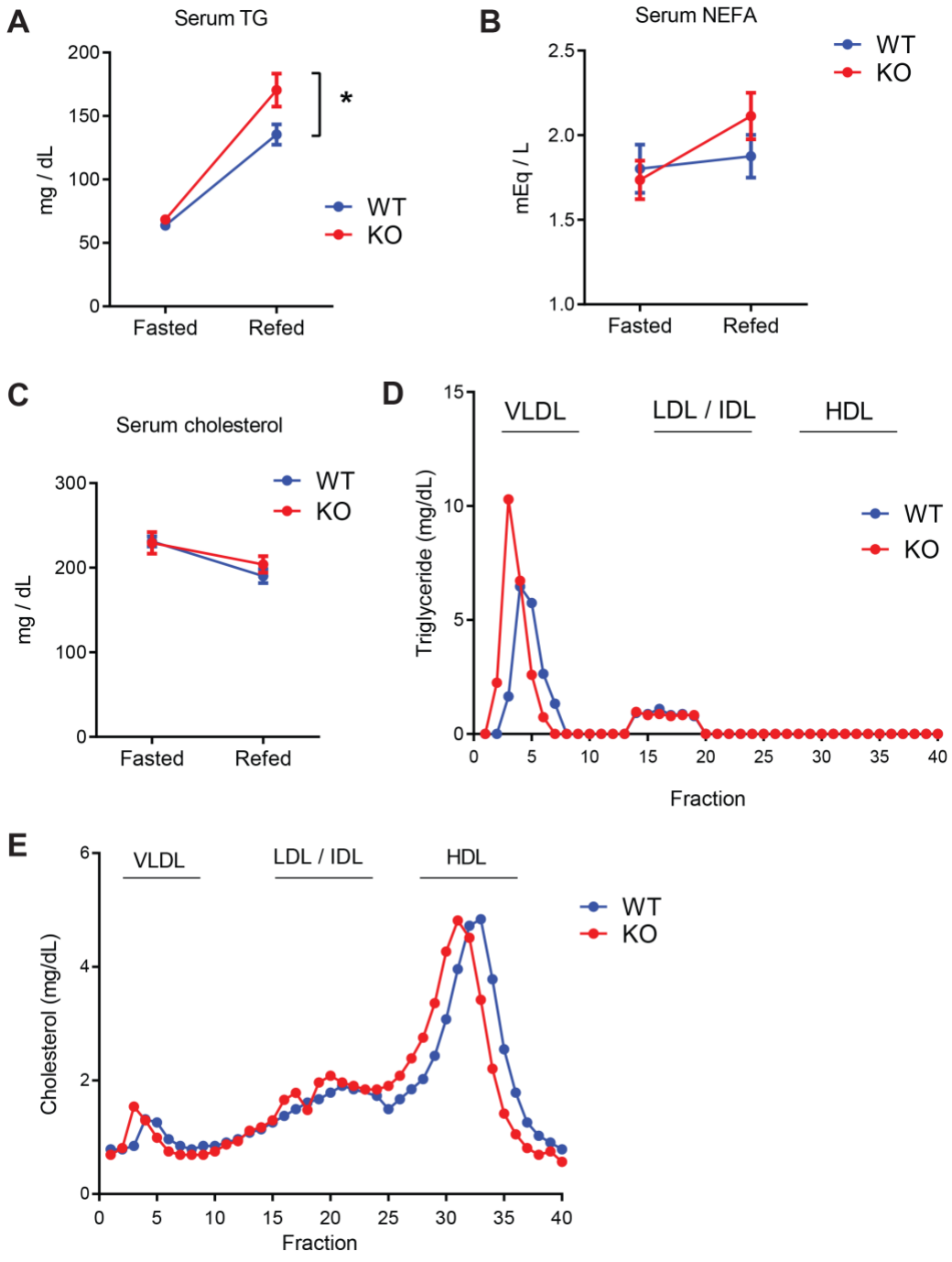

Figure 9. Higher postprandial VLDL-triglyceride levels in myonectin-KO male mice fed a high-fat diet. Serum triglyceride (TG; A), non-esterified free fatty acids (NEFA; B), and cholesterol (C) levels in male mice after an overnight 14-h fast ("fasted") or after an overnight fast followed by *ad-libitum* re-feeding for 2 h ("refed"). Mice (36 weeks of age) were euthanized after re-feeding for tissue collection. 2 WT mice did not eat during the re-feed period as assessed by 1) no increase in serum TG levels over fasting levels, and 2) an empty stomach. Therefore, re-fed data from these mice were not included in the analysis. Fasted: WT, n=12; KO, n=17. Re-fed: WT, n=10; KO, n=17. (D-E) Re-fed serum samples from 10 mice of each genotype were pooled and subjected to FPLC fractionation to separate lipoprotein species. Triglyceride (D) and cholesterol (E) levels were measured in each fraction. * $P < 0.05$

Loss of myonectin does not affect intestinal lipid absorption and secretion

Several mechanisms could affect lipid clearance from the circulation. For example, elevated serum TG levels in myonectin-KO mice after oral lipid gavage or *ad-libitum* feeding could be due to enhanced intestinal lipid absorption and/or greater secretion of TG-rich chylomicrons by the enterocytes. To test this, overnight-fasted mice were injected with poloxamer 407, a detergent that inhibits lipoprotein lipase (LPL) activity, preventing lipid uptake in peripheral tissue. After 1 h, mice were orally gavaged with intralipid. Accumulation of serum TG over time reflects intestinal lipid absorption and subsequent secretion of TG-rich chylomicrons. No differences in the kinetics of serum TG rise were noted between HFD-fed WT and KO mice (**Fig. 10A**). Alternatively, impaired lipid uptake into peripheral tissues could result in the elevated TG levels seen in KO animals. LPL plays a major role in the cellular uptake of lipids derived from circulating lipoprotein particles; the enzyme is located on the surface of endothelial cells in most tissues and hydrolyzes TG to liberate free fatty acids, which can then be taken up by peripheral tissues (71). We therefore measured whole-body LPL activity in post-heparin sera collected from mice in the postprandial state. As we previously observed, a 2-h *ad-libitum* feeding following an overnight fast was sufficient to induce a difference in serum TG between genotypes; the heparin-displaceable total LPL activity, however, was not different between WT and myonectin-KO mice (**Fig. 10B,C**).

Myonectin deletion alters adipose fat storage and lipid accumulation in liver

We next sought to determine whether myonectin deficiency alters lipid storage in peripheral tissues. Although HFD-fed WT and KO mice had similar body weights and body composition (**Fig. 3A,B**), the distribution of fat among tissues was altered. We noted that the KO

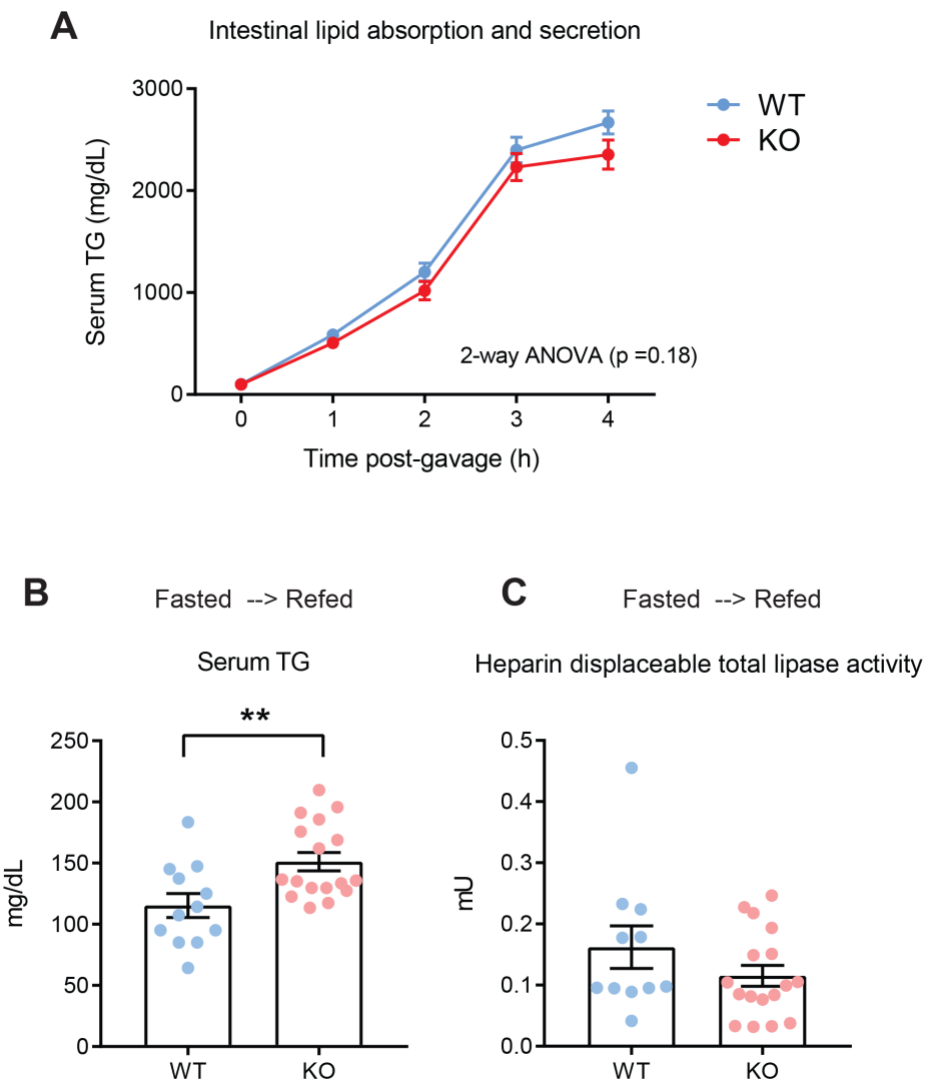

Figure 10. WT and myonectin-KO male mice fed a high-fat diet do not differ in intestinal lipid absorption or postprandial heparin-releasable serum lipase activity. (A) Serum TG levels over time during intestinal lipid absorption/secretion assay in male mice at 21 weeks of age (WT, n=12; KO, n=17). (B) Serum TG levels measured in serum samples collected after 2 h of re-feeding but before heparin injection in male mice (WT, n=12; KO, n=17). (C) Lipase activity in post-heparin serum from male mice at 34 weeks of age (WT, n=11; KO, n=17). ** $P < 0.01$

mice (39-week-old) had significantly increased fat mass (both visceral and subcutaneous fat depots) and a modest reduction in liver weight (**Fig. 11A-C** and **Table 4**). Liver histology revealed a marked reduction in steatosis in KO mice relative to WT littermates (**Fig. 11D**). Quantification of lipids also revealed significantly reduced hepatic TG content and lower cholesterol levels (**Fig.**

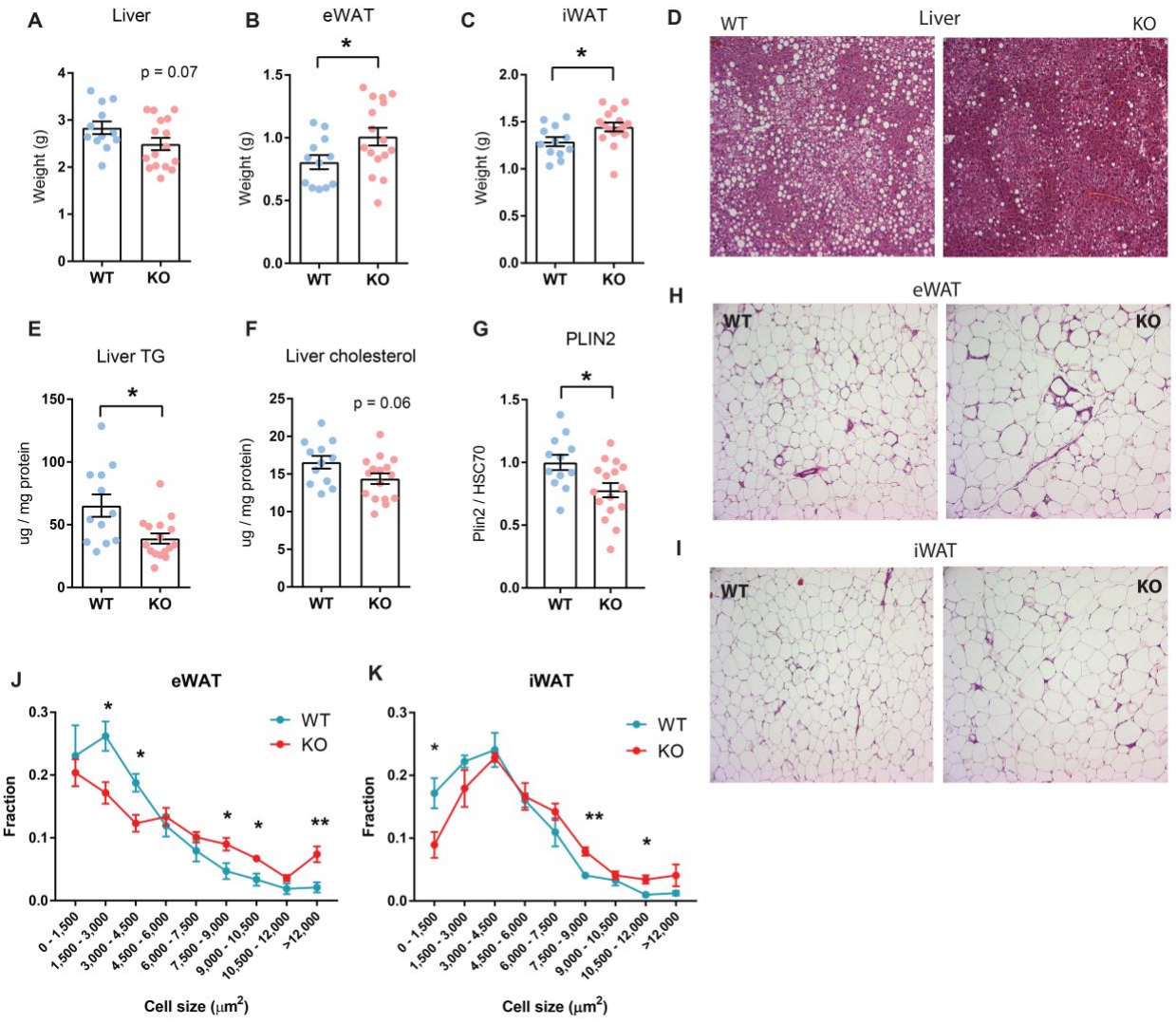

Figure 11. Myonectin deficiency alters lipid distribution in male mice fed a high-fat diet. WT and myonectin-KO mice were euthanized at 39 weeks of age after a 2–4-h fast in the morning. Unless otherwise specified, data in this figure are from analysis of WT (n=12) and KO (n=16) male mice. The wet weight of liver (A), visceral (gonadal) fat pad (B), and subcutaneous (inguinal) fat pad (C) are presented along with (D) representative images of H&E stained liver sections from WT and KO mice. (E-F) Quantification of TG (E) and cholesterol (F) levels in livers. (G) Western blot analysis of Perilipin 2. Two separate gels were run, each with WT (n=6) and KO (n=8) samples. PLIN2 levels were first normalized to HSC70 levels from the same gel and then normalized to the average WT value. Data were then combined from both gels for analysis. (H-I) Representative images of H&E stained epididymal white adipose tissue (eWAT) and inguinal white adipose tissue (iWAT) sections from WT and KO male mice. (J) Quantification of adipocyte size in eWAT sections (WT, n=5; KO, n=5). (K) Quantification of adipocyte size in iWAT sections (WT, n=4; KO, n=5). * $P < 0.05$, ** $P < 0.01$

11E,F). Consistent with the histologic data and hepatic TG content, the lipid droplet-associated protein perilipin 2 was also correspondingly reduced in myonectin-KO livers (**Fig. 11G**). Histologic analysis of visceral (epididymal) white adipose tissue (eWAT) and subcutaneous (inguinal) white adipose tissue (iWAT) indicated significantly larger adipocytes in myonectin-KO animals (**Fig. 11H,I**); this was further confirmed by cell size quantification (**Fig. 11J,K**). Differences in adipocyte cell size were more pronounced in the visceral fat depot (eWAT). These data suggest that myonectin plays a role in lipid partitioning between tissues and its deficiency promotes adipose tissue lipid storage and reduces lipid accumulation in liver.

Myonectin deletion alters multiple liver metabolite levels

Given the striking differences in lipid partitioning between adipose and liver of HFD-fed WT and KO animals, we measured circulating lipids from blood collected at the same time as tissue samples as shown in Fig. 11. Serum TG, NEFA, and β-hydroxybutyrate levels were similar between HFD-fed WT and KO male mice; serum cholesterol levels, however, were lower in myonectin-KO animals (**Fig. 12A-D**). To explore the genotypic difference in hepatic fat accumulation, we also performed unbiased metabolomics analysis to assess global changes in liver metabolites. Of the 642 metabolites quantified, only a small subset (32 in total) of metabolites significantly differed between WT and KO mice (**Fig. 12E**). Our data indicate that HFD-fed myonectin-KO male mice had elevated secondary bile acids, as well as increased levels of metabolites involved in one-carbon metabolism. Interestingly, the hepatic level of imidazole propionate, a molecule reported to induce insulin resistance (72), was also significantly elevated in myonectin-KO male mice; however, this did not impair insulin sensitivity in male mice as measured by glucose and insulin tolerance tests (**Fig. 3D,G**). In addition to metabolite profiling,

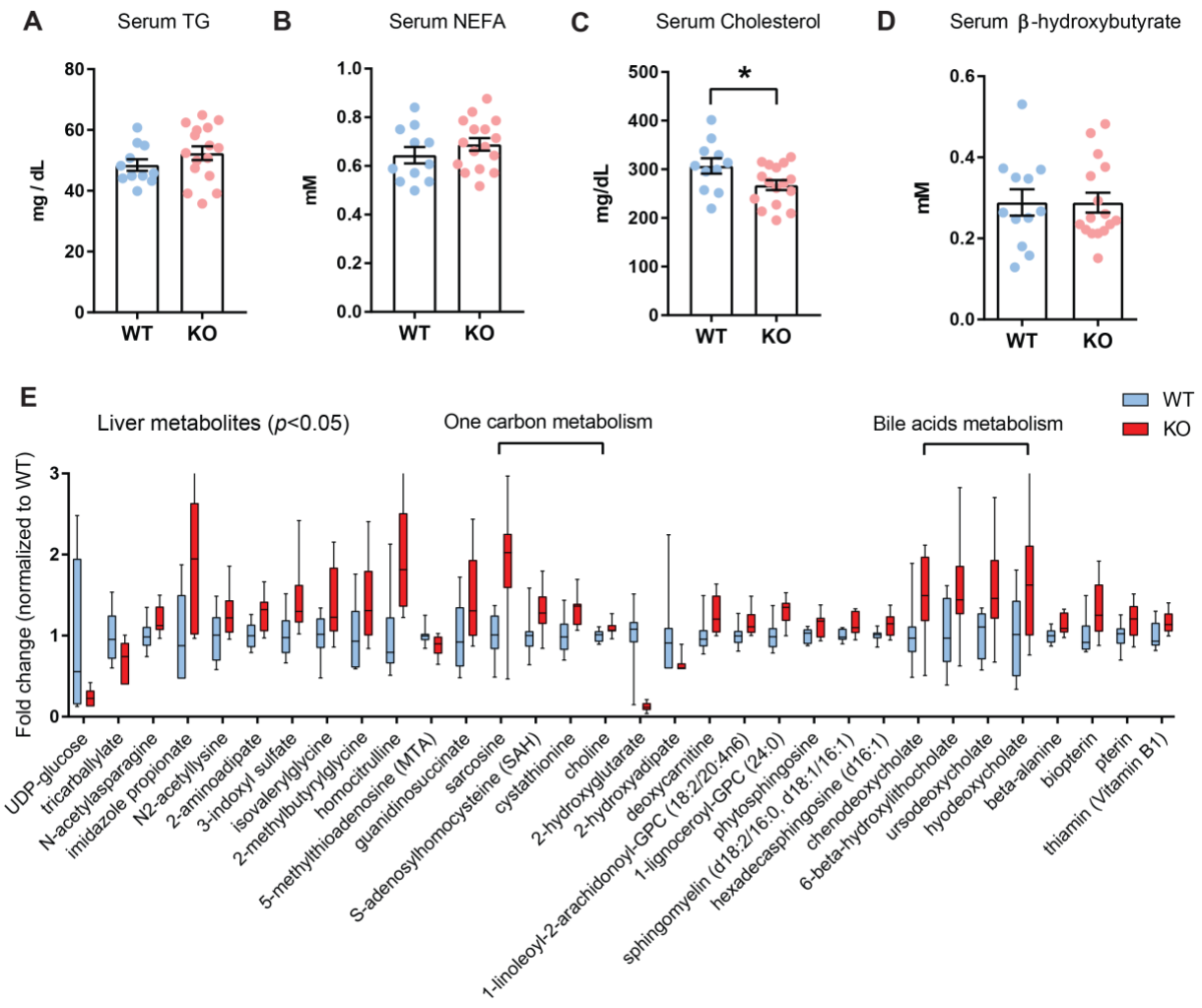

Figure 12. Steady-state serum and liver metabolite levels in WT and myonectin-KO male mice fed a high-fat diet. Sera and livers were harvested from mice (39 weeks old) 2-4 h after food removal (A-E). Quantification of serum triglyceride (TG; A), non-esterified free fatty acids (NEFA; B), cholesterol (C), and ketones (β-hydroxybutyrate; D) (WT, n=12; KO, n=16). (E) All liver metabolites that were significantly different ($p<0.05$) between WT (n=10) and myonectin-KO (n=10) male mice. * $P < 0.05$

we performed extensive quantitative PCR to assess the expression of genes involved in lipid synthesis and catabolism in liver and adipose tissue. Of the major genes involved in lipid synthesis and oxidation and lipoprotein and iron metabolism, there were no significant differences in the expression levels between genotypes in the liver or two major fat depots (**Fig. 13**). However, for genes involved in bile acid metabolism, the expression of *Cyp7a*, the rate limiting

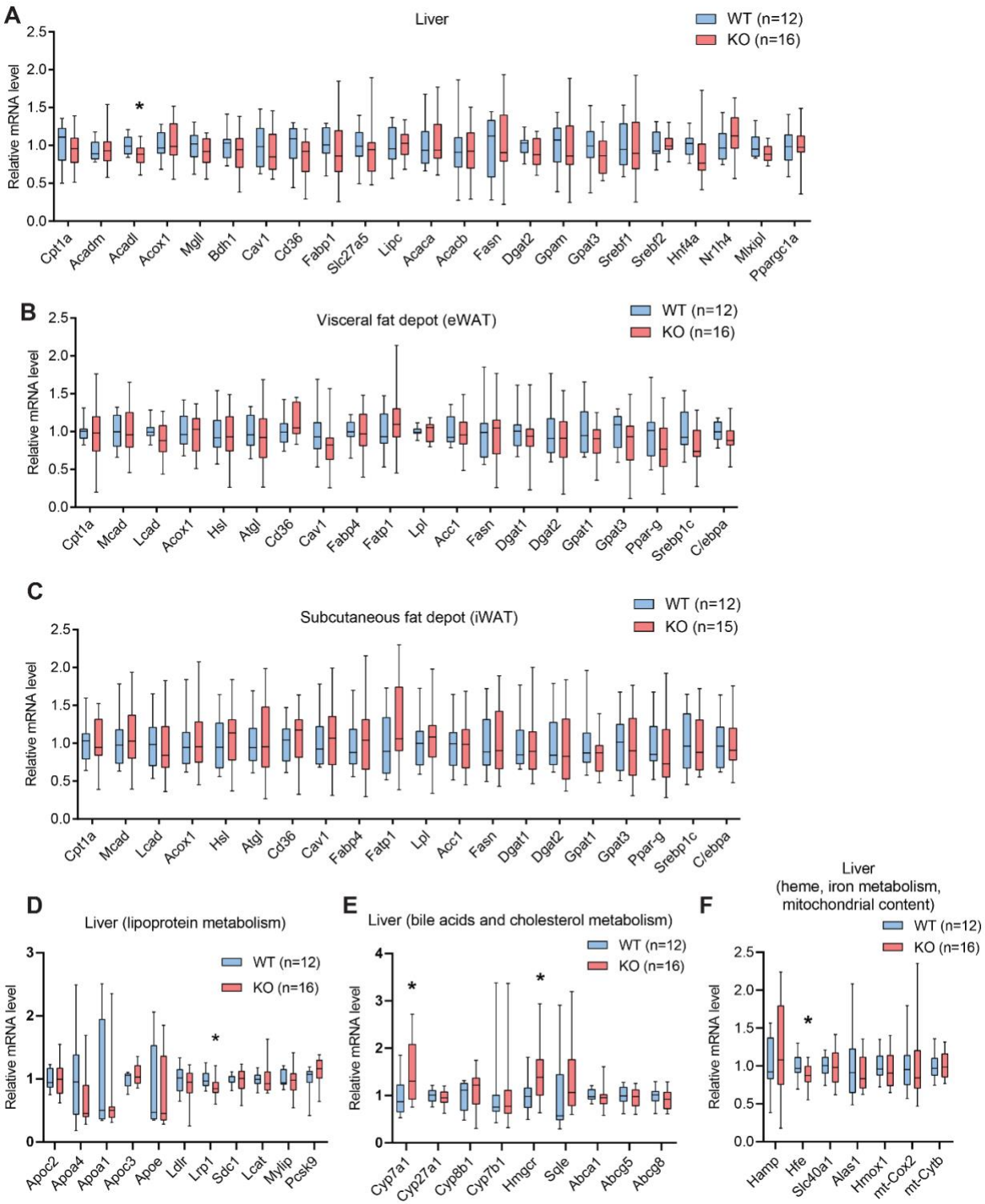

Figure 13. Expression of lipid metabolism genes in liver and visceral and subcutaneous fat depots of myonectin-KO and WT male mice fed a high-fat diet. (A-C) Expression of lipid metabolism genes in liver (A), epididymal white adipose tissue (eWAT; B), and inguinal white adipose tissue (iWAT; C) as measured by quantitative real-time PCR (WT, n=12; KO, n=15-16). (D-F) Expression of genes involved in

lipoprotein metabolism (D), bile acids and cholesterol metabolism (E), and heme and iron metabolism (F) in liver as measured by quantitative real-time PCR (WT, n=12; KO, n=16). Relative gene expression was first normalized to *36b4*, then normalized to the average WT value. All data are from mice sacrificed at 39 weeks of age following a 2–4-h fast in the morning. * $P < 0.05$

enzyme in bile acid synthesis, was significantly upregulated in the liver of myonectin-KO male mice (**Fig. 13E**).

Myonectin deficiency does not alter hepatic VLDL-TG secretion or fat oxidation

Since steady-state levels of metabolites (after 2 h of food removal) and gene expression could not fully explain the differential lipid accumulation in adipose and liver, we tested specific pathways of lipid flux *in vivo*. Reduced hepatic steatosis in HFD-fed KO mice could be due to increased hepatic VLDL-TG secretion. To test this, mice were first fasted for 4 h, beginning at 2 h into the light cycle, to ensure the absence of food-derived circulating chylomicrons secreted by enterocytes; in this physiological state, most of the circulating TG is likely derived from VLDL-TG particles secreted from liver. Mice were next injected with poloxamer 407 to inhibit lipid uptake in peripheral tissue. Thus, the accumulation of serum TG over time reflects hepatic VLDL-TG secretion. This experiment revealed no differences between WT and KO mice, indicating that hepatic VLDL-TG secretion cannot account for the reduced hepatic TG accumulation in myonectin-deficient male mice (**Fig. 14A**). Alternatively, enhanced hepatic fat oxidation can result in lower hepatic TG content. While not a direct measure of fat oxidation in liver, serum ketones are good proxies because ketogenesis in the liver is biochemically linked to fat oxidation (73); hence, circulating ketone levels correspond to the extent of hepatic fat oxidation. Circulating ketones (β-hydroxybutyrate) did not differ between WT and KO mice in either the fasted or fed

state, indicating that there were no differences in hepatic fat oxidation between genotypes (**Fig. 14B)**.

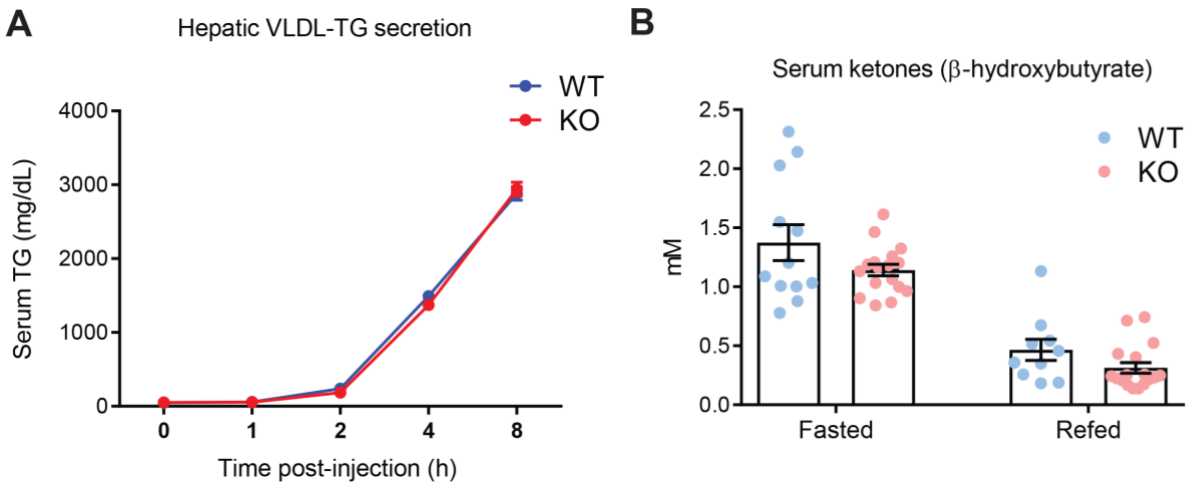

Figure 14. Hepatic VLDL secretion and fat oxidation in myonectin-KO and WT male mice fed a high-fat diet. (A) Serum TG levels over time during hepatic VLDL secretion assay in male mice at 20 weeks of age (WT, n=13; KO, n=17). (B) Serum levels of β-hydroxybutyrate in male mice at 36 weeks of age. Serum was collected after an overnight fast ("fasted"), and also collected upon overnight fast followed by refeeding ("refed"). Fasted: n=12 WT, 17 KO; refed: n=10 WT, 17 KO. Two WT mice did not eat during the re-fed period; therefore, refed serum data from these mice were not included in the analysis.

Myonectin deficiency does not alter adipose tissue lipolysis

Given that myonectin-KO mice had greater adiposity, decreased adipose tissue lipolysis could account for this phenotype. Although recombinant myonectin treatment does not affect *ex vivo* lipolysis in white adipose tissue explants (28), the impact of its deficiency on adipose lipolysis *in vivo* is unknown. To test this, mice were injected with a β_3-adrenergic receptor agonist (CL316,243) to stimulate lipolysis following a 5-h fast. CL-stimulated lipolysis was assessed by measuring serum glucose, glycerol, and NEFA before and 15 min post-injection; no differences were observed between WT and KO mice (**Fig. 15**). Our data thus indicate that both basal (no changes in steady-state serum NEFA levels; **Fig. 12B**) and stimulated lipolysis were not altered in mice lacking myonectin.

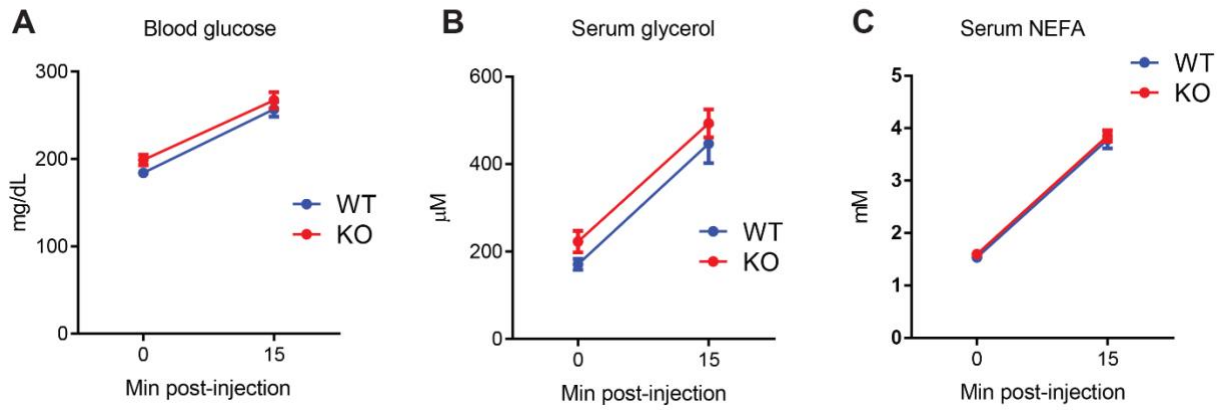

Figure 15. Myonectin-KO and WT male mice fed a high-fat diet do not differ in their capacity for stimulated white adipose tissue lipolysis. (A) Blood glucose, (B) serum glycerol, and (C) serum NEFA levels in male mice at 24 weeks of age during an experiment assessing β_3-adrenergic agonist (CL316,243)-stimulated lipolysis (WT, n=12; KO, n=17).

Myonectin-deficient male mice have higher postprandial LPL activity in the subcutaneous fat depot

Increased lipid uptake into adipocytes could result in greater adiposity. The capacity for peripheral tissues to take up circulating lipid is largely dependent on LPL whose activity is regulated in a tissue-specific and metabolic state-dependent manner (71). In WAT, LPL expression is downregulated during fasting to divert lipid away from adipose to other oxidative tissues. In contrast, LPL activity is activated in WAT postprandially to promote lipid uptake and storage. We therefore measured LPL activity in subcutaneous (iWAT) and visceral (eWAT) fat depots obtained from HFD-fed mice euthanized after 2 h of food removal or in a postprandial state (overnight fast followed by 2 h *ad-libitum* feeding). LPL activity was significantly increased in iWAT from KO mice relative to WT controls, but only in the postprandial state (**Fig. 16A,B**). Increased LPL enzymatic activity was not due to increased expression of LPL mRNA or protein in the iWAT from KO animals (**Fig. 16C-E**). Angiopoietin-like proteins and apolipoproteins are known to regulate LPL activity (74). We therefore assessed the expression of known LPL inhibitors

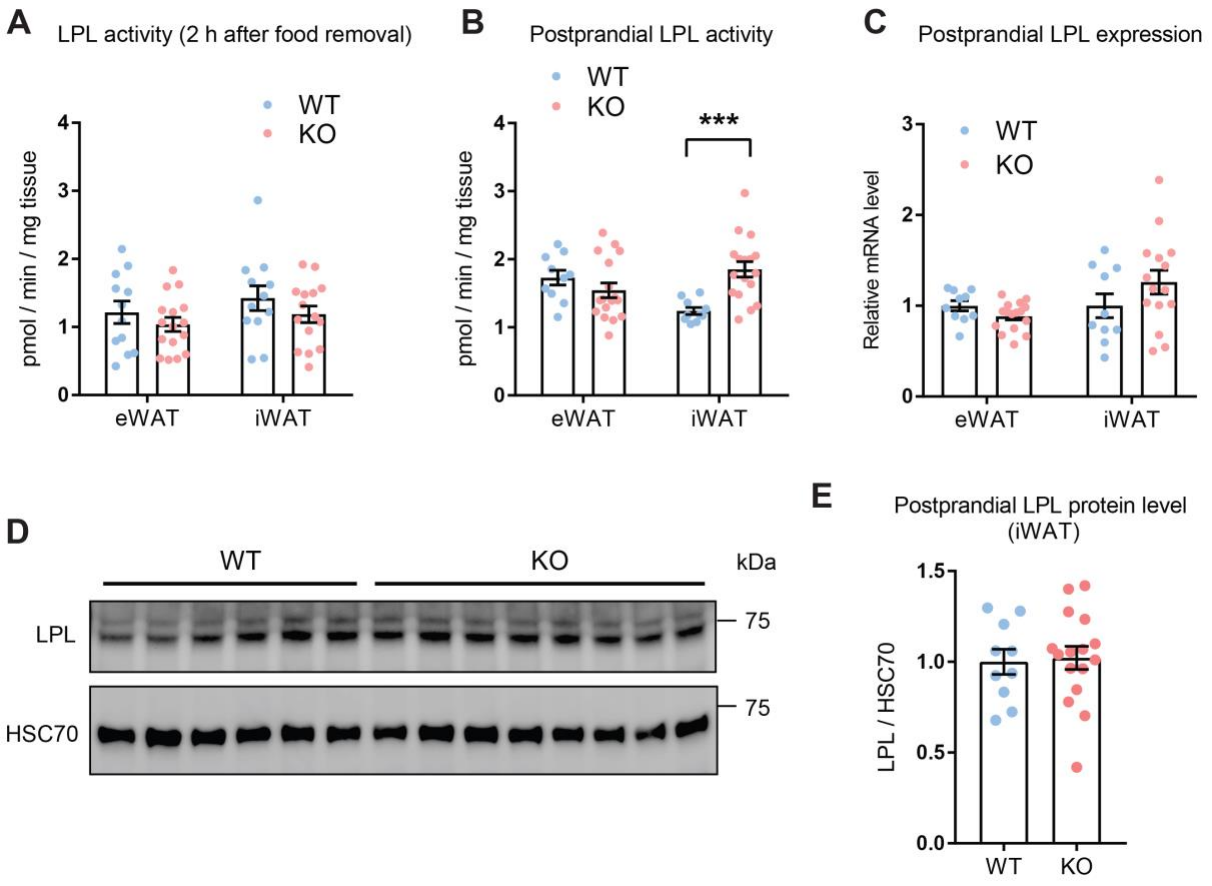

Figure 16. Postprandial lipoprotein lipase (LPL) activity in the subcutaneous (inguinal) fat depot is increased in myonectin-KO male mice fed a high-fat diet. (A) LPL activity in epididymal white adipose tissue (eWAT: WT, n=12; KO, n=16) and inguinal white adipose tissue (iWAT: WT, n=12; KO, n=15) from mice euthanized at 39 weeks of age following a 2–4-h fast in the morning. (B) LPL activity in eWAT and iWAT from mice (WT, n=10; KO, n=17) euthanized at 36 weeks of age after 2-h re-feeding following an overnight fast. (C) LPL mRNA expression in the same eWAT (WT, n=10; KO, n=16) and iWAT (WT, n=10; KO, n=15) samples as (B). (D-E) Western blot analysis of LPL in the same iWAT samples as in (B). Two separate gels were run, one with 6 WT and 8 KO samples, and the other with 4 WT and 8 KO samples. LPL levels were first normalized to HSC70 levels from the same gel, then normalized to the average WT value. Data were then combined from both gels for analysis (WT, n=10; KO, n=16) (E). Images from one gel are shown (D). *** $P < 0.001$

(*Angptl3*, *Angptl4*, *Angptl8*, and *ApoC3*) and activators (*ApoC2*, *ApoA4*, and *ApoA5*) in the same fat tissue samples as well as in liver. We also examined the level of *Fxr* mRNA, the transcriptional regulator of angiopoietin-like proteins and apolipoproteins, as well as *Gpihbp1* and *Vldlr* that are important for translocation of LPL to the cell surface. At the mRNA level, no significant genotypic

differences were observed for these transcripts in WAT and liver (**Fig. 17A-C**). We also measured protein levels of ANGPTL3 and ANGPTL4, two of the major LPL inhibitors, in fasting serum as well as the postprandial serum samples; their protein levels were also not significantly different between genotypes (**Fig. 17D-E**).

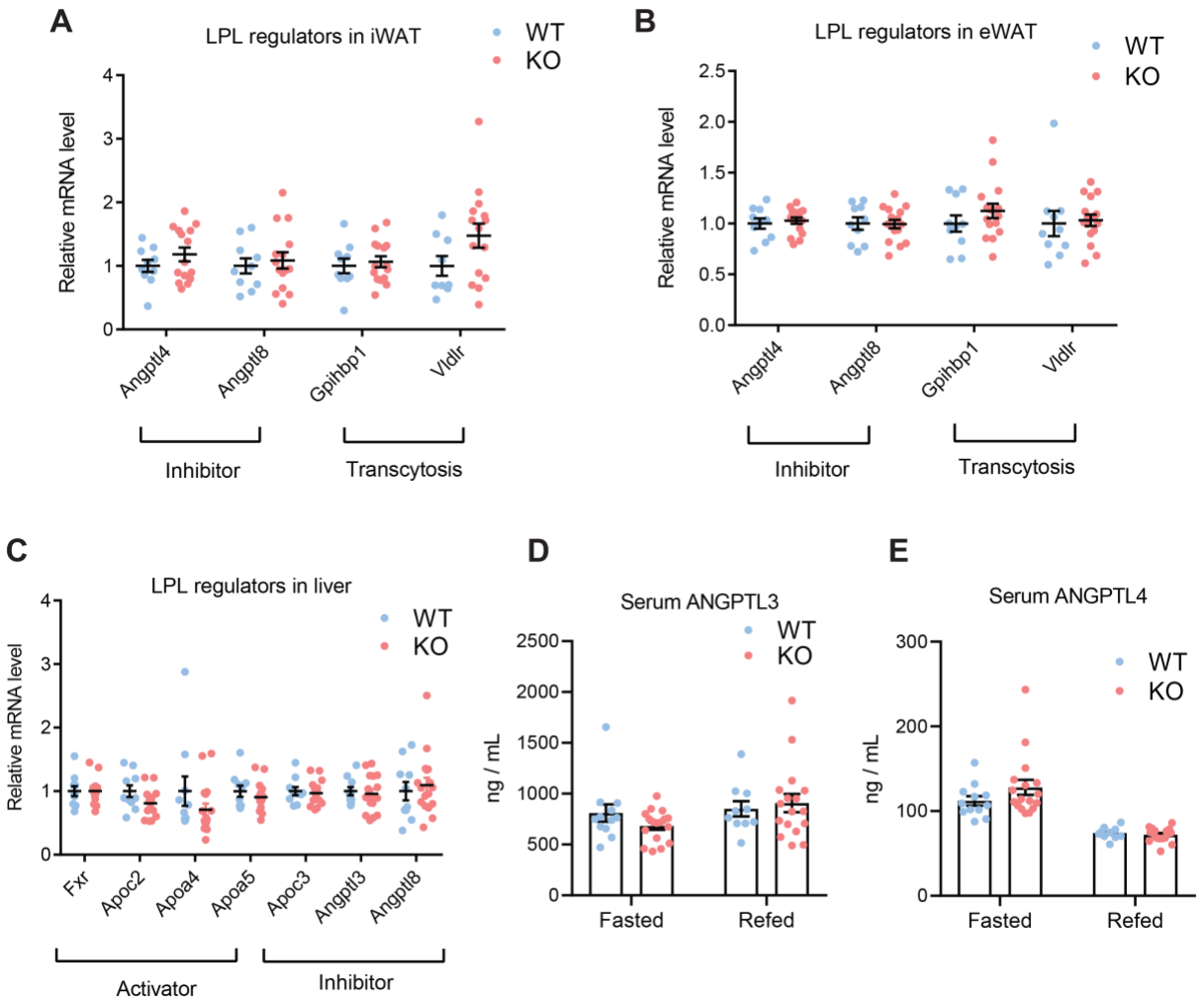

Figure 17. Serum levels and expression of genes involved in regulating lipoprotein lipase (LPL) activity or transcytosis in different fat depots and liver of myonectin-KO and WT male mice fed a high-fat diet. (A-C) Expression of LPL regulators, as measured by quantitative real-time PCR, in inguinal white adipose tissue (iWAT; A), epididymal white adipose tissue (eWAT; B), and liver (C) from mice sacrificed at 36 weeks of age after 2-h re-feeding following an overnight fast (WT, n=10; KO, n=15-17). Relative gene expression was first normalized to *36b4*, then normalized to the average WT value. (D-E) Serum levels of ANGPTl3 (D) and ANGPTl4 (E) in myonectin-KO and WT male mice after an overnight fast ("fasted") or following 2 h of re-feeding ("Refed"). Fasted: n=12 WT, 17 KO; refed: n=10 WT, 17 KO. Two WT mice did not eat during the re-fed period; therefore, refed serum data from these mice were not included in the analysis.

DISCUSSION

We used a genetic loss-of-function mouse model to determine whether myonectin is required physiologically to maintain metabolic homeostasis. Under basal conditions where mice were fed a control low-fat diet (LFD) comparable to standard chow, myonectin was largely dispensable for regulating whole-body carbohydrate and fat metabolism, consistent with a recent report (62). However, there is one notable phenotype in male mice fed a control LFD: myonectin deficiency significantly reduced physical activity in the *ad-libitum* fed state, as well as in the refed (post-prandial) state following a 24 hour fast. In the fasted state where mice typically have heightened foraging behavior, physical activity level was not significantly different between genotypes; thus, there appears to be a physiological state-dependent change in ambulatory and total physical activity in the KO animals. We speculate that myonectin may modulate, directly or indirectly, a central pathway controlling physical activity in male mice between two opposing (fed and fasted) metabolic states. Of note, the reduced physical activity seen in myonectin-KO male mice is not the result of a functional deficit in the skeletal muscle since the capacity for an exhaustive sprint or endurance run was not significantly different between genotypes, nor were the pre- and post-exercise blood glucose, lactate, NEFA, or ketone levels. The ability of skeletal muscle and liver to replenish their glycogen stores following exercise (with or without glucose gavage post exercise) was also not significantly different, indicating that myonectin is not required for the metabolic response or adaptation to a single bout of exercise. It appears that myonectin is also dispensable for physiologic adaptation to chronic voluntary exercise. When indirect calorimetry analyses were conducted in WT and KO mice with access to a running wheel, we observed no significant differences in metabolic rate, food intake, or the amount of voluntary

exercise (wheel running) between genotypes of either sex. Similarly, a recent report indicates that myonectin is not required for normal heart function under normal, non-stressed conditions (29).

In the pathophysiological context of obesity and insulin resistance induced by a high-fat diet (HFD), we observed two significant and notable phenotypes related to lipid metabolism in the myonectin-deficient animals. First, myonectin-KO mice displayed an impaired ability to handle an acute oral lipid load. Second, lipids appear to be partitioned differentially between adipose and liver; specifically, myonectin-KO male mice had strikingly reduced triglyceride accumulation in liver and, in parallel, a significant increase in adiposity due to greater lipid storage in hypertrophied adipocytes. These two lipid phenotypes in KO animals are sex-dependent. Apart of developing mild insulin resistance and a bigger gonadal fat pad, myonectin-KO female mice fed an HFD were largely indistinguishable from WT littermates with respect to whole-body lipid metabolism. It is known that female mice on a C57BL/6 genetic background are much less susceptible to diet-induced obesity (75, 76). Many studies (77), including our previous studies (54-56) and the present study, reinforce the importance of sex as a biological variable that can influence the impact and phenotypic outcomes of a given genotype. Intriguingly, although our current study and previous findings (62) do not support a major role for myonectin in regulating glucose metabolism, recent reports suggest that circulating myonectin in human blood is correlated with insulin resistance, impaired glucose metabolism, and type 2 diabetes (60, 61). Whether myonectin plays a causal role in human carbohydrate metabolism and insulin sensitivity, distinct from rodents, remains to be determined.

We previously showed that myonectin infusion lowers serum lipid levels in mice and, when given to cultured hepatocytes and adipocytes, also promotes lipid uptake into cells (28). Additionally, ingestion of lipid via oral gavage can upregulate myonectin expression (28). Based

on these previous findings, we hypothesized that myonectin deficiency would result in impaired lipid clearance following an oral lipid load. Indeed, myonectin-KO male mice exhibited a significantly greater rise in both serum TG and NEFA levels following an oral lipid challenge relative to WT littermates, a functional deficit we observed in multiple independent cohorts of HFD-fed male KO mice. Several mechanisms could account for the observed phenotype: 1) impaired lipid clearance and uptake by peripheral tissues as hypothesized, and/or 2) increased intestinal lipid absorption and chylomicron secretion. We ruled out the latter as the cause of the lipid intolerance seen in myonectin-deficient animals. To determine lipid uptake by peripheral tissues, we focused on LPL activity since this enzyme is a major determinant of lipid clearance in extrahepatic tissues (71). The biggest difference in serum lipid levels between genotypes was seen at 2 h after oral lipid gavage or 2 h post-feed following a fast; we therefore quantified the total heparin-displaceable LPL activity in the serum 2 h post-feeding. Although there were no significant genotypic differences in total lipase activity, we could not rule out potential differences in LPL-dependent lipid uptake between WT and KO mice. Of note, both WT and KO mice converged on the same baseline lipid levels 4 h after oral lipid gavage. Thus, the observed significant differences at earlier time points likely reflect differences in the kinetics of lipid uptake rather than the overall capacity for lipid disposal in peripheral tissues. For example, relative to WT littermates, the overall LPL activity may be lower in myonectin-KO mice shortly after oral lipid gavage, reflecting slower activation of the enzyme in response to altered nutritional state, which would result in a much greater rise in serum triglyceride at 0-2 h post-gavage that we observed. At later time points total LPL activity in KO mice may reach the same maximum level attained in WT mice, reflecting the marked decline in serum triglyceride observed in KO mice at 2-4 h post-gavage, leading to the same baseline lipid levels between genotypes 4 h after oral lipid challenge.

Hence, it is possible that when we measured total LPL activity at 2 h post-feeding, LPL activity in WT mice was in the process of decreasing back to baseline and the activity in the KO animals was increasing to its maximal level. Future studies will help to determine the total heparin-displaceable LPL activity at different time points after oral lipid challenge.

The second major phenotype observed in myonectin-KO male mice is a significant difference in lipid distribution between liver and adipose tissue. We observed significantly greater adipocyte hypertrophy, due to greater fat storage in lipid droplets, in both the visceral and subcutaneous fat depots of HFD-fed KO mice. Parallel to increased adiposity, we observed a striking reduction in fat accumulation in the liver of myonectin-deficient animals. Several mechanisms could underlie this phenotype, including liver-specific processes, adipose-specific processes, or a combination of both. Reduced hepatic steatosis could be a consequence of either increased fat oxidation, increased VLDL secretion, decreased lipid uptake from circulation, and/or decreased *de novo* lipogenesis. Serum ketones (β-hydroxybutyrate), a good proxy for liver fat oxidation (73), were not significantly different between WT and KO mice in either fed or fasting states, thus ruling out hepatic fat oxidation as the cause for reduced steatosis. We also ruled out enhanced hepatic VLDL-triglyceride secretion as a contributing factor to reduced fatty liver. Although lipid uptake and fatty acid synthesis have not been directly measured, our liver metabolite profiling, in addition to extensive PCR quantification of genes involved in hepatic lipid metabolism, does not suggest any differences in these two processes.

Interestingly, despite a striking reduction in ectopic lipid accumulation in liver, myonectin-KO male mice did not exhibit better hepatic glucose metabolism profiles relative to WT littermates; fasting blood glucose levels (dominated by hepatic gluconeogenesis) and insulin tolerance tests did not reveal any significant differences between genotypes. While fatty liver—

resulting from excessive ectopic fat deposition in the obese state— is frequently associated with impaired hepatic insulin action (as reflected in greater hepatic glucose output) (4), these two phenomena appear to be uncoupled in myonectin-KO animals. Intriguingly, one of the liver metabolites that was significantly upregulated in myonectin-KO male mice is imidazole propionate. This molecule, thought to be produced from histidine by gut microbiota, was recently reported to be elevated in obese humans with type 2 diabetes and when given to mice can induce insulin resistance (72). While it seems that diabetic humans have a relatively wide range of imidazole propionate concentrations relative to non-diabetic controls, the level of upregulation (2-3 fold) we observed in the myonectin-KO mice is not sufficient to disrupt normal insulin signaling as indicated by a lack of significant differences in fasting blood glucose, as well as glucose and insulin tolerance.

An alternative explanation for the reduced fat accumulation seen in myonectin-KO liver could be secondary to changes in fat storage in adipose tissue, leading to reduced ectopic lipid deposition in other organs and tissues. Enlarged adipocytes seen in our myonectin-KO mice could result from decreased lipolysis, increased lipid uptake and storage, decreased fat oxidation, and/or increased *de novo* lipogenesis. We ruled out reduced adipose lipolysis as a cause of increased adiposity, as neither basal nor β_3-adrenergic agonist stimulated lipolysis was significantly different between WT and KO mice. LPL activity was measured in adipose tissue as a proxy for the capacity for lipid uptake. Intriguingly, LPL activity was significantly greater in the subcutaneous (inguinal) fat depot of KO mice relative to WT littermates in the postprandial state. Increased fat uptake into adipocytes via LPL may, in part, account for the increase in adiposity and adipocyte cell size. However, this appears to be fat depot-specific; we did not observe a significant increase in LPL activity in the visceral (gonadal) fat of KO animals. Although fat oxidation and synthesis in adipose

tissue were not directly measured in this study, none of the lipid synthesis or catabolism genes we considered were significantly different in their expression levels between WT and KO mice. What accounts for the increased LPL activity seen in the iWAT of myonectin-KO mice is presently unclear, since none of the known regulators (angiopoetin-like proteins and apolipoproteins) of LPL activity and transcytosis were different in their expression or serum protein levels between WT and KO animals.

In summary, we provide here a detailed analysis of the metabolic consequences of myonectin deletion in a genetic mouse model. Whereas myonectin is largely dispensable for whole-body glucose metabolism, it plays an important role in regulating local and systemic lipid metabolism. Loss of myonectin causes lipid intolerance in response to oral lipid loading and it alters lipid distribution between adipose and liver. Thus, in addition to regulating stress erythropoiesis in the context of blood loss (38), myonectin/erythroferrone is also a secreted metabolic regulator of fat metabolism in the physiological context of diet-induced obesity. Future studies will help pinpoint the mechanisms by which myonectin controls fat metabolism in a tissue-specific manner, and the receptor (currently unknown) through which it exerts its biological functions.

REFERENCES

1. Wasserman, D. H., Kang, L., Ayala, J. E., Fueger, P. T., and Lee-Young, R. S. (2011) The physiological regulation of glucose flux into muscle in vivo. *J Exp Biol* **214**, 254-262
2. Roach, P. J., Depaoli-Roach, A. A., Hurley, T. D., and Tagliabracci, V. S. (2012) Glycogen and its metabolism: some new developments and old themes. *Biochem J* **441**, 763-787
3. Petersen, K. F., Dufour, S., Savage, D. B., Bilz, S., Solomon, G., Yonemitsu, S., Cline, G. W., Befroy, D., Zemany, L., Kahn, B. B., Papademetris, X., Rothman, D. L., and Shulman, G. I. (2007) The role of skeletal muscle insulin resistance in the pathogenesis of the metabolic syndrome. *Proc Natl Acad Sci U S A* **104**, 12587-12594
4. Samuel, V. T., and Shulman, G. I. (2012) Mechanisms for insulin resistance: common threads and missing links. *Cell* **148**, 852-871
5. Pedersen, B. K. (2013) Muscle as a secretory organ. *Compr Physiol* **3**, 1337-1362
6. Pedersen, B. K., and Febbraio, M. A. (2012) Muscles, exercise and obesity: skeletal muscle as a secretory organ. *Nat Rev Endocrinol* **8**, 457-465
7. Henningsen, J., Rigbolt, K. T., Blagoev, B., Pedersen, B. K., and Kratchmarova, I. (2010) Dynamics of the skeletal muscle secretome during myoblast differentiation. *Mol Cell Proteomics* **9**, 2482-2496
8. Chan, X. C., McDermott, J. C., and Siu, K. W. (2007) Identification of secreted proteins during skeletal muscle development. *J Proteome Res* **6**, 698-710
9. Hartwig, S., Raschke, S., Knebel, B., Scheler, M., Irmler, M., Passlack, W., Muller, S., Hanisch, F. G., Franz, T., Li, X., Dicken, H. D., Eckardt, K., Beckers, J., de Angelis, M. H., Weigert, C., Haring, H. U., Al-Hasani, H., Ouwens, D. M., Eckel, J., Kotzka, J., and Lehr, S. (2014) Secretome profiling of primary human skeletal muscle cells. *Biochim Biophys Acta* **1844**, 1011-1017
10. McPherron, A. C., and Lee, S. J. (2002) Suppression of body fat accumulation in myostatin-deficient mice. *J Clin Invest* **109**, 595-601
11. Shan, T., Liang, X., Bi, P., and Kuang, S. (2013) Myostatin knockout drives browning of white adipose tissue through activating the AMPK-PGC1alpha-Fndc5 pathway in muscle. *FASEB J* **27**, 1981-1989
12. Guo, T., Bond, N. D., Jou, W., Gavrilova, O., Portas, J., and McPherron, A. C. (2012) Myostatin inhibition prevents diabetes and hyperphagia in a mouse model of lipodystrophy. *Diabetes* **61**, 2414-2423
13. Pedersen, B. K. (2009) Edward F. Adolph distinguished lecture: muscle as an endocrine organ: IL-6 and other myokines. *J Appl Physiol* **107**, 1006-1014
14. Hojman, P., Pedersen, M., Nielsen, A. R., Krogh-Madsen, R., Yfanti, C., Akerstrom, T., Nielsen, S., and Pedersen, B. K. (2009) Fibroblast growth factor-21 is induced in human skeletal muscles by hyperinsulinemia. *Diabetes* **58**, 2797-2801
15. Izumiya, Y., Bina, H. A., Ouchi, N., Akasaki, Y., Kharitonenkov, A., and Walsh, K. (2008) FGF21 is an Akt-regulated myokine. *FEBS Lett* **582**, 3805-3810
16. Zeng, L., Akasaki, Y., Sato, K., Ouchi, N., Izumiya, Y., and Walsh, K. (2010) Insulin-like 6 is induced by muscle injury and functions as a regenerative factor. *J Biol Chem* **285**, 36060-36069
17. Ouchi, N., Oshima, Y., Ohashi, K., Higuchi, A., Ikegami, C., Izumiya, Y., and Walsh, K. (2008) Follistatin-like 1, a secreted muscle protein, promotes endothelial cell function and revascularization in ischemic tissue through a nitric-oxide synthase-dependent mechanism. *J Biol Chem* **283**, 32802-32811
18. Broholm, C., Laye, M. J., Brandt, C., Vadalasetty, R., Pilegaard, H., Pedersen, B. K., and Scheele, C. (2011) LIF is a contraction-induced myokine stimulating human myocyte proliferation. *J Appl Physiol* **111**, 251-259

19. Haugen, F., Norheim, F., Lian, H., Wensaas, A. J., Dueland, S., Berg, O., Funderud, A., Skalhegg, B. S., Raastad, T., and Drevon, C. A. (2010) IL-7 is expressed and secreted by human skeletal muscle cells. *Am J Physiol Cell Physiol* **298**, C807-816
20. Quinn, L. S., Anderson, B. G., Strait-Bodey, L., Stroud, A. M., and Argiles, J. M. (2009) Oversecretion of interleukin-15 from skeletal muscle reduces adiposity. *Am J Physiol Endocrinol Metab* **296**, E191-202
21. Nishizawa, H., Matsuda, M., Yamada, Y., Kawai, K., Suzuki, E., Makishima, M., Kitamura, T., and Shimomura, I. (2004) Musclin, a novel skeletal muscle-derived secretory factor. *J Biol Chem* **279**, 19391-19395
22. Subbotina, E., Sierra, A., Zhu, Z., Gao, Z., Koganti, S. R., Reyes, S., Stepniak, E., Walsh, S. A., Acevedo, M. R., Perez-Terzic, C. M., Hodgson-Zingman, D. M., and Zingman, L. V. (2015) Musclin is an activity-stimulated myokine that enhances physical endurance. *Proc Natl Acad Sci U S A* **112**, 16042-16047
23. Bostrom, P., Wu, J., Jedrychowski, M. P., Korde, A., Ye, L., Lo, J. C., Rasbach, K. A., Bostrom, E. A., Choi, J. H., Long, J. Z., Kajimura, S., Zingaretti, M. C., Vind, B. F., Tu, H., Cinti, S., Hojlund, K., Gygi, S. P., and Spiegelman, B. M. (2012) A PGC1-alpha-dependent myokine that drives brown-fat-like development of white fat and thermogenesis. *Nature* **481**, 463-468
24. Welc, S. S., and Clanton, T. L. (2013) The regulation of interleukin-6 implicates skeletal muscle as an integrative stress sensor and endocrine organ. *Exp Physiol* **98**, 359-371
25. Staiger, H., Bohm, A., Scheler, M., Berti, L., Machann, J., Schick, F., Machicao, F., Fritsche, A., Stefan, N., Weigert, C., Krook, A., Haring, H. U., and de Angelis, M. H. (2013) Common genetic variation in the human FNDC5 locus, encoding the novel muscle-derived 'browning' factor irisin, determines insulin sensitivity. *PLoS One* **8**, e61903
26. Egan, B., and Zierath, J. R. (2013) Exercise metabolism and the molecular regulation of skeletal muscle adaptation. *Cell Metab* **17**, 162-184
27. Trayhurn, P., Drevon, C. A., and Eckel, J. (2010) Secreted proteins from adipose tissue and skeletal muscle - adipokines, myokines and adipose/muscle cross-talk. *Arch Physiol Biochem* **117**, 47-56
28. Seldin, M. M., Peterson, J. M., Byerly, M. S., Wei, Z., and Wong, G. W. (2012) Myonectin (CTRP15), a novel myokine that links skeletal muscle to systemic lipid homeostasis. *J Biol Chem* **287**, 11968-11980
29. Otaka, N., Shibata, R., Ohashi, K., Uemura, Y., Kambara, T., Enomoto, T., Ogawa, H., Ito, M., Kawanishi, H., Maruyama, S., Joki, Y., Fujikawa, Y., Narita, S., Unno, K., Kawamoto, Y., Murate, T., Murohara, T., and Ouchi, N. (2018) Myonectin Is an Exercise-Induced Myokine That Protects the Heart From Ischemia-Reperfusion Injury. *Circ Res* **123**, 1326-1338
30. Wong, G. W., Krawczyk, S. A., Kitidis-Mitrokostas, C., Ge, G., Spooner, E., Hug, C., Gimeno, R., and Lodish, H. F. (2009) Identification and characterization of CTRP9, a novel secreted glycoprotein, from adipose tissue that reduces serum glucose in mice and forms heterotrimers with adiponectin. *FASEB J* **23**, 241-258
31. Wong, G. W., Krawczyk, S. A., Kitidis-Mitrokostas, C., Revett, T., Gimeno, R., and Lodish, H. F. (2008) Molecular, biochemical and functional characterizations of C1q/TNF family members: adipose-tissue-selective expression patterns, regulation by PPAR-gamma agonist, cysteine-mediated oligomerizations, combinatorial associations and metabolic functions. *Biochem J* **416**, 161-177
32. Wong, G. W., Wang, J., Hug, C., Tsao, T. S., and Lodish, H. F. (2004) A family of Acrp30/adiponectin structural and functional paralogs. *Proc Natl Acad Sci U S A* **101**, 10302-10307
33. Wei, Z., Peterson, J. M., Lei, X., Cebotaru, L., Wolfgang, M. J., Baldeviano, G. C., and Wong, G. W. (2012) C1q/TNF-related protein-12 (CTRP12), a novel adipokine that improves insulin sensitivity and glycemic control in mouse models of obesity and diabetes. *J Biol Chem* **287**, 10301-10315

34. Wei, Z., Peterson, J. M., and Wong, G. W. (2011) Metabolic regulation by C1q/TNF-related protein-13 (CTRP13): activation of AMP-activated protein kinase and suppression of fatty acid-induced JNK signaling. *J Biol Chem* **286**, 15652-15665
35. Wei, Z., Seldin, M. M., Natarajan, N., Djemal, D. C., Peterson, J. M., and Wong, G. W. (2013) C1q/Tumor Necrosis Factor-related Protein 11 (CTRP11), a Novel Adipose Stroma-derived Regulator of Adipogenesis. *J Biol Chem* **288**, 10214-10229
36. Seldin, M. M., Lei, X., Tan, S. Y., Stanson, K. P., Wei, Z., and Wong, G. W. (2013) Skeletal muscle-derived myonectin activates the mTOR pathway to suppress autophagy in liver. *J Biol Chem* **289**, 36073-36082
37. Kautz, L., Jung, G., Nemeth, E., and Ganz, T. (2014) Erythroferrone contributes to recovery from anemia of inflammation. *Blood* **124**, 2569-2574
38. Kautz, L., Jung, G., Valore, E. V., Rivella, S., Nemeth, E., and Ganz, T. (2014) Identification of erythroferrone as an erythroid regulator of iron metabolism. *Nat Genet* **46**, 678-684
39. Peterson, J. M., Aja, S., Wei, Z., and Wong, G. W. (2012) C1q/TNF-related protein-1 (CTRP1) enhances fatty acid oxidation via AMPK activation and ACC inhibition. *J Biol Chem* **287**, 1576-1587
40. Peterson, J. M., Seldin, M. M., Wei, Z., Aja, S., and Wong, G. W. (2013) CTRP3 attenuates diet-induced hepatic steatosis by regulating triglyceride metabolism. *Am J Physiol Gastrointest Liver Physiol* **305**, G214-224.
41. Peterson, J. M., Wei, Z., Seldin, M. M., Byerly, M. S., Aja, S., and Wong, G. W. (2013) CTRP9 transgenic mice are protected from diet-induced obesity and metabolic dysfunction. *Am J Physiol Regul Integr Comp Physiol* **305**, R522-533
42. Peterson, J. M., Wei, Z., and Wong, G. W. (2010) C1q/TNF-related Protein-3 (CTRP3), a Novel Adipokine That Regulates Hepatic Glucose Output. *J Biol Chem* **285**, 39691-39701
43. Byerly, M. S., Swanson, R., Wei, Z., Seldin, M. M., McCulloh, P. S., and Wong, G. W. (2013) A Central Role for C1q/TNF-Related Protein 13 (CTRP13) in Modulating Food Intake and Body Weight. *PLoS One* **8**, e62862
44. Enomoto, T., Ohashi, K., Shibata, R., Higuchi, A., Maruyama, S., Izumiya, Y., Walsh, K., Murohara, T., and Ouchi, N. (2011) Adipolin/C1qdc2/CTRP12 functions as an adipokine that improves glucose metabolism. *J Biol Chem* **286**, 34552-34558
45. Su, H., Yuan, Y., Wang, X. M., Lau, W. B., Wang, Y., Wang, X., Gao, E., Koch, W. J., and Ma, X. L. (2013) Inhibition of CTRP9, a novel and cardiac-abundantly expressed cell survival molecule, by TNFalpha-initiated oxidative signaling contributes to exacerbated cardiac injury in diabetic mice. *Basic Res Cardiol* **108**, 315-326
46. Uemura, Y., Shibata, R., Ohashi, K., Enomoto, T., Kambara, T., Yamamoto, T., Ogura, Y., Yuasa, D., Joki, Y., Matsuo, K., Miyabe, M., Kataoka, Y., Murohara, T., and Ouchi, N. (2013) Adipose-derived factor CTRP9 attenuates vascular smooth muscle cell proliferation and neointimal formation. *FASEB J* **27**, 25-33
47. Kambara, T., Ohashi, K., Shibata, R., Ogura, Y., Maruyama, S., Enomoto, T., Uemura, Y., Shimizu, Y., Yuasa, D., Matsuo, K., Miyabe, M., Kataoka, Y., Murohara, T., and Ouchi, N. (2012) CTRP9 protein protects against myocardial injury following ischemia-reperfusion through AMP-activated protein kinase (AMPK)-dependent mechanism. *J Biol Chem* **287**, 18965-18973
48. Sun, Y., Yi, W., Yuan, Y., Lau, W. B., Yi, D., Wang, X., Wang, Y., Su, H., Gao, E., Koch, W. J., and Ma, X. L. (2013) C1q/Tumor Necrosis Factor-Related Protein-9, a Novel Adipocyte-Derived Cytokine, Attenuates Adverse Remodeling in the Ischemic Mouse Heart via Protein Kinase A Activation. *Circulation* **128**, S113-120
49. Appari, M., Breitbart, A., Brandes, F., Szaroszyk, M., Froese, N., Korf-Klingebiel, M., Mohammadi, M. M., Grund, A., Scharf, G. M., Wang, H., Zwadlo, C., Fraccarollo, D., Schrameck, U., Nemer, M., Wong, G. W., Katus, H. A., Wollert, K. C., Muller, O. J., Bauersachs, J., and Heineke, J. (2017) C1q-TNF-Related Protein-9 Promotes Cardiac Hypertrophy and Failure. *Circ Res* **120**, 66-77

50. Yan, W., Guo, Y., Tao, L., Lau, W. B., Gan, L., Yan, Z., Guo, R., Gao, E., Wong, G. W., Koch, W. L., Wang, Y., and Ma, X. L. (2017) C1q/Tumor Necrosis Factor-Related Protein-9 Regulates the Fate of Implanted Mesenchymal Stem Cells and Mobilizes Their Protective Effects Against Ischemic Heart Injury via Multiple Novel Signaling Pathways. *Circulation* **136**, 2162-2177
51. Kambara, T., Shibata, R., Ohashi, K., Matsuo, K., Hiramatsu-Ito, M., Enomoto, T., Yuasa, D., Ito, M., Hayakawa, S., Ogawa, H., Aprahamian, T., Walsh, K., Murohara, T., and Ouchi, N. (2015) C1q/Tumor Necrosis Factor-Related Protein 9 Protects against Acute Myocardial Injury through an Adiponectin Receptor I-AMPK-Dependent Mechanism. *Mol Cell Biol* **35**, 2173-2185
52. Yuasa, D., Ohashi, K., Shibata, R., Mizutani, N., Kataoka, Y., Kambara, T., Uemura, Y., Matsuo, K., Kanemura, N., Hayakawa, S., Hiramatsu-Ito, M., Ito, M., Ogawa, H., Murate, T., Murohara, T., and Ouchi, N. (2016) C1q/TNF-related protein-1 functions to protect against acute ischemic injury in the heart. *FASEB J* **30**, 1065-1075
53. Lei, X., Seldin, M. M., Little, H. C., Choy, N., Klonisch, T., and Wong, G. W. (2017) C1q/TNF-related protein 6 (CTRP6) links obesity to adipose tissue inflammation and insulin resistance. *J Biol Chem* **292**, 14836-14850
54. Petersen, P. S., Lei, X., Wolf, R. M., Rodriguez, S., Tan, S. Y., Little, H. C., Schweitzer, M. A., Magnuson, T. H., Steele, K. E., and Wong, G. W. (2017) CTRP7 deletion attenuates obesity-linked glucose intolerance, adipose tissue inflammation, and hepatic stress. *Am J Physiol Endocrinol Metab* **312**, E309-E325
55. Rodriguez, S., Lei, X., Petersen, P. S., Tan, S. Y., Little, H. C., and Wong, G. W. (2016) Loss of CTRP1 disrupts glucose and lipid homeostasis. *Am J Physiol Endocrinol Metab* **311**, E678-E697
56. Tan, S. Y., Little, H. C., Lei, X., Li, S., Rodriguez, S., and Wong, G. W. (2016) Partial deficiency of CTRP12 alters hepatic lipid metabolism. *Physiol Genomics* **48**, 936-949
57. Wei, Z., Lei, X., Petersen, P. S., Aja, S., and Wong, G. W. (2014) Targeted deletion of C1q/TNF-related protein 9 increases food intake, decreases insulin sensitivity, and promotes hepatic steatosis in mice. *Am J Physiol Endocrinol Metab* **306**, E779-790
58. Wolf, R. M., Lei, X., Yang, Z. C., Nyandjo, M., Tan, S. Y., and Wong, G. W. (2016) CTRP3 deficiency reduces liver size and alters IL-6 and TGFbeta levels in obese mice. *Am J Physiol Endocrinol Metab* **310**, E332-345
59. Lu, L., Zhang, R. Y., Wang, X. Q., Liu, Z. H., Shen, Y., Ding, F. H., Meng, H., Wang, L. J., Yan, X. X., Yang, K., Wang, H. B., Pu, L. J., Zhang, Q., Chen, Q. J., De Caterina, R., and Shen, W. F. (2016) C1q/TNF-related protein-1: an adipokine marking and promoting atherosclerosis. *Eur Heart J* **37**, 1762-1771
60. Li, K., Liao, X., Wang, K., Mi, Q., Zhang, T., Jia, Y., Xu, X., Luo, X., Zhang, C., Liu, H., Zhen, H., Li, L., and Yang, G. (2018) Myonectin Predicts the Development of Type 2 Diabetes. *J Clin Endocrinol Metab* **103**, 139-147
61. Toloza, F. J. K., Mantilla-Rivas, J. O., Perez-Matos, M. C., Ricardo-Silgado, M. L., Morales-Alvarez, M. C., Pinzon-Cortes, J. A., Perez-Mayorga, M., Arevalo-Garcia, M. L., Tolosa-Gonzalez, G., and Mendivil, C. O. (2018) Plasma Levels of Myonectin But Not Myostatin or Fibroblast-Derived Growth Factor 21 Are Associated with Insulin Resistance in Adult Humans without Diabetes Mellitus. *Front Endocrinol (Lausanne)* **9**, 5
62. Coffey, R., Sardo, U., Kautz, L., Gabayan, V., Nemeth, E., and Ganz, T. (2018) Erythroferrone is not required for the glucoregulatory and hematologic effects of chronic erythropoietin treatment in mice. *Physiol Rep* **6**, e13890
63. Tang, T., Li, L., Tang, J., Li, Y., Lin, W. Y., Martin, F., Grant, D., Solloway, M., Parker, L., Ye, W., Forrest, W., Ghilardi, N., Oravecz, T., Platt, K. A., Rice, D. S., Hansen, G. M., Abuin, A., Eberhart, D. E., Godowski, P., Holt, K. H., Peterson, A., Zambrowicz, B. P., and de Sauvage, F. J. (2010) A mouse knockout library for secreted and transmembrane proteins. *Nat Biotechnol* **28**, 749-755
64. Qiao, L., Zou, C., van der Westhuyzen, D. R., and Shao, J. (2008) Adiponectin reduces plasma triglyceride by increasing VLDL triglyceride catabolism. *Diabetes* **57**, 1824-1833

65. Mizunoya, W., Haramizu, S., Shibakusa, T., Okabe, Y., and Fushiki, T. (2005) Dietary conjugated linoleic acid increases endurance capacity and fat oxidation in mice during exercise. *Lipids* **40**, 265-271
66. Schmittgen, T. D., and Livak, K. J. (2008) Analyzing real-time PCR data by the comparative C(T) method. *Nat Protoc* **3**, 1101-1108
67. Little, H. C., Tan, S. Y., Cali, F. M., Rodriguez, S., Lei, X., Wolfe, A., Hug, C., and Wong, G. W. (2018) Multiplex Quantification Identifies Novel Exercise-regulated Myokines/Cytokines in Plasma and in Glycolytic and Oxidative Skeletal Muscle. *Mol Cell Proteomics* **17**, 1546-1563
68. Leick, L., Wojtaszewski, J. F., Johansen, S. T., Kiilerich, K., Comes, G., Hellsten, Y., Hidalgo, J., and Pilegaard, H. (2008) PGC-1alpha is not mandatory for exercise- and training-induced adaptive gene responses in mouse skeletal muscle. *Am J Physiol Endocrinol Metab* **294**, E463-474
69. Mathis, D., and Shoelson, S. E. (2011) Immunometabolism: an emerging frontier. *Nat Rev Immunol* **11**, 81
70. Winzell, M. S., and Ahren, B. (2004) The high-fat diet-fed mouse: a model for studying mechanisms and treatment of impaired glucose tolerance and type 2 diabetes. *Diabetes* **53 Suppl 3**, S215-219
71. Wang, H., and Eckel, R. H. (2009) Lipoprotein lipase: from gene to obesity. *Am J Physiol Endocrinol Metab* **297**, E271-288
72. Koh, A., Molinaro, A., Stahlman, M., Khan, M. T., Schmidt, C., Manneras-Holm, L., Wu, H., Carreras, A., Jeong, H., Olofsson, L. E., Bergh, P. O., Gerdes, V., Hartstra, A., de Brauw, M., Perkins, R., Nieuwdorp, M., Bergstrom, G., and Backhed, F. (2018) Microbially Produced Imidazole Propionate Impairs Insulin Signaling through mTORC1. *Cell* **175**, 947-961 e917
73. McGarry, J. D., and Foster, D. W. (1980) Regulation of hepatic fatty acid oxidation and ketone body production. *Annu Rev Biochem* **49**, 395-420
74. Zhang, R. (2016) The ANGPTL3-4-8 model, a molecular mechanism for triglyceride trafficking. *Open Biol* **6**, 150272
75. Yang, Y., Smith, D. L., Jr., Keating, K. D., Allison, D. B., and Nagy, T. R. (2014) Variations in body weight, food intake and body composition after long-term high-fat diet feeding in C57BL/6J mice. *Obesity (Silver Spring)* **22**, 2147-2155
76. Hong, J., Stubbins, R. E., Smith, R. R., Harvey, A. E., and Nunez, N. P. (2009) Differential susceptibility to obesity between male, female and ovariectomized female mice. *Nutr J* **8**, 11
77. Varlamov, O., Bethea, C. L., and Roberts, C. T., Jr. (2014) Sex-specific differences in lipid and glucose metabolism. *Front Endocrinol (Lausanne)* **5**, 241

CURRICULUM VITAE

Hannah Little Version date: 4/26/19

Educational History:

Ph.D. expected	2019	Program: Biochemistry, Cellular, and Molecular Biology Mentor: G. William Wong, PhD	Johns Hopkins University School of Medicine
B.S.	2013	Biological Sciences	University of California, Irvine

Other Professional Experience:

Undergraduate researcher	2011-2013	Mentor: Zhibin Guan, PhD	University of California, Irvine
Summer intern	Summers 2009-2012	Mentors: Shannon Holloway, PhD; Toshihiko Kawano, PhD	Los Alamos National Laboratory

Scholarships and Fellowships:

Fellowship 2017-2019 National Institute of Diabetes and Digestive and Kidney Diseases — Johns Hopkins University School of Medicine
(F31DK116537; F31 pre-doctoral fellowship; $88,088)

Fellowship 2015-2017 American Heart Association — Johns Hopkins University School of Medicine
(15PRE25710315; Pre-doctoral fellowship; $50,000)

Scholarship 2013 UC Irvine Department of Biological Sciences — University of California, Irvine
(Jane Unzelman Scholarship; $3,000)

Scholarship 2013 UC Irvine Department of Biological Sciences — University of California, Irvine
(UC Irvine Biological Sciences Leadership Scholars Program Scholarship; $10,000)

Scholarship 2009-2013 University of California Regents — University of California, Irvine
(UC Irvine Regents' Scholarship; $10,000)

Peer-Reviewed Publications:

Rodriguez, S.; **Little, H.C.**; Shepard, B.D.; Wolfe, A.; Cheema, M.U.; Jandu, S.; Woodward, O.M.; Talbot Jr., C.C.; Berkowitz, D.E.; Pluznick, J.L.; Wong, G.W. (2019) Late-onset renal hypertrophy and dysfunction in mice lacking CTRP1. *FASEB J.* Under review.

Little, H.C.; Rodriguez, S.; Lei, X.; Tan, S.Y.; Stewart, A.N.; Sahagun, A.; Sarver, D.C.; Wong, G.W. (2019) Myonectin deletion promotes adipose fat storage and reduces liver steatosis. *FASEB J.* [Epub ahead of print]

Little, H.C.; Tan, S.Y.; Cali, F.M.; Rodriguez, S.; Lei, X.; Wolfe, A.; Hug, C.; Wong, G.W. (2018) Multiplex quantification identifies novel exercise-regulated myokines/cytokines in plasma and in glycolytic and oxidative skeletal muscle. *Mol. Cell. Proteomics*. **17**, 1546 – 1563. (PMCID: PMC6072542)

Lei, X.; Seldin, M.M.; **Little, H.C.**; Choy, N.; Klonisch, T.; Wong, G.W. (2017) C1q/TNF-related protein 6 (CTRP6) links obesity to adipose tissue inflammation and insulin resistance. *J. Biol. Chem.* **292**, 14836-14850. (PMCID: PMC5592665)

Petersen, P.S.; Lei, X.; Wolf, R.M.; Rodriguez, S.; Tan, S.Y.; **Little, H.C.**; Schweitzer, M.A., Magnuson, T.H.; Steele, K.E.; Wong, G.W. (2017) CTRP7 deletion attenuates obesity-linked glucose intolerance, adipose tissue inflammation, and hepatic stress. *Am. J. Physiol. Endocrinol. Metab.* **312**, E309-E325. (PMCID: PMC5406989)

Tan, S.Y.; **Little, H.C.**; Lei, X.; Li, S.; Rodriguez, S.; Wong, G.W. (2016) Partial deficiency of CTRP12 alters hepatic lipid metabolism. *Physiol. Genomics.* **48**, 936-949. (PMCID: PMC5206390)

Rodriguez, S.; Lei, X.; Petersen, P.S.; Tan, S.Y.; **Little, H.C.**; Wong, G.W. (2016) Loss of CTRP1 disrupts glucose and lipid homeostasis. *Am. J. Physiol. Endocrinol. Metab.* **311**, E678-E697. (PMCID: PMC5241556)

Zeng, H.; **Little, H. C.**; Tiambeng, T.; Williams, G. A.; Guan, Z. (2013) Multifunctional Dendronized Peptide Polymer for Effective siRNA Delivery. *J. Am. Chem. Soc.* **135**, 4962-4965.

Poster Presentations:

Little, H.C.; Tan, S.Y.; Lei, X.; Rodriguez, S.; Petersen, P.S.; Wong, G.W. (2018) Myonectin Deficiency Alters Lipid Metabolism in High Fat Fed Mice. Abstract for poster presentation, Keystone Symposia on Organ Crosstalk in Obesity and NAFLD. Keystone, CO, January 21, 2018.

Little, H.C.; Tan, S.Y.; Lei, X.; Rodriguez, S.; Petersen, P.S.; Wong, G.W. (2017) Myonectin Deficiency Alters Lipid Metabolism in High Fat Fed Mice. Abstract for poster presentation, Navigating Lipid Research in Baltimore. Baltimore, MD, May 5, 2017.

Little, H.C.; Tan, S.Y.; Lei, X.; Rodriguez, S.; Petersen, P.S.; Wong, G.W. (2016) Myonectin Deficiency Alters Lipid Metabolism in High Fat Fed Mice. Abstract for poster presentation, Kern Lipid Conference. Vail, CO, August 8, 2016.

Service and Leadership:

Co-founder	2016-present	Graduate Student Peer Mentoring Program	Johns Hopkins University, School of Medicine

(Co-founded a peer mentoring program that facilitates organized peer support among graduate students by hosting monthly discussions and workshops focused on common hardships faced in graduate school)

Lead mentor	2013-2017	Thread	Non-profit organization, Baltimore, MD

(Mentored an at-risk Baltimore City high school student for four years; oversaw three other mentors of the same student and delegated roles and tasks based on each mentor's strengths)